

# UC Berkeley

## UC Berkeley Electronic Theses and Dissertations

### Title

Impactful Design: from Microfluidic Devices for Modeling the Spine to Equipment for Pandemic Relief

### Permalink

<https://escholarship.org/uc/item/0bx6p17t>

### Author

McKinley, Jonathan

### Publication Date

2023

Peer reviewed|Thesis/dissertation

Impactful Design: from Microfluidic Devices for Modeling the Spine to Equipment for  
Pandemic Relief

By

Jonathan Patrick McKinley

A dissertation submitted in partial satisfaction of the

requirements for the degree of

Doctor of Philosophy

in

Engineering - Mechanical Engineering

in the

Graduate Division

of the

University of California, Berkeley

Committee in charge:

Professor Grace D. O'Connell, Chair

Professor Kevin Healy

Professor Mohammad Mofrad

Spring 2023

Impactful Design: from Microfluidic Devices for Modeling the Spine to Equipment for  
Pandemic Relief

Copyright 2023  
By  
Jonathan Patrick McKinley

## Abstract

Impactful Design: from Microfluidic Devices for Modeling the Spine to Equipment for  
Pandemic Relief

By

Jonathan Patrick McKinley

Doctor of Philosophy in Engineering - Mechanical Engineering

University of California, Berkeley

Professor Grace D. O'Connell, Chair

Lower back pain is the leading cause of physical disability worldwide. In the United States, annual costs associated with lower back pain exceed \$100 billion, as 70%-80% of Americans experience debilitating back pain at least once in their lifespan, limiting quality of life and ability to work. Disc degeneration is a major incurable cause of back pain often brought on or exacerbated by excessive loading of the spine. To enable the development of treatments for disc degeneration, more physiological relevant models which include the harsh mechanical environment of the human disc are needed. The dissertation research focused on the Annulus-on-a-Chip (AoC) design, fabrication, and testing of primary cells experimentally and computationally to replicate harsh strains in the annulus fibrosis of the human disc. Strains proved to be controllable, multidirectional, and uniform with magnitudes ranging from -10% in compression to 12% in tension in the axial, radial, and circumferential directions. The dissertation is the first of its kind to replicate complex mechanical loading on a microscale. The Annulus-on-a-Chip was designed to be reconfigurable for other uses such as the modeling of cardiovascular vessels, lymphatic vessels, and the cervix.

Due to the COVID-19 pandemic, the dissertation includes design for pandemic response to help rapidly address the inadequate supply of personal protective equipment (PPE). During the pandemic, shortages of PPE in rural and low-income healthcare settings were thrust into an international bidding war for N95 respirators due to global supply chain disruptions. To extend stockpiles of N95 respirators, benchtop devices for treating N95 respirators with Ultraviolet-C (UVC) germicidal light uniformly, rapidly, and inexpensively were developed and tested. Design iterations improved user safety, efficacy, and process flow, resulting in a set of open-source designs.

Finally, the lessons learned while targeting improvements to societal healthcare through engineering design of the AoC and pandemic response devices led to the ideating, proposing, and implementing of the College of Engineering Business Minor for Engineering PhDs. Intended

to complement the strengths specific to PhDs at UC Berkeley, the Engineering Business Minor was designed to significantly support the many students looking to make an impact with their research.

To all of my loved ones.

# Contents

<b>Contents</b>	<b>ii</b>
<b>List of Figures</b>	<b>iv</b>
<b>List of Tables</b>	<b>ix</b>
<b>1 Introducing the Load Bearing Intervertebral Disc, Both Healthy and Degenerated</b>	<b>1</b>
1.1 The Rigid Yet Flexible Load Bearing Spine . . . . .	1
1.2 Conventional Mechanically Active Models for the Healthy and Degenerated Intervertebral Discs in the Spine . . . . .	4
1.3 Next Generation Mechanically Active Cell Culture Models Including Micro-Bioreactors . . . . .	7
1.4 Objectives and Scope of the Dissertation . . . . .	7
<b>2 State-of-the-Art Review of Complex Loading Devices for Modeling the Disc</b>	<b>10</b>
2.1 Introduction . . . . .	10
2.2 Review Methods . . . . .	12
2.3 Identified Conditions for Complex Loading . . . . .	13
2.4 Macro-Bioreactor or Whole Organ <i>ex vivo</i> Systems . . . . .	17
2.5 Micro-bioreactors or Mechanically Active Microphysiological Systems (Organ-chips) . . . . .	19
2.6 Exemplar Micro-bioreactor Devices . . . . .	21
2.7 Discussion . . . . .	25
2.8 Limitations . . . . .	27
<b>3 Design of a Flexing Organ-chip to Model <i>in situ</i> Loading of the Intervertebral Disc</b>	<b>28</b>
3.1 Abstract . . . . .	28
3.2 Introduction . . . . .	29
3.3 Results and Discussion . . . . .	32

3.4	Methods . . . . .	40
<b>4</b>	<b>Impactful Design for Pandemic Response</b>	<b>45</b>
4.1	Introduction . . . . .	46
4.2	Results and Discussion . . . . .	47
4.3	Methods . . . . .	56
<b>5</b>	<b>Conclusions and Outlook</b>	<b>62</b>
5.1	Design and Development of the Annulus-on-a-Chip . . . . .	62
5.2	Rapid Design for Pandemic Response . . . . .	63
5.3	Business Minor Specifically Designed for Engineering PhDs . . . . .	63
	<b>Bibliography</b>	<b>67</b>



# List of Figures

- 1.1 (a) The intervertebral disc provides structure support and mobility for the spine (Image sourced from 3D Muscle Lab). Discs in the lumbar spine bear the greatest loads compared to those in the thoracic or cervical spine, given their supporting position at the base of the spine. (b) Degeneration of the disc can be seen with Magnetic Resonance Imaging (MRI) as a loss of height and discoloration, graded in severity using the Pfirrmann Grading Scale (images sourced from the Cornell Pain Clinic). (c) A degenerated disc losses its height, but also losses its ability to withstand compressive loads properly. Load normally shared by the NP is transferred entirely to the AF when NP pressure is lost. Like the walls of a deflated tire, the AF experiences changes in load (shown with red arrows) from tension to compression when pressure is lost as degeneration progresses.[232] . . . . . 2
- 1.2 (a) The intervertebral disc is made up of the nucleus pulposus (NP) and the annulus fibrosus (AF). Cell type, morphology, and density are different between the NP and AF.[132] (b) Like the jelly in a filled donut, the NP fills the interior of the AF. Meanwhile, the AF surrounds the NP with layers like those of an onion.[196] (c) Degeneration is brought on by numerous factors including genetics, aging, habits (e.g., smoking), and injury (e.g., change in load). Degeneration is marked by decreased nutrient availability, tissue structural changes, inflammation, and innervation which contributes to cell death, immune response, and back pain. A cascade occurs when cell death, immune response, and back pain lead to further changes in degeneration.[18] . . . . . 5
- 2.1 This figure demonstrates multiscale loading in the disc. Compressive forces applied at the organ-level results in complex stresses throughout the NP and AF (e.g., radial and circumferential tensile stress), which is experienced by embedded cells. In the healthy disc, the AF experiences both direct axial compression and tensile stresses due to internal pressure from the NP. Despite off-axis loading from supporting trunk muscles while performing daily activities like bending. Two-sided arrows indicate that diurnal loading is often cyclic. . . . . 13

- 2.2 Mechanically active bioreactors were categorized as macro-bioreactors that culture entire organs to maintain disc integrity or micro-bioreactors that culture disc cells for tissue engineering. Grey arrows indicate either applied loads, displacements, or strains of known magnitude, direction, and frequency. Blue arrows indicate unknown strains that need to be measured or calculated. . . . . 17
- 2.3 Overview of the complex micromechanical environments created by applied strain on cell chambers in micro-bioreactors. Except for the (A) independently controlled cell chamber which is many centimeters in width, each cell chamber is on the order of tens or hundreds of microns tall and wide. (A) While still 2D, a PDMS membrane with independently actuated corners represents a departure from conventional 2D stretch culture that could be programmed to achieve more disc-like strains.[74] (B) Disc shaped cell scaffolds are compressed on top and bottom to achieve complex strain in the interior when walls are unconfined.[117] (C) Unlike most devices with a single strain type, this confined chamber can be strained in tension or compression to achieve complex strain relevant for articular cartilage or heart muscle.[159, 139] (D) Embedded within a cell chamber placed in a bulk PDMS form that is bent, cells experience tension and compression depending on the chamber wall. Tension and compression can be flipped if the device is bent in the opposite direction. Complex strain similar to that applied by hoop strain is relevant for annular structures such as the annulus fibrosus, cardiac vessels or the cervix.[142] . . . . . 22
- 3.1 (a) The AoC bent by hand to demonstrate the process of applying strain through device deformation. Blue markings in the channel are for reference only. Scale bar: 4 mm. (b) Schematic and dimensions of the AoC including the embedded channel. (c) Schematic showing the process of applying strain to cells in the channel by bending while the channel is imaged from below with an inverted microscope. (d) Schematic of vertebra and disc with positive axial, radial, and circumferential (or hoop) directions labeled. (e) When the posterior AF is under combined flexion, compression, and axial rotation, it assumes a state of strain where the axial and radial strains are inversely proportional and the circumferential strains are minimal and variable in comparison. This strain condition was replicated in the AoC channel when the device is flexed. . . . . 29

- 3.2 (a) Exploded view of the experimental setup in SOLIDWORKS (overall dimensions: 15 cm x 15 cm x 4.4 cm). (b) Representative image of the experimental setup. The AoC was held between a 3D printed barrel structure and a 1 mm thick glass slide placed on top of the microscope stage for imaging. Micropipette tips with equal volumes of cell culture media were plugged into ports at either end of the channel. Polypropylene ‘packing’ tape was used to connect the device to servo motor horns and apply cyclic force on the device. As the servo horns rotated upward in tandem, the tape pulled tight, forcing the device to conform to the 3D printed barrel structure. Scale bar: 4 mm. (c) Cross-section of the AoC with the relevant dimensions to compute the tensile strain,  $\epsilon_x$ , in the channel. . . . . 31
- 3.3 (a) Quarter symmetrical color map of strain in the x direction (radial strain) under maximum flexion. (b) Experimentally measured strains (open symbols) are plotted against the beam theory estimation (solid line) and the FE model (dashed line). Based on the model, the centroidal axis was offset from the neutral axis by 0.2 mm (difference in the intersection at the x-axis). (c) Components of 3D strains, including radial, circumferential (circ.), and axial strains, are plotted for the element at the midpoint of the channel as the device is flexed from a flat starting position to a maximum angle based on the curvature of the barrel. Tensile and compressive strains were positive and negative, respectively. Radial, axial, and circ. strains correspond to x, y, and z strains. (d) Strains plotted along the channel demonstrated uniformity in the strain fields applied throughout the channel. Data is presented only for half of the channel due to symmetry. (e) Axial:radial and circumferential:radial strain ratios for the AoC were plotted along the length of the channel. . . . . 33
- 3.4 (a) Live/dead staining of an AF cell population (nearly 2000 cells/channel) after three weeks of culture. Cell density varied throughout the channel, with the greatest number near the media port (black circle). Scale bar = 100  $\mu\text{m}$ . (b) Cells with sufficient contrast were segmented with polygon selections to compare before and during strain. Scale bar = 100  $\mu\text{m}$ . (c) A Brightfield image was taken after strain was applied to confirm that cells remained attached to the channel for at least an hour after loading. Polygon selections are included to distinguish each cell. Scale bar = 100  $\mu\text{m}$ . . . . . 36
- 4.1 Made from readily available parts, the UVC Blaster Mini required  $< 4ft^2$  in bench space and could process five N95 respirators in ten minutes or less. (30 N95 Respirators / hour) This system processes the front and back of the respirator simultaneously. A UVC Blaster with higher capacity but greater cost was also designed. . . . . 47
- 4.2 Iterative design resulted in two UVC Blasters models, depending on cost and throughput. The UVC Blaster Mini was designed to sit on a cart or benchtop while the UVC Blaster XL could either sit on a benchtop or be built into a temporary wall in order to separate clean and dirty zones in a hospital. . . . . 48

4.3	User needs and wants were defined in collaboration with rural community health-care workers. . . . .	49
4.4	In addition to preventing risks through engineering design, potential risks were displayed in the user manual as well as on the device itself. . . . .	53
4.5	The device was created to be safe by mechanical design instead of safe by protocol. However, safety warnings were displayed in the user manual to add a layer of safety for the user. . . . .	54
4.6	Design elements were included to ensure user safety and treatment effectiveness. A clean and dirty handle on the Mini eliminated the need for additional personnel or additional PPE to operate the device. A barrier separating a clean room from a dirty room afford better process control. . . . .	55
4.7	Compared to aluminum, ePTFE was chosen as a more UVC reflective surface, which improved chamber performance by increasing UVC intensity and UVC scattering (Image from Porex Corporation). Treatment time was reduced, and treatment coverage improved qualitatively. . . . .	55
4.8	The UVC Blaster Mini compared favorably to the state-of-the-art systems of the time with respect to metrics important for rural and low income healthcare settings. (Left) The University of Nebraska Medicine Center paved the way for UVC use for decontaminating respirators in hospitals, but the initial investment was too expensive. (Middle) Costs for the Battelle hydrogen peroxide vapor system were almost entirely covered by the federal government and could treat respirators at scale but could not treat respirators outside its range in rural settings. (Right) In addition to the low cost, the UVC Blaster Mini was designed to be easy to operate with built-in safety elements that could keep nearly any healthcare worker safe even without training. . . . .	56
4.9	A Sper light meter was used to measure UVC intensity, while test strips were used to measure UVC dose (intensity per time). A jig was created to move the light meter sensor reliably to various coordinates within the chamber. Intensity was recorded in spreadsheets as depicted in this figure. The test strips which turned green in the presence of sufficient UVC light were pasted at various locations on the respirator including the inside, any edges, and the straps. Dose was recorded by photographing the test strips and comparing color to a reference shown in the top right. . . . .	58
4.10	A grid of irradiance values ( $mW/cm^2$ ) measured throughout the chamber was faster and more reliable than simulating values. . . . .	59
4.11	A grid of irradiance values ( $mW/cm^2$ ) for the XL model was also measured. Besides a higher intensity, the pattern of values similar with respect to edge effects. . . . .	60
4.12	Relative spectral intensity by wavelength from the Sper Scientific UVC Light Meter user manual. The crosshairs indicate the calibration point. . . . .	61

5.1 The entire Engineering PhD student body was surveyed regarding their interest in a business minor. Favorable responses from 132 PhDs indicated that there was a need. . . . . 65

5.2 Engineering PhD students interested in a business minor were spread across numerous departments in the college including Electrical Engineering and Computer Science (EECS), Mechanical Engineering (ME), Material Science Engineering (MSE), BioEngineering (BioE), Applied Science and Technology (AST), Civil and Environmental Engineering (CEE), Industrial Engineering Operations Research (IEOR), and Nuclear Engineering (NE). . . . . 66

# List of Tables

3.1	Comparison of strain ratios in the posterior AF within bone-disc-bone segments under flexion, the AoC, and commercial uniaxial cell stretchers. . . . .	36
-----	---	----

## Acknowledgments

I have enjoyed nearly twelve years at UC Berkeley while completing my bachelors, masters, and PhD. During those twelve years there have been countless individuals who have changed my life for the better, including friends, family, and mentors. Special thanks to my parents, who cultivated my belief in the power of community, which played a large part in my Berkeley experience. To my brothers who taught me that even the most audacious vision is achievable. To my coach who instilled the belief in the power of Consistent Hard Work Over Time. To Professor Grace O'Connell, who encouraged me to pursue my interests in design and encouraged me through her own actions to try to change the outcome of the COVID-19 Pandemic. To the many volunteers that teamed up to rapidly develop engineering designs presented in this dissertation aimed at improving the conditions for healthcare workers in the pandemic. And to Professor Lee Fleming, Dean Tsu-Jae King Liu, Rhonda Shrader, and Professor Lisa Pruitt for supporting me and the new Business Minor for engineering PhDs designed by the students for the students. Thank you!

# Chapter 1

## Introducing the Load Bearing Intervertebral Disc, Both Healthy and Degenerated

The following chapter includes healthy and degenerated conditions for the intervertebral discs from an anatomical, compositional, and cellular point of view. Emphasis is placed on mechanical function of the spine, such as the bearing of static and dynamic load while enabling flexibility along its length with the use of soft yet strong intervertebral discs between the bony vertebral bodies. Injury, degeneration, back pain or a combination of all three greatly impacts mechanical functioning of the spine which can result in lessened quality of life.

### 1.1 The Rigid Yet Flexible Load Bearing Spine

#### Load Bearing Anatomy of the Intervertebral Disc

The spine is made up of alternating rigid vertebral bones and flexible intervertebral discs (IVD) (see Fig. 1.1A). When supported by trunk muscles and ligaments, the spine offers the rigidity and flexibility needed to bend and lift loads.[166] These loads in turn are applied to the spine before being transferred to each bone-disc-bone segment. A disc under compression from the bones results in a pressurized nucleus pulposus (NP) with a strained annulus fibrosus (AF) (see Fig. 1.2A-B). Pressurization of the NP is due to the attraction of water, while the AF strain comes from surrounding and containing the pressurized NP. Just as the walls of a pressurized vessel or car tire undergo tensile circumferential strain or hoop strains to counteract an internal pressure, the AF experiences tensile strains to counteract the internal pressure of the hydrated NP.[232]

Disc hydration is lost steadily throughout the day, which results in a loss of disc height and an increase in disc stiffness.[20] Hydration, height, and viscoelasticity is regained when



sleeping horizontally due to the decrease in load on the spine. This natural diurnal cycle illustrates the dependence of disc health on loading which can be described by magnitude, frequency, and duration of strains as recorded with sensors on humans completing everyday tasks.[181] While there is some loading that is beneficial for cell health and the movement of nutrients, loading that is too great in magnitude, duration, or frequency can disrupt the homeostasis of the disc (see Fig. 1.2C).

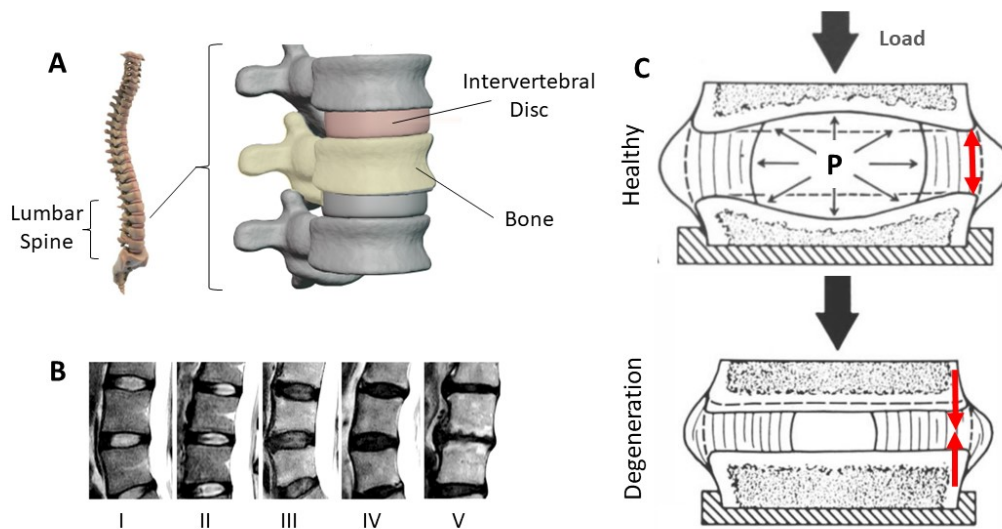


Figure 1.1: (a) The intervertebral disc provides structure support and mobility for the spine (Image sourced from 3D Muscle Lab). Discs in the lumbar spine bear the greatest loads compared to those in the thoracic or cervical spine, given their supporting position at the base of the spine. (b) Degeneration of the disc can be seen with Magnetic Resonance Imaging (MRI) as a loss of height and discoloration, graded in severity using the Pfirrmann Grading Scale (images sourced from the Cornell Pain Clinic). (c) A degenerated disc loses its height, but also loses its ability to withstand compressive loads properly. Load normally shared by the NP is transferred entirely to the AF when NP pressure is lost. Like the walls of a deflated tire, the AF experiences changes in load (shown with red arrows) from tension to compression when pressure is lost as degeneration progresses.[232]

## Composition

The IVD has tissue gradients in the radial direction with respect to the NP in the center (see Fig. 1.2A). While the NP is largely uniform, cell density, cell phenotype, collagen concentrations and mechanics all differ between the NP, inner AF and outer AF. Aligned, in long organized fibers, more collagen type I is present in the outer AF than the inner, and vice versa for collagen II and proteoglycans (GAGs).[54] Composition dictates load bearing capabilities. The highly negatively charged polar GAGs attract and hold water, which is effective at resisting compression when confined by the AF. The fibrous bundles of collagen in the AF, meanwhile, are most effective at withstanding tensile loads as if part of a tendon. One tissue type is ineffective alone. Instead, the combination of tissue types with a gradient of material properties in between is needed to provide both loading and flexibility.

## Cellular/Biochemical

Blood vessels in the IVD are limited to the outer edges or periphery of the AF where cellularity is greatest.[67, 138] With limited blood supply to the IVD, acidity and osmolarity is high and nutrients are low which results in a harsh cellular environment.[220] The presence of loading changes the availability of water and large molecules by moving the molecules through the disc by way of convection.[2] Strains on a tissue can change the flow of water and nutrients available to these cells because cyclic compression and relaxation on the surrounding tissue forces fluid flow, an alternative to vasculature.[52] By way of convection and diffusion, metabolic byproducts and nutrients are transported depending on concentration and molecule size (glucose, oxygen, sulfate, and lactate can diffuse).[138] IVD cells also respond favorably to loads transferred directly to the cell.[102, 145] In the NP, cells are rounded and chondrocyte-like under hydrostatic pressure. The outer AF cells are elongated and fibroblast-like, given matrix bound adhesion sites tethered to F-actin filaments for load transfer. In between, a gradient of loading as well as cell aspect ratio is present.[24]

## Intervertebral Disc Degeneration

The lumbar spine rather than the thoracic or cervical is chosen for further discussion given both its risk of failure due to high loads combined with a large range of motion and its impact on quality of life. Degeneration can be brought on in several ways due to multifactorial etiology which includes both genetics and lifestyle. In one documented population, rowers, the link between loading and degeneration in the lumbar spine is clear.[226]

## Anatomy

Higher static and cyclic loads from injured disc tissue, excessive body weight or strenuous exercise, increase loading on the disc. These loads can far exceed intradiscal hydrostatic pressure, leading to unrecoverable loss in fluid and in disc height. Magnetic Resonance Imaging (MRI) can determine levels of degeneration using the Pfirrmann grading system by

comparing disc height and disc composition (see 1.1B). Lost internal NP pressure can be seen on the images as if the air was let out of a tire. Without intradiscal water acting as a shock absorber responsible for sharing some load, the disc becomes stiffer, and the extracellular matrix and cells take on more load. Even though the tissues are made for tension, the AF must withstand the compressive loads previously shared by the NP (see 1.1C). In addition to a change from tension to compression, strain magnitudes can more than double in the presence of tears associated with degeneration. With the increase in strain magnitude as well as the change in strain state, degeneration in the AF can lead to further degeneration. This positive feedback loop of degeneration known as a cascade acts not only mechanically in the case of annular tears that can lead to more annular tears, but also acts biochemically as seen in the presence of inflammation.

Much like diurnal loading, degeneration can lead to lost disc height. It can also lead to or be caused by rupture, stiffening, and cell death. Hyperphysiological or overloading with respect to magnitude, frequency, or duration can alter the anabolic/catabolic balance important for homeostasis. The disc cellular environment becomes even harsher mechanically and chemically.

### **Composition**

Layers of the AF once bound by collagen and elastin become loose and disorganized.[50] Disc mechanics become stiffer with an NP that behaves more like a solid instead of a viscoelastic material, resulting in higher stresses on cells throughout for a given strain. The permeable endplates calcify, limiting the flow of nutrients from the vertebral body.

### **Cellular/Biochemical**

The AF relies on a healthy NP for the movement of nutrients. A disrupted NP can limit the flow of water and nutrients necessary for cell health. As a result, a more neutral pH is no longer maintained (7.1-7.4 pH instead of 6.2-6.5 pH with degeneration).[72] The availability of oxygen can also be compromised because overloading can reduce oxygen diffusivity through the AF. Cellularity therefore greatly depends on level of degeneration.[215] When the disc is torn from overloading, blood vessels can penetrate deeper. The normally isolated disc is suddenly exposed to the immune and nervous systems, which then provide macrophages and neutrophils, resulting in inflammation and innervation.

## **1.2 Conventional Mechanically Active Models for the Healthy and Degenerated Intervertebral Discs in the Spine**

From whole organisms, to tissues, to cells, conventional models of the disc that are mechanically active span multiple scales.

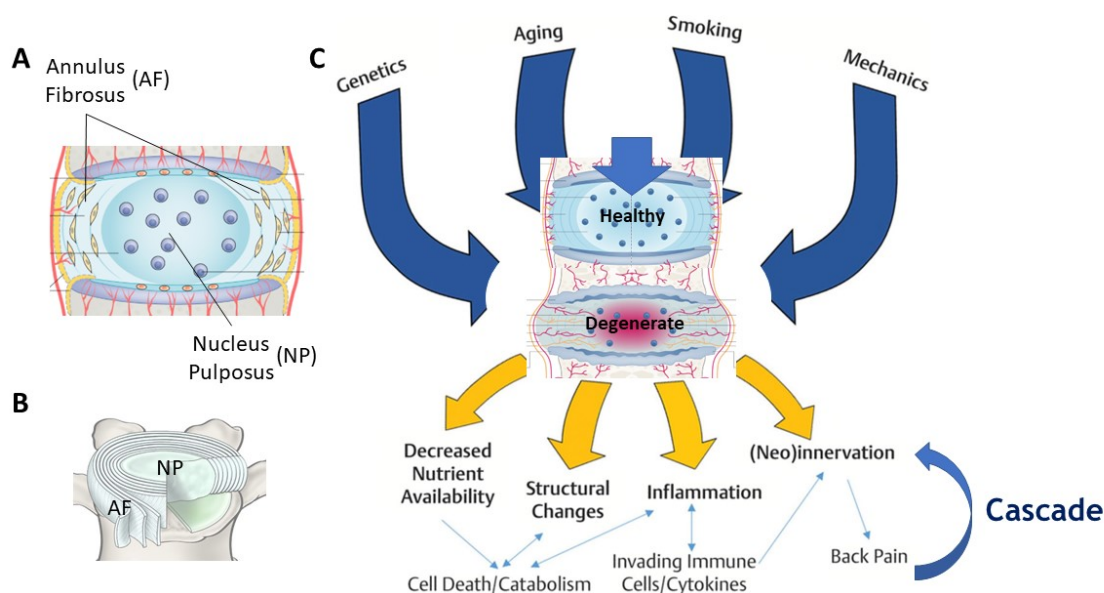


Figure 1.2: (a) The intervertebral disc is made up of the nucleus pulposus (NP) and the annulus fibrosus (AF). Cell type, morphology, and density are different between the NP and AF.[132] (b) Like the jelly in a filled donut, the NP fills the interior of the AF. Meanwhile, the AF surrounds the NP with layers like those of an onion.[196] (c) Degeneration is brought on by numerous factors including genetics, aging, habits (e.g., smoking), and injury (e.g., change in load). Degeneration is marked by decreased nutrient availability, tissue structural changes, inflammation, and innervation which contributes to cell death, immune response, and back pain. A cascade occurs when cell death, immune response, and back pain lead to further changes in degeneration.[18]

## Animal Models for Disc

Pre-clinical assessment of biological therapeutics heavily rely on small animal models like mice or rats which are readily available and can be modified with knock-out or surgical techniques to replicate degeneration.[76, 103, 77, 147] These small animal models can also replicate loading on the disc using exercise, external loading devices, or surgical modifications such as with the bipedal mouse model.[51, 129] However, translatability is limited, findings from small animal models do not translate well to humans in general but especially in the disc due to differences in biomechanics and disc cell type. Of the therapeutics tested successfully in small animals, 88% go on to fail clinical trials in humans, which further drives up the cost of therapeutics that reach market approval (\$2.9 Billion).[55] As a result of high failure

rates, therapeutic development is risky and time-consuming with some drugs requiring more than a decade of research with costly and ethically concerning large non-human primates such as bonobos. In response, animal models for studying therapeutics are being reduced, refined, and replaced by alternatives.

## **Mechanically Active Tissue Culture or Macro-Bioreactors**

One such alternative is a macro-bioreactor capable of maintaining whole disc resected from cadavers. Rather than use the entire organism, the disc can be resected and isolated for culture to gain control over applied stimulus as well as biomechanical and biochemical testing.[84] Resected tissue can include partial or whole organs that are kept viable in media for weeks to months.[169] While there are disadvantages of isolating a tissue or a cell population from the whole organism and interactions with the cardiovascular and nervous systems, the isolation can make it possible to ask more direct scientific questions about the function or structure of the disc as a whole or about specific tissue within the disc such as the AF.[192] By placing human tissue in these macro-bioreactors, physiological relevance is improved with the necessary cell type (recreates spontaneous degeneration) and human-like biomechanical loading. The presence of human cells allows for spontaneous degeneration, a cellular attribute critical to the pathology of disc degeneration that is unique to humans and few other animal models.[128] The human-like or physiologically relevant loading is important in the disc for maintaining cellular and tissue homeostasis which is key to enabling long term cell culture. Discussion of mechanically active tissue culturing or macro-bioreactors will continue in Chapter 2. Rather than expanding cells for clinical use, bioreactors discussed include models of healthy and pathological tissues.

## **Mechanically Active Cell Culture or 2D Stretch Culture**

After harvesting cells from the disc, healthy or degenerated cells can be studied by growing them in monolayers on hard or soft substrates. Soft substrates are advantageous for disc modeling because they can be stretched, which applies uniaxial or biaxial strain to adhered cells (Flexcell).[43, 121, 176, 203, 71] In this configuration, the cells can be chemically stimulated by additions to the media bath such as cytokines or other degenerative additives. While these cells can be mechanically and chemically stimulated and studied in highly controllable ways, the physiological relevance is limited with the two-dimensionality of the cell monolayers. Differences in cell behavior and morphology of 2D cell layers compared to disc cells in 3D *in vivo* tissue are detailed in the coming chapter.

### 1.3 Next Generation Mechanically Active Cell Culture Models Including Micro-Bioreactors

By using human cells in highly controllable micro-scaled 3D tissue constructs, organ-chips, also known as microphysiological systems or micro-bioreactors, have shown the potential to revolutionize the benchtop-to-bedside process of pharmaceutical treatment discovery, development, and approval.[62] These devices that are manufactured with computer chip processes, can be tailored to study disease progression, drug dosing, and treatment efficacy or to be used to pick drug targets or to inform clinical trial design for a range of tissue types and associated diseases.[130] However, the untreatable disc degeneration behind the leading cause of years lived with disability (YLD), lower back pain, is yet to be modeled fully on a micro-physiological system.[95, 135, 190, 86] In order to increase the drug discovery for disc degeneration of the intervertebral disc, better models are needed that can match the unique mechanical activity, composition, and cell type of the disc. Most microphysiological systems (organ-chips) could match disc composition and cell type. A mechanically activated microphysiological system or micro-bioreactor is also needed to match mechanical activity. A micro-bioreactor capable of mimicking the disc could be crucial in eliciting predictable *in vitro* catabolic and anabolic responses characteristic of disc degeneration specific to humans. These upgrades to conventional animal or conventional cell culture models could further enable drug discovery and development. Resulting therapeutics could provide the first non-invasive early-response treatment to answer the growth in back pain. Additionally, devices designed for application in the disc can be impactful when adapted for other tissues in the body such as tendon, ligaments, and the cervix.

### 1.4 Objectives and Scope of the Dissertation

This dissertation is focused on impactful design. Included in the next two chapters are the necessary information for the design and development of the first micro-bioreactor for the spine, called the Annulus-on-a-Chip. Chapter 4 is dedicated to novel designs and development of devices to extend personal protective equipment (PPE) stockpiles in the pandemic. Both examples target a major societal problem.

## Chapter 2: State-of-the-art Review of Complex Loading Devices with Application in Modeling the Disc

A non-systematic literature review was conducted across multiple fields in order to identify devices and their design elements that could be adapted for use in modeling the disc at several scales. After identifying conditions for complex loading throughout the body, micro- and macro-bioreactors capable of applying these complex loads were identified in peer-reviewed literature (patent databases were not included). While macro-bioreactor

were included for reference, emphasis was placed on the smaller, more customizable micro-bioreactors given their higher potential impact on treatments for disc degeneration and back pain outlined above. Micro-bioreactor devices related to intervertebral discs, cardiovascular tissue, and articular cartilage were all included given the possibility for sharing design elements. Challenges of implementing both micro- and macro-bioreactor systems were detailed to enable a designer or researcher to arrive at the optimum scale for modeling the disc for their purposes. Future device concepts were included with particular relevance to the disc, such as the incorporation of active driven membranes instead of the current use of passive membranes, fast actuation mechanisms to replicate trauma conditions in the disc, and multicell models to replicate degenerative conditions with the presence of immune and nervous system responses. Ultimately, the review supports the need and proves the novelty of the micro-bioreactor Annulus-on-a-Chip (AoC) presented in Chapter 3.

### **Chapter 3: Design and Development of the Annulus-on-a-chip, a First of its Kind Micro-bioreactor)**

The AoC designed to replicate complex strains felt by soft tissue in the spine was both modeled and manufactured as part of the development of the patentable way of applying complex strain. While mechanical stimulus is derived from human spine data, other animal models are considered. Although there exists an interplay between various types of stimuli in regard to spine health, other forms of stimuli such as chemical or electrical are excluded from consideration to isolate the effects of mechanical stimuli. The development of patentable device for applying complex strains is not dependent on cellular work. However, a complete microphysiological system is made up of the device itself in combination with the cellular interface, whether a biocompatible surface or matrix. Instead of developing the device and the cell-device interface in parallel, the device mechanics were determined before the cell-device interface was studied separately, so as it eliminate a host of additional variables that come with a new device design. As a result of this split approach, cell-device interface was developed into a separate chapter in which cellular response to soft substrates are investigated, typical of most microphysiological systems.

### **Chapter 4: Rapid Impactful Design to Protect Healthcare Workers with Limited Supplies of Personal Protective Equipment in a Pandemic**

The COVID-19 pandemic relief design and engineering led to the development of the UVC Blaster over six iterations. To meet the needs of healthcare workers in rural hospital settings, each iteration included changes due to availability of parts, manufacturability, fail-safety, and reproducibility. While the other aspects of the UVC Blaster design are included, fail-safety and reproducibility are the focus. Biological work to determine the efficacy of the UVC Blaster was limited due to limited access to necessary SARS-CoV-2 model viruses. Instead

of determining the direct effectiveness of the device on the transmission of COVID-19 on PPE, the indirect effectiveness of the design on SARS-CoV-2 is determined by measuring the reproducibility of UVC light at the most germicidal wavelength throughout the device and on all PPE surfaces. All aspects of the design were based on guidelines by the Centers for Disease Control and Prevention (CDC) at the time. CDC guidelines shifted from week to week, ultimately settling on more stringent criteria which eliminated the use of the UVC Blaster for purposes of decontamination as determined by a germicidal effectiveness measured. While future designs would incorporate a higher germicidal effectiveness, the effectiveness standard of the UVC Blaster was balanced between speed of manufacturing/deployment and sufficient effectiveness based on the CDC guidelines of late Spring 2020. The design of the UVC Blaster was also dependent on the assumption that the use of the device would change depending on PPE materials or personal objects that needed to be treated. The UVC Blaster designs were developed in California and flown to New England, where supplies and new methodologies were most needed.

## **Chapter 5: Conclusions and Outlook**



## Chapter 2

# State-of-the-Art Review of Complex Loading Devices for Modeling the Disc

This is my review aimed at informing present and future designs of disc specific models capable of replicating physiologically relevant complex loading. Device examples applying complex loading to other tissues such as cardiovascular tissue and articular cartilage were included to increase the knowledge base for work in the spine. Macro-bioreactors were included, however, emphasis was placed on the smaller more customizable micro-bioreactors given their greater potential to lead to treatments for disc degeneration and back pain outlined in Chapter 1. Micro-bioreactor devices related to intervertebral discs, cardiovascular tissue, and articular cartilage were all included given the possibility to share design elements. Upon completion of the review, the novelty and need for the Annulus-on-a-Chip (AoC), a micro-bioreactor device designed to apply the complex loading necessary for modeling the disc, was confirmed.

### 2.1 Introduction

Osteoarthritis and lower back pain are the leading causes for physical disability worldwide. In the United States, annual costs associated with lower back pain are greater than \$100 billion, as 70%-80% of Americans experience debilitating back pain at least once in their lifespan, limiting quality of life and ability to work.[183, 236, 228, 111] Causes for lower back pain are multifactorial and include risk factors such as smoking tobacco, obesity, fat infiltration of muscles, facet degeneration, and disc degeneration.[70, 245, 211, 120, 110] While most occurrences of lower back pain goes undiagnosed, a definitive diagnosis for painful disc degeneration was found in nearly 40% of lower back pain patients.[190, 167] Since not all are symptomatic, the patient population with lumbar disc degeneration in general is much larger especially in an elderly population (near 70-75% degeneration).[212] Disc degeneration

is not only associated with age and back pain but also genetics, diabetes, smoking tobacco, obesity, and occupational tasks resulting in excessive loading on the spine. [172, 9, 143, 6] Compared to the general population, rowers are five times more likely to have a form of lumbar disc degeneration due to the repetitive high loads on the disc in a fully flexed position.[49, 89, 177]

The disc is made up of the annulus fibrosus (AF) which is a highly organized multi-layered fiber-reinforced tissue made up of type I collagen that surrounds and supports a gelatinous nucleus pulposus (NP) composed of type II collagen.[232, 242] When healthy, the intervertebral disc provides flexibility and structural support to withstand loads in the face of dynamic axial compression, torsion, bending, and extension during daily activities. As loads are applied to the disc, the AF acts like the thick walls of a pressurized vessel as embedded fibers are engaged by hoop stresses to contain the NP.[33] Axial loads on the organ translate through the tissue to become multiaxial or complex loads at the cellular level (see Fig. 2.1). Fully confined by the AF, the pressurization of the NP offers load support to the spinal column and uniform load transfer back to the AF. However, when pressurization is reduced in the case of internal disc disruption and other forms of degeneration, the AF shares more of the load which can lead to bulging of the disc, nerve impingement, and the narrowing of the nearby spinal canal (i.e., spinal stenosis).[131, 110, 234, 153, 156] Loads from daily activities are already considered harsh or complex as they can far exceed body weight, are multiaxial, are highly dynamic and are dictated by anisotropic material behavior.[180, 193] With degeneration, the harsh environment only worsens. Progression of degeneration increases loads and changes loading type across the AF, which furthers degeneration in a cascade.[205, 232]

Loading type and magnitude play a role in the catabolic/anabolic balance in cell response. Low dynamic loads or physiological loads can create a net anabolic effect, however, overloading or static prolonged loading (> 24 hours) on human cells especially in dehydrated discs can lead to a catabolic response.[222, 223] When healthy, homeostasis is achieved when cells express extracellular matrix catabolic proteins such as collagen I, collagen II, glycosaminoglycan (GAG), aggrecan and others that provide structure and attract water critical for maintaining disc pressure and nutrient/metabolite diffusion. However, in addition to progressively worsening biomechanical loading, disc degeneration also leads to a cascade of worsening cell health. A decline in anabolic cellular function marked by inflammatory/catabolic response leads to further cell death.[69] In this state, senescent cells associated with aging or degeneration, accumulate and secrete pro-inflammatory cytokines and contribute to the cascade by creating senescence in neighboring cells.[58]

There has been growing interest in minimally invasive biological strategies to treat symptomatic disc degeneration, including molecular therapies for reprogramming the catabolic disc environment, gene therapies (Mesenchymal Stem Cell-targeted Senescence inhibitors), cell-based therapies (anti-inflammatory and immunosuppressive autologous mesenchymal stem cells), and injectable biomaterials.[107, 127, 238, 186, 222, 188] However, clinical uses of these approaches have been limited. Currently, only one biological treatment strategy has been approved by the FDA (Food and Drug Administration) where full-thickness articular

cartilage defects in the knee are replaced with autologous cellularized collagen scaffolds.[30]

Development of more effective and less invasive biological treatment strategies for the disc has proven more challenging without better tests for efficacy. Existing *in vitro* tests for treatment development have poor predictive value and species-dependent differences (e.g., presence of regenerative notochordal cells) mean that existing *in vivo* models or animal models have limited translational value to clinical observations.[127, 136] Furthermore, the larger size of human discs compared to animal models results in a harsher mechanical and chemical environment with worse nutrient transport which could limit the lifespan of any injected cells.[168] Any treatment, whether an injected biomaterial or a gene edited stem cell, needs to overcome this harsh environment. To do so, bioreactors for disease modeling, drug screening, tissue regeneration, or for basic mechanobiology are needed for relevant and accurate testing in these harsh conditions.[10, 187]

Cells in healthy AF and NP tissues are exposed to hypoxic conditions, hyperosmotic stresses, complex mechanical loads, and deficiencies in nutrient delivery and waste removal.[127] Replicating the harsh microenvironment, including acidity, abnormal loading, and inflammation, is critical for assessing potential biological repair strategies to treat early to moderate disc degeneration.[207, 151] While each aspect of the microenvironment is important for cell health and the degenerative process, this review will focus on bioreactor platforms used to replicate the complex mechanical microenvironment, since altering non-mechanical or physicochemical cues (e.g., osmotic loading, oxygen, nutrients, inflammatory compounds, pH) can be done more simply by altering the culture media or altering conditions in the incubator.[149, 79] The bioreactors in this review have been categorized into macro- and micro-bioreactors to cover complex loading with application in the disc from a multiscale perspective. Macro-bioreactors or *ex vivo* organ culture models refer to whole disc culture, whereas micro-bioreactors or *ex vivo* cell culture models reference mechanically active microphysiological systems or organ-chips with harvested cells embedded in 3D gels to enable complex loading. Several expert reviews highlight animal disc models and their comparison to micro- and macro-bioreactors.[210]

This review focuses on complex mechanical activity in both micro- and macro-bioreactors with direct application or future application to the disc. Benefits and challenges with disc related micro- and macro-bioreactors are presented to inform future design of a novel device to test disc therapies.

## 2.2 Review Methods

A non-systematic literature review was conducted across multiple fields in order to identify designs elements that could be adapted for use in modeling the disc, specifically the AF. Micro- and macro-bioreactors were sampled from peer-reviewed literature only. Patents were not included.

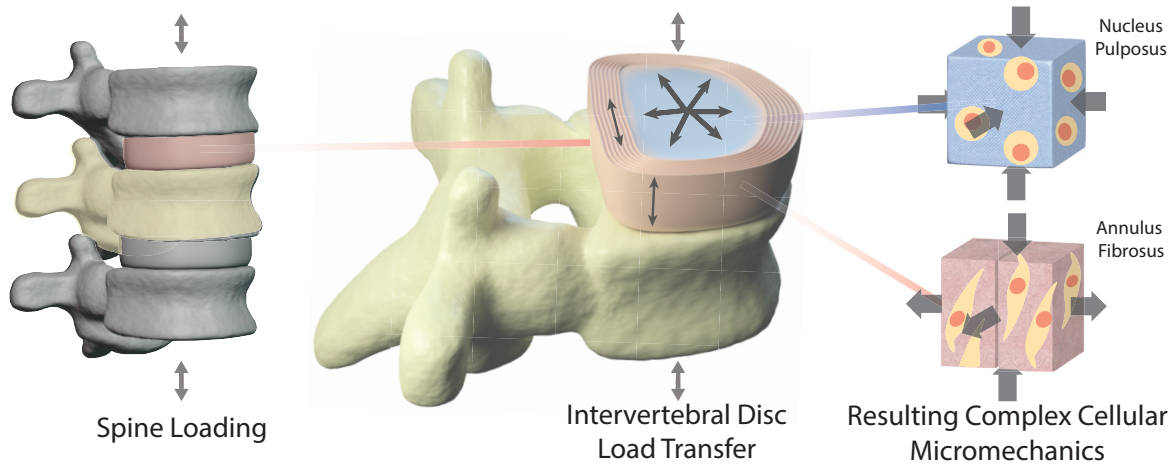


Figure 2.1: This figure demonstrates multiscale loading in the disc. Compressive forces applied at the organ-level results in complex stresses throughout the NP and AF (e.g., radial and circumferential tensile stress), which is experienced by embedded cells. In the healthy disc, the AF experiences both direct axial compression and tensile stresses due to internal pressure from the NP. Despite off-axis loading from supporting trunk muscles while performing daily activities like bending. Two-sided arrows indicate that diurnal loading is often cyclic.

## 2.3 Identified Conditions for Complex Loading

Disc mechanics can be measured at the organ (global level) or tissue scale but needs to be calculated at the cellular or local level using mathematical models (e.g., finite element modeling) or measured with magnetic resonance imaging (MRI).[246, 156] Both micro- and macro-bioreactors offer multiaxial loading with many degrees of freedom to apply complex loads to cells. Mechanical activity at the microscale is referred to as micromechanics, that is, mechanical activity on a small population of cells embedded in a matrix. While this manuscript covers multiscale loading, from loads at the organ scale (e.g., bone-disc-bone motion segment) transferred to the cellular level, it does not cover loads on and within a single cell for brevity and focus. Thus, microfluidics for single-cell manipulation were not included.[98]

Local collagen fiber orientation and matrix composition comprising the extracellular environment mediates load transfer and cell phenotype. Similar to the fibroblasts in tendons, AF cells take on spindle-like shapes and orient along load paths in the direction of highly aligned collagen fibers.[216] NP cells have a rounded morphology due to large hydrostatic pressures applied during diurnal loading and a lack of collagen fibers.[233] *In vitro* studies

have shown that cell phenotype can be altered through mechanical forces which are dictated by the mechanical properties of the surrounding tissue.[118, 219] For example, Work by Bonnevie and coworkers showed that AF cells in rabbits lose spindle-like morphology as they spread and initiate disease progression when prestrain and fiber alignment in the AF is lost because of an injury.[19]

In addition to transferring load, physiologically relevant 3D gels (i.e., engineered matrix) also attract interstitial water, which provides a realistic alternative to the media bath in 2D. Interstitial water (70%-80% of the disc by weight) removes waste and provides nutrients with hydrostatic forces and osmotic pressure gradients. [101, 78] While the disc is healthy, interstitial fluids attracted by the extracellular matrix share compressive loads on the disc at short time scales by way of hydrostatic pressure. When the extracellular matrices of tissues are properly replicated, mechanical load stimulates cells in multiple ways: directly by way of matrix compression and indirectly through fluid movement. Thus, the very presence of a 3D gel which enables interstitial fluid further complicates loading.

Osmolarity also contributes to the micromechanical loading condition, and work by Wuertz and coworkers showed that osmotic loading even has a greater effect on gene expression than mechanical loading.[237, 193] Fluid uptake by the disc is impacted by the surrounding osmotic environment, where hyperosmotic conditions results in lower fluid uptake and an increase in the effective stiffness of the disc joint.[15] Furthermore, the surrounding osmotic environment has been shown to alter fluid uptake by the cell, altering cell membrane stiffness, and altering subsequent tissue production. Healthy NP cells embedded in an agarose hydrogel had greater glycosaminoglycan (GAG) production and thereby improving mechanical properties when cultured in hyper-osmotic conditions.[154, 179, 185] However, dynamic loading also induces fluid movement into and out of the disc, with diurnal loading contributing to fluctuations in water composition up to 25%, which also causes changes in the osmotic microenvironment of disc cells.[163, 105]

Much of the mechanobiological research has been limited to studying the effects of strain magnitude or frequency on 2D cell culture bioreactors (referred to as '2D stretch culture' in this paper). These 2D cell cultures use elastic membranes as substrates and do not replicate physiological loading for several reasons. First, nearly all applied strain is directly transferred from the 2D substrate to the cells (80% Strain Transfer Ratio (STR)), whereas cells *in vivo* (30-65% STR) and in engineered gels experience a much smaller fraction (50% STR for chondrocytes in alginate gels) due to strain attenuation from the surrounding matrix.[73, 117, 85] While a researcher could apply a lower magnitude strain on the 2D substrate to make up the difference in strain transfer the cells would still exhibit counter-intuitive behavior and would produce less matrix. Fibroblasts loaded on a 2D substrate *in vitro* aligned perpendicular to the loading direction, whereas cells in a 3D gel aligned in parallel as expected *in vivo*. [39] In addition, Gruber et al. showed that human AF cells in 3D gels led to more disc-like matrix production (i.e., collagen I and II) than in 2D culture.[81]

Finally, cells themselves apply forces on microenvironments which have been shown to align fibers, change cell morphology, and compact engineered tissues. While this self-assembled loading is an example of complex loading, it is not included as a bioreactor ex-

ample, but rather as a reference for bioreactor design. When embedded in 3D collagen gels shaped like rings about a rigid core (collagen gel contraction assay) cell-mediated gel contraction aligns and elongates the cells and rearranges the collagen to make a more dense ring structure (reduction of area = 80%) with circumferential collagen fibrils.[244, 22] Both the boundary conditions and the presence of fibers is an important element of bioreactor design that directs cell loading in a distributed manner that would be difficult to apply externally. Prearranged fibers acting as cell substrates can also be used in bioreactor design to alter cell orientation and expression of collagen-I in the case of fibroblasts on fibers with large diameters.[59, 248, 141]

## Bioreactors for Comparing Simple and Complex Loading

Many bioreactor studies rely on conventional 2D uniaxial loading conditions, where strain magnitude and frequency are altered. Few studies have evaluated differences between single and multi-loading modalities (e.g., combinations of tension, compression, and/or shear) on cell response and tissue production. Studies that decouple complex mechanical stimuli into its simple components help identify benefits of complex loading with respect to tissue components with relevance to health and integrity, such as GAG content. In the following subsections, we compare simple loading (uniaxial tension) to more complex, multi-axial loading devices in cardiovascular and articular cartilage research to gain insights that can further the disc community in its ability to model complex systems. We specifically looked at these two research areas because cardiovascular vessels can be disc-like with their thick walls which experience cyclic tensile and other strains due to internal pressure, similar to the AF under compression. Furthermore, like the disc, articular cartilage experiences large compressive and shear forces during daily loading. The studies discussed below evaluated loading modalities independently before combining them to assess the impacts from the resulting complex loads. These studies use the simple loading conditions as the control instead of the typical static control.

## Intervertebral Disc Bioreactors

The osmotic environment in the disc is greater and fluctuates more than most tissues in the body.[243] Change in osmolarity, a form of loading due to the forces on cells from swelling, is known to have a large effect on disc gene expression and protein production.[154] The less studied combined effects of osmolarity and mechanical load can be modeled with a custom bioreactor comprised of disc cells seeded in a collagen type I scaffold that can vary osmolarity and control load by way of hydrostatic pressure (0.25 MPa, 0.1 Hz) or cyclic tension (4%, 1Hz).[237] Effects of loading with or without osmotic pressure is studied with respect to aggrecan (i.e., GAG) and collagen II given their importance in attracting water necessary for maintaining osmolarity, nutrient diffusion, structure, and function in the NP as well as the inner AF. Collagen I is also studied, given its load bearing importance in the AF. When osmolarity increased from hypo (300 milliosmoles) to hyperosmolarity (500

milliosmoles) for annulus fibrosus cells, there was more than a three-fold increase in collagen II mRNA and nearly a three-fold increase in aggrecan mRNA. Meanwhile, loading on its own effected collagen II mRNA and aggrecan, but to a much lesser extent. When hyperosmolarity and mechanical loading were combined, Wuertz et al. showed a surprising 20% decrease in human cell collagen I mRNA.[237] The interplay between osmolarity and mechanical loading therefore needs to be considered along with other physiochemical microenvironmental factors when modeling physiologically relevant mechanically active tissues.[149]

## Cardiovascular Bioreactors

Even though discs are for the most part avascular, vascular tissue engineering can provide examples of complex loading that share similarities with loads in the disc.[88] Due to blood flow and fluctuating blood pressure, cells in blood vessel walls withstand multi-directional cyclic strains (axial, circumferential, and radial) combined with shear.[96] These combined forces can be modeled in both macro or micro-bioreactors.[200, 83] A macro-bioreactor for vascular scaffolds which decouples and independently controls shear stress and strain showed that combined loading had a more anabolic synergistic effect on tissue regeneration and inflammation than without.[113] In addition, a custom macro-bioreactor with independent control over fluid-induced shear stress and mechanical strain demonstrated that mesenchymal stem cells (MSCs) produced 75% more collagen when combined complex loads were applied to heart valve scaffolds instead of simple loads.[61]

## Articular Cartilage Bioreactors

Articulating joints can provide additional insights into the comparison between complex loads and simple ones. Bioreactors have been used for maintaining native cartilage tissue composition and mechanical integrity and for improved *de novo* tissue production.[194] Much like the disc, GAGs are important components of articular cartilage, along with collagen. Axial compression is the primary loading condition used for cartilage bioreactors; however, loading that combines compression and shear better replicates repeated loading and sliding experienced while walking or articulating the knee and hip joint.[235, 45] Applying 10% compression strain and 1% shear strain (at 1 Hz for both) simultaneously to engineered cartilage 3D gels resulted in 50% more GAG production, compared to compression alone (collagen production and cell alignment was not analyzed).[170]

The presence of interstitial fluids in 3D gels and *in vivo* tissues alter cell response in the presence of loading, or bulk tissue strain. The application of bulk tissue strain deforms the matrix and increases fluid pressure gradients, interstitial fluid flow, and fluid-induced shear which can stimulate GAG production in chondrocytes.[202] To study only the effects of matrix deformation on cells shear strain was applied to minimize interstitial fluid movement.[68] Shear strain (1-3% at 0.01-1.0 Hz) without the interstitial fluid flow resulted in 50% more protein synthesis and 25% more GAGs in bovine collagen explants from the knee.[104]

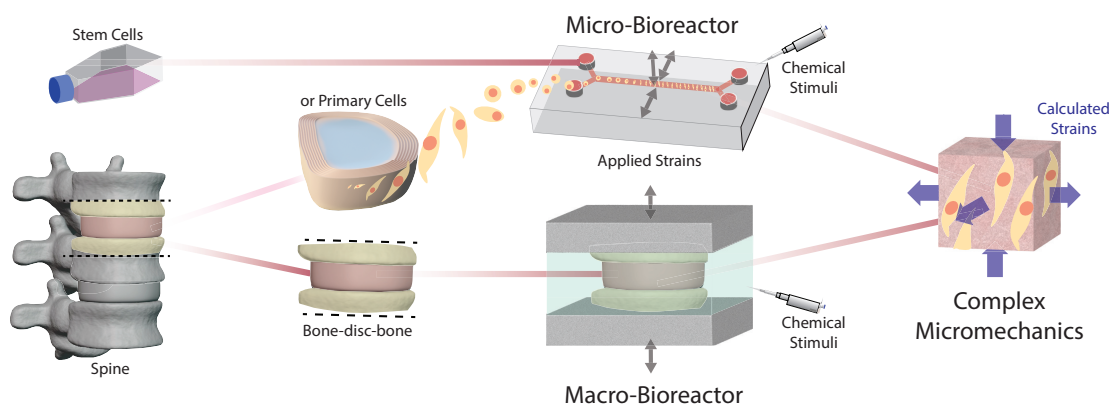


Figure 2.2: Mechanically active bioreactors were categorized as macro-bioreactors that culture entire organs to maintain disc integrity or micro-bioreactors that culture disc cells for tissue engineering. Grey arrows indicate either applied loads, displacements, or strains of known magnitude, direction, and frequency. Blue arrows indicate unknown strains that need to be measured or calculated.

Another articular cartilage bioreactor used a mass (100g) dropped at a height (10 cm) to model injury and the onset of osteoarthritis in response to trauma. The impact was studied with changes in osmolarity or cell volume. Swollen chondrocytes due to hypo-osmotic conditions were more prone to injury/death as measured by a cell injury marker (lactate dehydrogenase) and a cell viability test. Meanwhile, increased osmolarity lead to cell shrinkage, resulting in protection from injury/death.[26]

## 2.4 Macro-Bioreactor or Whole Organ *ex vivo* Systems

Adopted from loaded cell scaffold models, three-dimensional *ex vivo* organ culture models have been used to approximate the loads on the human spine from daily activity by housing large animal discs within reservoirs of media and applying force by way of mechanical testing devices (see the lower half of Fig 2.2).[3] By removing the entire disc from a cadaver and placing it in a mechanically active bioreactor, more control is gained over the mechanical stimulus. With macro-bioreactors, loads can be programmed instead of being based on animal behavior in live animal models. Discs can be used from most species, including human. Alternatively, samples can be engineered to be disc-like constructs using *ex vivo* cells in an artificial scaffold to achieve self-assembled tissue.[3] When provided the right mechanical signal, cells self-assemble their extracellular matrix, organize tissue structure,



increase strength all while restoring cell phenotype or furthering differentiation of MSCs for tissue engineered constructs by increasing cartilage-like gene expression.[213]

No matter the sample, applied loads are typically limited to only uniaxial unconfined compression on the disc, however, when uniaxial strain is applied to a tissue with anisotropic properties and spatial heterogeneity, complex loading occurs at the micromechanical level on the cell. Uniaxial compression was applied statically until 2009 when cyclic loading was applied to ovine discs with intact endplates subjected to malnourishment for upwards of 21 days.[108] A deficient glucose supply led to a decrease in cell viability by more than half, suggesting proper media in addition to cyclic loading is needed for sustained disc culture, at least when the endplates remain intact.

Torsion was added in addition to and in combination with cyclic compression in 2013. Cell viability was maintained above 70% with all loading regimes. However, a strong upregulation of matrix genes and matrix remodeling genes in the most complex loading regime (combined cyclic compression with cyclic torsion) was observed in addition to a change in cell morphology within the NP.[35]

By 2016, additional degrees of freedom were added to a bioreactor to mimic bilateral bending with compression. Cell viability improved over 14 days of culture relative to the unloaded disc. [11] While removal of the bony endplates allows for nutrient flow and limits blood clotting possible in the endplate, devices that apply the most complex loading leave the bony endplates for better load transfer. [34] In these examples, endplates are potted with a polymer which complicates nutrient transport.

## Challenges of Macro-bioreactors

Macro-bioreactors require whole cadaveric human discs. While discs from other species can offer similar biomechanics as human discs, their cellular response deviates with respect to disc pathologies, including the lack of spontaneous disc degeneration.[157, 51] To eliminate the need for whole cadaveric discs, more available human cells could be harvested from patient biopsies before placement in scaffolds. However, without the precise and localized flow of media provided by micro-bioreactors, cell viability can be harmed by poor nutrient transport through macro-sized scaffolds.[37] To maintain cell viability for cellular or cadaveric studies, macro-bioreactors require external heating and gas regulation given a typical size too large for conventional incubators.

In order to achieve proper fixation between the mechanical testing device and the bone to apply the most complex loading types beyond just compression, end plates are carved and potted in hard polymer which forms an artificial endplate.[191] As a result, the healthy nutrient flow through the endplate and into the NP and inner AF is disrupted as if there was endplate calcification as seen in advanced degenerated discs.[99] Without access to capillary beds in the endplates of adjacent vertebral bodies for nutrient and metabolite exchange by way of diffusion (small molecules) and mechanically driven convection (large molecules) the disc is starved of nutrients.[220, 140] To mimic fluid exchange seen *in vivo*, plattens from the

testing equipment and potted sections from the disc can be made porous for partial nutrient diffusion, however, cellular conditions remain disadvantageous.

Meanwhile, a static reservoir of cell media in the bioreactor maintains tissue health and enables the administration of drugs. Of concern when stimulating whole discs is the free swelling of the tissue from changes in osmolarity that occurs outside the spine, which can alter load transfer from the disc to the cells and can change biochemical response including GAG stimulus.[97] This free swelling can be addressed with precise control of annulus fibrosus hydration for accurate physiological mechanics and composition including osmolarity.[231]

While the whole disc provides the most physiologically relevant modeling as far as tissue structure and function, the study of cell response is limited to post test analysis such as histology and gene expression instead of monitoring the cell response throughout the test. Without monitoring, the macro-bioreactor tests tend to run much longer, which can lead to higher risks in contamination and results in lower overall throughput.

## 2.5 Micro-bioreactors or Mechanically Active Microphysiological Systems (Organ-chips)

Micro-bioreactors commonly known as mechanically active microphysiological systems or organ-chips offer more control over nutrient flow, drug delivery and applied strains than conventional cell stretch culture or macro-bioreactor whole organ culture (see the upper half of Fig. 2.2).[65] Micro-bioreactors have micron-sized manufactured structures or channels that can house cells or that can act like capillaries to deliver fluids with precision. In addition, these micro-bioreactors can control microenvironments or micromechanics while providing real-time monitoring with the possibility of single cell resolution. Control can mean precise programmable control of substrate mechanics, fluid forces, or both at the single cellular level.

Organ-chips have multiple use cases from 1) drug discovery, 2) drug dosing/toxicology, to 3) studying the biology of disease, which includes biological mechanisms and related patient specificities that can't be modeled with a mouse. Studying the biology of disease is the first use case which establishes the organ-chip design, dosing and toxicology come later. However, later organ-chip uses like dosing and toxicology are important to keep in mind as they can influence design requirements such as testing throughput.

Rather than use the entire organ, only the most relevant tissue and its functional response are recapitulated.[119] The chosen tissue to model is dependent on the scientific objective at hand, such as the recapitulation of complex diseases like disc degeneration or the mimicry of clinical outcomes with respect to drug efficacy/toxicity.[122]) Functional responses in the disc that are important to recapitulate include spontaneous degeneration, inflammatory response, and tissue remodeling in the presence of complex loading. To recapitulate these responses, a device complete with a chamber of cells (10-1000 cell count) within sight of a microscope that can withstand complex loading and deliver media or therapeutics is needed.[241, 78]

## High Quality Visual, Chemical, and Mechanical Information

Micro-bioreactors provide high quality information by combining visual, chemical, and mechanical results with precise spatial and temporal positioning. Due to optically clear device materials, cells can be monitored visually for cell kinetics or morphology with immunofluorescence staining or dyes. They can also monitor biochemical outcomes on a single or multicellular basis which include PCR-ELISA or qPCR for gene expression.[94] Microfluidics have been utilized for studying the disc, however, these platforms have only recently been mechanically activated.[135] Although some tests like gene expression are destructive, samples can still be monitored if they run in parallel and sacrificed at different time points.

## Highly Customizable Study Design

Microfluidic design offers more study design customization compared to macro-bioreactors. By using similar manufacturing processes for computer chips, instead of a single test for every bench-top mechanical testing machine, an array of devices can be made in just the surface area of a postage stamp. As a result, many devices can be made and tested in parallel to create replicates for greater statistical power. The multitude of devices also enables sensitivity studies across a physiological range for a given variable such as strain magnitude (14-34%).[117]

## Higher Sample Availability

Compared to the whole disc, human IVD cell donations are more frequent given the greater prevalence of procedures that excise disc tissue: biopsies, discectomies, and spine fusion.[237] In addition to greater sample availability, the microscale also means costs are reduced due to less need for reagent. Made in parallel with a multitude of devices in each batch, micro-bioreactors are cheap and dispensable.

## Adapting Existing Micro-bioreactors

Micro-bioreactors have yet to be designed for the intervertebral disc, however, the more common cardiovascular micro-bioreactors could be adapted.[201] Mechanically active micro-bioreactors are a subset of organ-chips which typically rely on pneumatics to deliver strain on a structure or tissue to mimic strains in the body such as the expanding of alveolar sacs.[214, 92] Mechanically active micro-bioreactors are limited for use in the disc and are limited in use for the soft tissue in the musculoskeletal system in general (tendons, articular cartilage, ligaments, connective tissue) which share similarities in terms of cell type, structure, and functionality as the AF.[135] However, the designs presented in the previous section for use in simulating other load bearing tissues like cartilage could be tuned for use in the disc. A good example of a micro-bioreactor in one application tuned for another is the beating heart-on-a-chip by Marsano et al. which applied tensile strain on a 3D hydrogel for modeling the

myocardium before being converted to applying confined compression on articular cartilage-on-a-chip Occhetta et al.[159, 139] The dual compartmentalized pneumatically controlled device chassis remained the same for both applications while the array of hanging posts used to contain the cell laden 3D gel was made rigid to provide full confinement of the cartilage.

## 2.6 Exemplar Micro-bioreactor Devices

Early mechanically active organ-chips used deformable microporous Polydimethylsiloxane (PDMS) membranes as cell substrates to apply strain uniaxially for approximating the mechanics of thin walled tissues such as the balloon-like alveolar sacs undergoing continuous multi-axial strains from breathing.[93, 92] More physiologically relevant biaxial strain was then achieved by using a similar organ-chip by using vacuum-driven actuators on four sides of the membrane instead of only two.[218] To further diversify the mechanobiological applications for this membrane-based mechanically active organ-chip Gizzi et al. accomplished programmable multi-axial loading by independently controlling the four vacuum-driven actuators surrounding the membrane which could create injury related strain concentrations.[74]

While the membrane based devices can apply strains in numerous profiles to test anything from uniform cellular strains to irregular injury-like strains, the tissues stimulated are limited to two dimensions, which limits applicability. In an effort to make *in vitro* studies more translatable, strain complexity applied by mechanically active bioreactors needs to mimic *in vivo* conditions. The following devices demonstrate various forms of applied complex strain with design elements applicable for the disc. For a representative sample of applied complex strain, see Figure 2.3.

### Three-dimensional Unconfined Compression

In 2019, two bioreactors applying complex loads on gels were created. Using pneumatics, Lee et al. built a microfluidic platform to apply varying magnitudes of cyclic load across an array (5×5 separate gels) of hydrogel discs with growth plate chondrocytes.[116] The 3D unconfined compression applied by the device resembled that of macro-bioreactors applying compression in cells in scaffolds without the native tissue except for the precise control of drugs and nutrients.[3] Fluid readily flowed around each disc to wash away waste, distribute nutrients and administer drugs. Discs made of an alginate scaffold for transferring strain to the cells were bonded to a glass plate and remained unconfined. Fluorescent imaging enabled the measurement of strain attenuation similar to that of *in vivo* conditions from device (33.8% compression) to cell (16% compression) by imaging each cell before and after mechanical stimulus. While gene expression was not analyzed, the device was designed to retrieve each disc for downstream analysis.

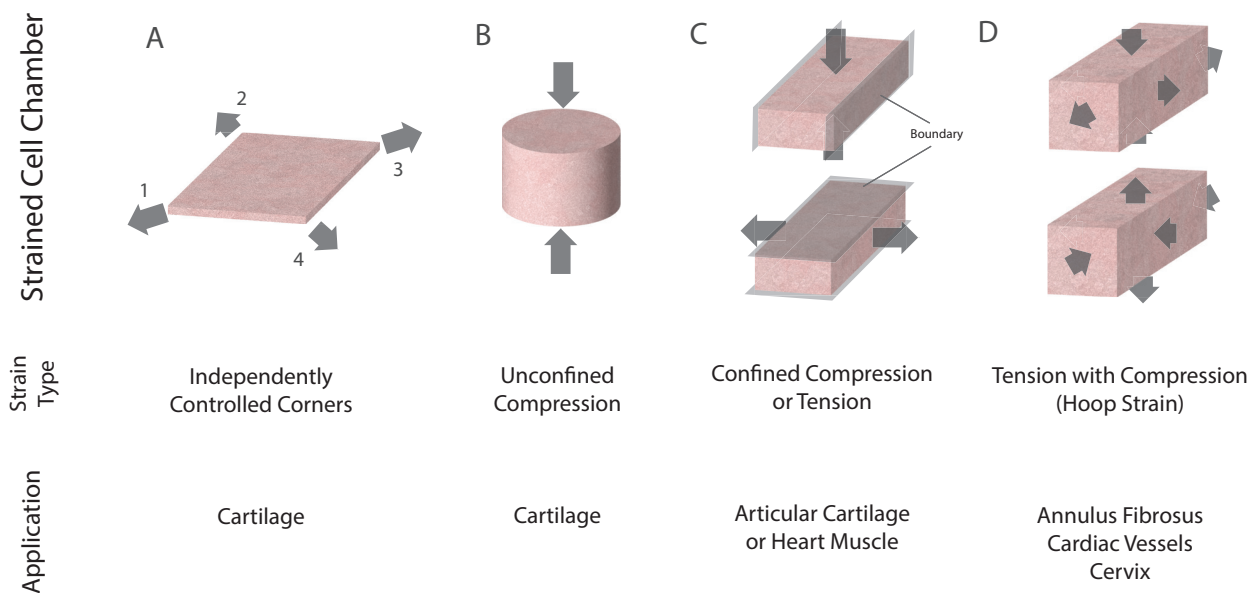


Figure 2.3: Overview of the complex micromechanical environments created by applied strain on cell chambers in micro-bioreactors. Except for the (A) independently controlled cell chamber which is many centimeters in width, each cell chamber is on the order of tens or hundreds of microns tall and wide. (A) While still 2D, a PDMS membrane with independently actuated corners represents a departure from conventional 2D stretch culture that could be programmed to achieve more disc-like strains.[74] (B) Disc shaped cell scaffolds are compressed on top and bottom to achieve complex strain in the interior when walls are unconfined.[117] (C) Unlike most devices with a single strain type, this confined chamber can be strained in tension or compression to achieve complex strain relevant for articular cartilage or heart muscle.[159, 139] (D) Embedded within a cell chamber placed in a bulk PDMS form that is bent, cells experience tension and compression depending on the chamber wall. Tension and compression can be flipped if the device is bent in the opposite direction. Complex strain similar to that applied by hoop strain is relevant for annular structures such as the annulus fibrosus, cardiac vessels or the cervix.[142]

## Three-dimensional Confined Compression

Full confinement of the micro tissue on three sides with a rigid yet deformable fourth side enables the cartilage-on-a-chip to apply uniform strain at hyperphysiological levels (30% compression) on a gel.[159] However, a confined chamber alone would limit the nutrient and metabolite transport. For this reason, undersized gaps in the walls of the cell chamber mimic capillaries as they allow for the flow of media without the extrusion of cells. When hyperphysiological compression is applied, cells exhibit signs of catabolism and inflammation similar to the clinical outcomes of osteoarthritis. The design therefore can be used as a screening tool for patients undergoing therapies. With respect to tuning the device for use in the disc, hyperphysiological compressive loads both static and dynamic also occur in the disc when the diseased condition amplifies strains.[48]

## Three-dimensional Bulk Shear

Three pneumatic chambers were created along the length of a micro tissue made up of chondrocytes embedded in a gel.[164] Each chamber was independently programmed to either be pressurized or to be held under vacuum to achieve compressive strains (5-12%), tensile strains, and a gradient of strains on the tissue. If a pressurized chamber sat adjacent a chamber held under vacuum, bulk shear ( $9.8 \pm 2.9$  milliradians) could also be applied to the tissue which is common in the annulus fibrosus, especially under spinal flexion.[100]

## Three-dimensional Complex Strains: Tension with Compression

In 2022, we developed and implemented the flexing AoC (presented in detail in Chapter 3) as a proof-of-concept design for mimicking complex strains measured in the AF uniformly. Strains were applied uniformly across a large cell chamber (16 mm in length) and designed to accommodate a wide range of strain magnitudes in both tension and compression (-19% to 12%). Instead of the use of pneumatic actuation, complex strains were achieved through geometrical placement within a deformable bulk PDMS device. The cell chamber was kept near one edge of the device to keep all cells within the working distance of a standard microscope. Device capabilities were reported in two bi-axial ratios that describe the entire 3D complex micromechanical engineered environment, which allow future comparisons. The device satisfies the gap in applied mechanical activity capable of both tensile and compressive strains as seen in the hoop stresses of annular tissues like the disc, cervix, and thick-walled blood vessels.

## Challenges of Micro-bioreactors

Until devices are miniaturized and made compatible with existing laboratory robotic handling and imaging systems, the practical complexity of micro-bioreactors outlined below remains a great barrier. As a result, throughput will continue to be a big trade-off for

the higher complexity that enables higher quality modeling necessary for translatability to humans.[165]

## Scaffold Requirements

The required process of cell harvesting for use in micro-bioreactors separates cells from their native extracellular matrix. Each micro-bioreactor therefore requires an engineered scaffold that elicits the desired biological cellular response for self-assembled tissues.[14] The transfer of strain from device to cell via the scaffold is just one of many scaffold characteristics relevant to a mechanically active organ-chip. More than just strain transfer ratio there are numerous additional considerations that affect cell response self-assembly of the tissue and the diffusion of nutrients/cell waste when selecting a scaffold: focal adhesion site density, viscoelasticity, work-ability (on-chip linking/setting/forming/maturing techniques), biocompatibility, type (synthetic/natural/hybrid), fiber inclusion (collagen), biodegradability, and interstitial fluid perfusion.[21] There are several hydrogel scaffolds and techniques that can balance mechanical properties for desired tissue strength and physiologically relevant cell response (low proliferation rates and high GAG secretion), however, these scaffolds have not been standardized.[32, 8] Micro-bioreactor design can compensate for scaffold differences with respect to nutrient diffusion if channels are altered to increase the flow of media resulting in improved diffusion gradients of nutrients, gases, and cell waste.[182] However, micro-bioreactor design depends on strain transfer of hydrogels.

## Imaging Requirements

To determine true mechanical stimulus on the cell despite varying scaffold characteristics, strains need to be measured optically on multiple scales: whole cell strains and device strains.[116] While measuring cellular strains comes with its unique challenges given dependence on time, cell orientation, cell location, cell stiffness, cytoskeleton organization, etc. this measure could more readily compare tissue properties and the true mechanical stimulus to the cells.[229] Alternatively, embedded microbeads could elucidate scaffold strains.[164]

## Complexity from Micro Scaled Devices

Micro-bioreactors are limited to a few thousand cells per device, which is not enough for biochemical and gene expression analysis. Several devices must be pooled for sufficient cell counts to run assays for collagen content and gene expression with ELISA. Alternative methods using amplification (PCR-ELISA) are possible for gene expression analysis, but they add to the complexity of the protocol. A clean room is required for device manufacturing, since the small scale of micro-bioreactors leaves them prone to channel clogging. [209] Once a reusable mold is made using photolithography, devices can be manufactured inexpensively in parallel. Parallel manufacturing increases the number of duplicates needed in case of contamination or manufacturing defects.

## 2.7 Discussion

Between computational, *in vitro*, and animal, there are numerous models that can be used to study minimally invasive therapies on intervertebral discs in the presence of mechanical activity. However, there are few models that can replicate the three-dimensional strain environment in the disc, including micro- and macro-bioreactors. Due to heterogeneous tissue properties, complex mechanical stimulus is applied to cells in the disc even when a uniform uniaxial force is applied in the case of a macro-bioreactor. Resulting nonuniform strain distribution can be seen on strain maps at tissue and cellular scales.[47, 229] While both micro- and macro-bioreactors can apply physiologically relevant complex strain, the control of the microenvironment down to a single cellular level in combination with a highly customizable platform makes micro-bioreactors more promising for studying more than just tissue mechanics but also drug and treatment evaluation.[135]

Both micro- and macro-bioreactors are discussed with respect to their mechanical capabilities (including osmotic loading), however these platforms could also control oxygen levels, pH, access to nutrients, as well as the presence of therapeutics. In this way, these bioreactors of multiple scales offer control of the microenvironment otherwise not possible in small or large animal *in vivo* models. While the bioreactors are less adept at modeling pain or immune response as compared to *in vivo* models, they do provide control over nearly all other relevant characteristics of disc degeneration.[146, 198]

## Future Bioreactor Design Advancements

### Combinations of Micro- and Macro-bioreactor Design Features

Between the *in vitro* micro-bioreactors and the *ex vivo* macro-bioreactors lies an exception to the framework outlined in this manuscript; devices that utilize aspects of both device classes, such as the combination of microfluidics with *ex vivo* discs. As one example, whole discs from mice were placed in perfusion chambers where media for nutrients were precisely controlled with the use of microfluidic channels.[50] Compared to the loose lamella and dead cells in the static group, precise perfusion of nutrients in the disc-on-a-chip maintained a disc structure of dense collagen fibers and cell viability for 21 days. Precise control of fluids past whole organs extended the culture from days to months. Perfusion by way of microfluidics or mesofluidics could be used to eliminate contamination, continuously elute metabolites, and deliver drugs in either micro- or macro-bioreactors.

Our proof-of-concept tests indicate that microfluidics could also be combined with the mechanical testing equipment used by macro-bioreactors to apply compression to whole discs. The whole disc would be replaced by a manufacturer PDMS disc with similar size, shape, and material properties (Young's modulus and Poisson's ratio). Microfluidic channels embedded in a bulk PDMS form could then be actuated if a mechanical tester compressed the entire form. Disc-like material properties, including the NP and the AF, can be achieved by altering the PDMS component ratios of cross linker and matrix.[230] The softer NP PDMS



mix can be poured in the middle of the AF PDMS mix to achieve a disc shape with a soft interior, a more rigid exterior, and a gradient of material properties in between. Higher and more physiologically relevant strains could be achieved if microfluidic channels housing cells were placed in locations within the bulk PDMS disc, representative of the AF, the NP, or the boundary in between. Degeneration could be modeled by adding cuts in the PDMS exterior as if internal disc disruption was present. While adjacent perfusion channels would also experience the actuation, the design of these channels could still allow for fluid control.

### **Active Driven Membranes Replacing External Actuators**

Nearly all micro-bioreactors operate with passive driven membranes in that the membrane deformations within the device are driven by external stimuli by way of hydrostatic pressure, pneumatic pressure, or by way of linkage from a motor. However, there is a new class of materials that use active driven membranes with the use of electromechanically active polymers, piezoelectric or smart polymers.[114] These smart polymers can deform the cell scaffold itself or make dielectric elastomer actuators (DEAs) for a microfluidic device to apply stimulus to the scaffold.[57] These DEAs controlled by cyclic voltage can apply relatively high stress and large strains which can be effective for disease models. The use of smart polymers to stimulate cells has long been studied for simple loading applications, however, the technology is largely unexplored for use in micro-bioreactors that apply complex strain.[44] Costa et al. demonstrated the use of a DEA that has promise in applying complex strains in 3D to cells.[46]

### **Fast Actuation for Modeling Trauma**

An alternative membrane substrate based design was created with a dielectric elastomer actuator (DEA) capable of applying both large tensile (38%) strains and compressive strains (12%) within the same cycle at ultra-high frequencies. High speed actuation enables the modeling of traumatic injuries as well as degeneration from vibration, an occupational hazard for helicopter pilots and truck drivers.[27, 53, 171, 115] Acute high speed and magnitude impacts (30% compression in one second) to the whole human disc have been shown to cause significant cell death, loss of GAGs, damage to aggrecan, neurite sprouting with increased nerve growth factor and cartilage endplate cracking.[5]

### **Multicell Type Modeling**

Healthy discs are isolated from immune and nerve cells until degeneration or an injury disrupts the outer AF tissues and lowers the intradiscal pressure necessary for sheltering the disc from the rest of the body.[208] A multicell type environment is then created when neurons, immunocytes, and vascular endothelial cells enter the injured disc leading to pain, inflammation, and matrix remodeling all of which has been modeled in mice.[197] If equipped with multiple cell types or the byproducts of multiple cell types, micro-bioreactors could offer improved translatability compared to the mouse model. For example, Moy et al. took a

preexisting osteoarthritis joint-on-a-chip perfusion micro-bioreactor and added sensory neurons to provide insight into the nervous system response during joint stimulus.[146, 125] Meanwhile, rather than add immune host cells Hwang et al. achieved a multicell type tissue response with the addition of products from immune cells such as pro-inflammatory cytokines (interleukin IL-1 $\beta$  and tumor necrosis factor-alpha (TNF- $\alpha$ )) important to degenerative cascades.[94] The micro-bioreactor platform allows for the analysis of resulting phenotypic and genotypic changes.

## 2.8 Limitations

Most applied strain considered in this review corresponds with healthy tissues. However, hyperphysiological strains occur in degenerated or injured tissue which can more than double peak strains.[87] In addition, the loading type can switch from tension to compression in the AF with lost NP integrity.[232] Most bioreactors can not switch between tension and compression and have a limitation on maximum applied strain, therefore accounting for hyperphysiological strain greatly complicates bioreactor design.

Scaffold choice should be taken into account with respect to device design. Mechanically active organ-chips or microfluidic devices are typically discussed with respect to the device mechanics but not with respect to the choice of cell scaffold even though it can alter device mechanics with respect to strain transfer to the cells.[31] Additionally, scaffold selection is important considering not all scaffolds are compatible with the model at hand, the cells, or device manufacturing methods.

This review is limited to experimental devices and does not include computational modeling, which more readily enables the study of both the healthy and the degenerate conditions. Ultimately, computational modeling should be used in tandem with bioreactors to fill in gaps of knowledge in experimental work. One such example of an experimental gap modeled computationally is the study of collagen fiber and tissue matrix interactions with or without injury.[247, 151] Fibers are an important element of load bearing soft tissue that are challenging to incorporated in scaffolds for micro-bioreactors.[66]

## Chapter 3

# Design of a Flexing Organ-chip to Model *in situ* Loading of the Intervertebral Disc

Jonathan P. McKinley, Andre R. Montes, Maple N. Wang, Anuya R. Kamath, Gissell Jimenez, Jianhua Lim, Siddharth A. Marathe, Mohammad R. K. Mofrad, and Grace D. O'Connell

This work was published in the Journal of Biomicrofluidics. Given the interchangeability of terms, this work uses the term mechanically active organ-chip instead of micro-bioreactor as previously described in Chapters 1 and 2.

### 3.1 Abstract

The leading cause of disability of all ages worldwide is severe lower back pain. To address this untreated epidemic, further investigation is needed into a main cause for back pain, intervertebral disc degeneration. In particular, microphysiological systems modeling critical tissues in a degenerative disc, like the annulus fibrosus (AF), are needed to investigate the effects of complex multiaxial strains on AF cells. By replicating these mechanobiological effects unique to the AF that are yet understood, we can advance therapies for early-stage degeneration at the cellular level. To this end, we designed, fabricated, and collected proof-of-concept data for a novel microphysiological device called the flexing Annulus-on-a-Chip (AoC). We used computational models and experimental measurements to characterize the device's ability to mimic complex physiologically relevant strains. As a result, these strains proved to be controllable, multi-directional, and uniformly distributed with magnitudes ranging from  $-10$  to  $12\%$  in the axial, radial, and circumferential directions which differ greatly from applied strains possible in uniaxial devices. Furthermore, the AoC evaluated favorably for long-term cell culture by withstanding accelerated life testing (66K cycles of  $10\%$  strain)

and later culturing 2000 bovine AF cells without loading for more than three weeks. Additionally, after strain (3.5% strain for 75 cycles at 0.5 Hz) was applied to a monolayer of AF cells in the AoC, a population remained adhered to the channel with spread morphology. The AoC can also be tailored for other annular structures in the body, such as in cardiovascular vessels, lymphatic vessels, and in the cervix.

## 3.2 Introduction

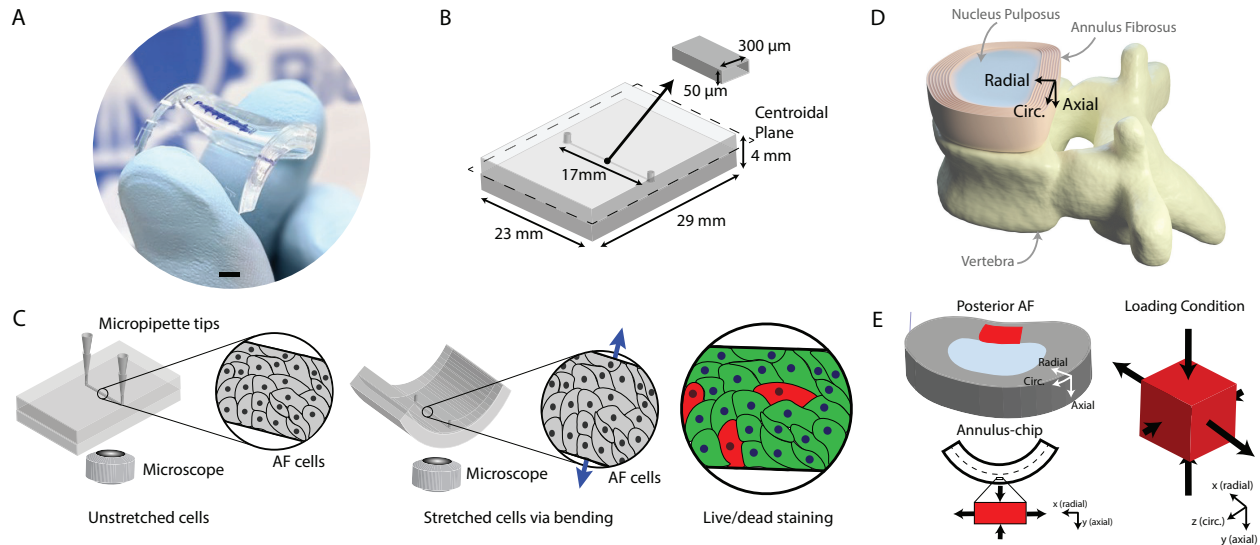


Figure 3.1: (a) The AoC bent by hand to demonstrate the process of applying strain through device deformation. Blue markings in the channel are for reference only. Scale bar: 4 mm. (b) Schematic and dimensions of the AoC including the embedded channel. (c) Schematic showing the process of applying strain to cells in the channel by bending while the channel is imaged from below with an inverted microscope. (d) Schematic of vertebra and disc with positive axial, radial, and circumferential (or hoop) directions labeled. (e) When the posterior AF is under combined flexion, compression, and axial rotation, it assumes a state of strain where the axial and radial strains are inversely proportional and the circumferential strains are minimal and variable in comparison. This strain condition was replicated in the AoC channel when the device is flexed.

Severe lower back pain is the leading cause of disability worldwide. In the United States, lower back pain affects 70-80% of Americans [131, 228, 183] and costs \$100 Billion annually; [111] yet, long-term treatment for lower back pain has been limited. [227] Of those patients with chronic lower back pain, 40% have Internal Disc Disruption (IDD) or damage to the intervertebral disc as part of early disc degeneration. [190] Thus, to address the

back pain epidemic, further investigation is needed into IDD and related intervertebral disc degeneration.

IDD is marked by radial fissures in the annulus fibrosus (AF) which is critical to spine health and function. The AF constrains the nucleus pulposus (NP), increasing intradiscal pressure, which allows the disc to withstand large compressive loads. Tears or fissures to the AF greatly increase internal strains. With additional loading, these tears are at risk of propagating further through the AF and triggering degenerative tissue remodeling. [232, 184, 190, 221, 12, 144, 195, 16, 239] Moderate and severe degeneration has been noted with a decrease in disc height and water content, and increased tissue fibrosis. [156, 175] These changes lead to even greater AF strains and annular fissures, inducing the self-perpetuating degenerative cascade. [224, 177, 225, 90, 1, 85, 240, 195]

The cause of IDD and the degenerative cascade is not well understood due to its multifactorial etiology stemming from both genetics and lifestyle. However, studies have recently pointed to cell-mediated, mechanobiological signaling as a potential initiator. [150, 64] Therefore, cell-based experiments which can model the complex strains specific to the disc are necessary to elucidate the role of disc mechanobiology in the degenerative cascade, thereby enabling drug development for lower back pain or tissue regeneration.

To this end, multiple 2D and 3D cell-straining studies have been conducted to characterize differences in cell signaling between normal and degenerated AF cells. [150, 64, 145] 2D studies impart uniaxial tensile loads on monolayers of AF cells and monitor cellular structure, adhesion, and inflammatory response.[152, 29, 173, 1] Efforts to investigate the effects of compressive loads in 3D microenvironments have focused on culturing AF cells in cell-laden gels, bioreactors, or hydrostatic pressure chambers before analyzing activity due to static or cyclic compression. [145] For each of these 2D and 3D studies, loading magnitude, type, and frequency are controlled, but only applied uniaxially either in compression or in tension. Microphysiological systems, or organ-chips, can model disease progression and repair. They can also apply more complex *in situ* loading modalities as demonstrated with the strain gradient generator for hydrogels created by Hsieh et al.[91] However, the miniaturization of AF complex strains in a microphysiological system has yet to be engineered academically or commercially, despite its relevance in disc degeneration.[199, 7, 214]

While conventional cell stretching studies offer the ability to isolate cell response from applied strain, the applied strains have limited physiological relevance given their over simplified configuration (e.g., uniaxial loading). Tissue-, or organ-culture models promise more physiologically relevant strains, but these approaches are complex and linking the multiaxial loading conditions to corresponding cell responses within a single tissue (e.g., AF within disc organ culture) is challenging. Understanding the link between disc mechanics and cell responses could allow for a more targeted strategy to address *in situ* disease initiation and propagation at the cellular level. Specifically, uncovering the distinctive cellular effects between uniaxial and multiaxial loading types is important because it separates the unique contributions from both loading modalities to mechanobiological factors that potentially initiate the degenerative cascade. Therefore, there is a need for a more complete system that can isolate specific cell responses to loading conditions while maintaining physiological

relevance.

Therefore, the objective of this study is to present a microphysiological tool that can investigate the effects of physiologically relevant stretching of AF cells in 2D and 3D cultures. To achieve this goal, we designed, fabricated and conducted initial testing of a flexing organ-chip that can apply either uniaxial or multiaxial stretching to AF cells secured within a single chamber (Fig. 3.1A-C); we developed our platform to mimic loading conditions applied to AF cells *in situ* by recapitulating proportional strains in the axial, radial, and circumferential directions (Fig. 3.1D). In this proof-of-concept study, we provide preliminary experimental and computational data to demonstrate the feasibility of our system, the flexing Annulus-on-a-Chip (AoC).

The novelty of the AoC lies in the highly physiologically relevant 3D strain made possible by bending an embedded chamber of cells, which better matches observed *in situ* strains in the AF.[214] This unique strain field integrated into a microfluidic platform satisfies an unmet need in intervertebral disc research [135] which will enable new avenues for studying disease progression and regeneration. In other words, by combining the capabilities of a microphysiological system with the mechanical stimulus of an animal model, the AoC impacts intervertebral disc research by providing an improved research tool to study therapies for disc degeneration which can not be studied to the same extent in conventional cell stretching devices. In this manuscript, we focus on highlighting the design work, the impactful intervertebral disc application, and the preliminary biological study behind the novel contribution of the device – complex loading that is physiologically relevant to the AF.

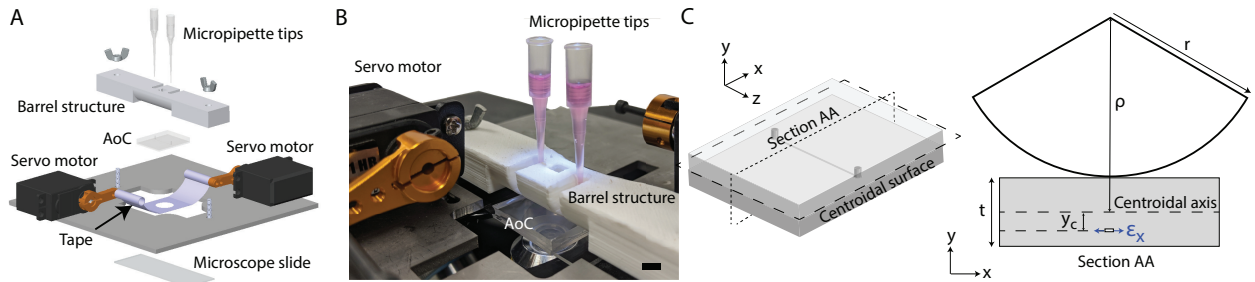


Figure 3.2: (a) Exploded view of the experimental setup in SOLIDWORKS (overall dimensions: 15 cm x 15 cm x 4.4 cm). (b) Representative image of the experimental setup. The AoC was held between a 3D printed barrel structure and a 1 mm thick glass slide placed on top of the microscope stage for imaging. Micropipette tips with equal volumes of cell culture media were plugged into ports at either end of the channel. Polypropylene ‘packing’ tape was used to connect the device to servo motor horns and apply cyclic force on the device. As the servo horns rotated upward in tandem, the tape pulled tight, forcing the device to conform to the 3D printed barrel structure. Scale bar: 4 mm. (c) Cross-section of the AoC with the relevant dimensions to compute the tensile strain,  $\epsilon_x$ , in the channel.

### 3.3 Results and Discussion

#### AF Physiological Strain Analysis to Design the Annulus-on-a-Chip

Strains applied to the intervertebral disc are translated to the AF and NP.[232] Degeneration reduces internal pressure from the NP, increasing the magnitude of AF strains and the prevalence of tears.[82, 155] When designing the AoC, we chose to replicate strains in a degenerated posterior AF [195] because of its susceptibility to tearing and initiating IDD. [190]

Much of the literature on AF mechanics has focused on uniaxial tissue stretching, [82, 158] which applies large tensile strains in one direction and unconstrained contractile strains in the transverse directions due to the cell's Poisson's ratio. In contrast, *in situ* loading with additional boundary conditions results in more complex constraints that may increase the risk of AF tissue failure. [13, 247] For example, under combined flexion, compression, and axial rotation, the posterior AF experiences inversely proportional tensile and contractile strains with low and variable circumferential strains.[155, 13, 7] By considering the strains on an 'engineering element' within the posterior AF we can consider different strain ratios with respect to the orientation commonly used for the disc (e.g., Axial:Radial or Circumferential:Radial strain ratios; Fig. 3.1E). These strain ratios make it possible to translate from whole disc loading of all types on one scale to strain on the smaller scale in the AF.

To create a target for strain orientation and proportionality for the AoC, we analyzed results from Amin et al.[7] which evaluated axial, radial, and circumferential strains during the cyclic application of combined flexion, compression, and axial rotation on 12 degenerated discs (Pfirrmann Grades II-III). We integrated the contributions from each strain direction by calculating strain ratios (axial:radial and circumferential:radial) across these discs at 20,000 cycles. The means and standard deviations were calculated from ratios of averaged strains to provide a physiological relevant strain window for the posterior AF. Circumferential:radial and axial:radial ratios were  $0.05 \pm 0.35$  and  $-0.95 \pm 1.17$ , respectively. The large standard deviations compared to the mean are due to variation in circumferential strain directionality and not from variation in axial or radial strains. Ultimately, the AoC strain ratios were designed to fit within this physiologically relevant window by leveraging bending mechanics.

#### Device Design and Development

Several microfluidic devices have been developed which apply complex strains to cells that are viewable under Brightfield microscopes.[135, 109] While these devices do not replicate the complex strains needed for the AF, their designs were referenced in the development of the AoC.

A device created by Hsieh et al. in 2014, for example, applies complex strains to annular hydrogel structures using unconfined compression.[91] Concentric rings of hydrogel structures mean a gradient of complex strain is achieved. Compression is applied statically for simplicity. In 2019, Lee et al. also used unconfined compression on hydrogel structures but

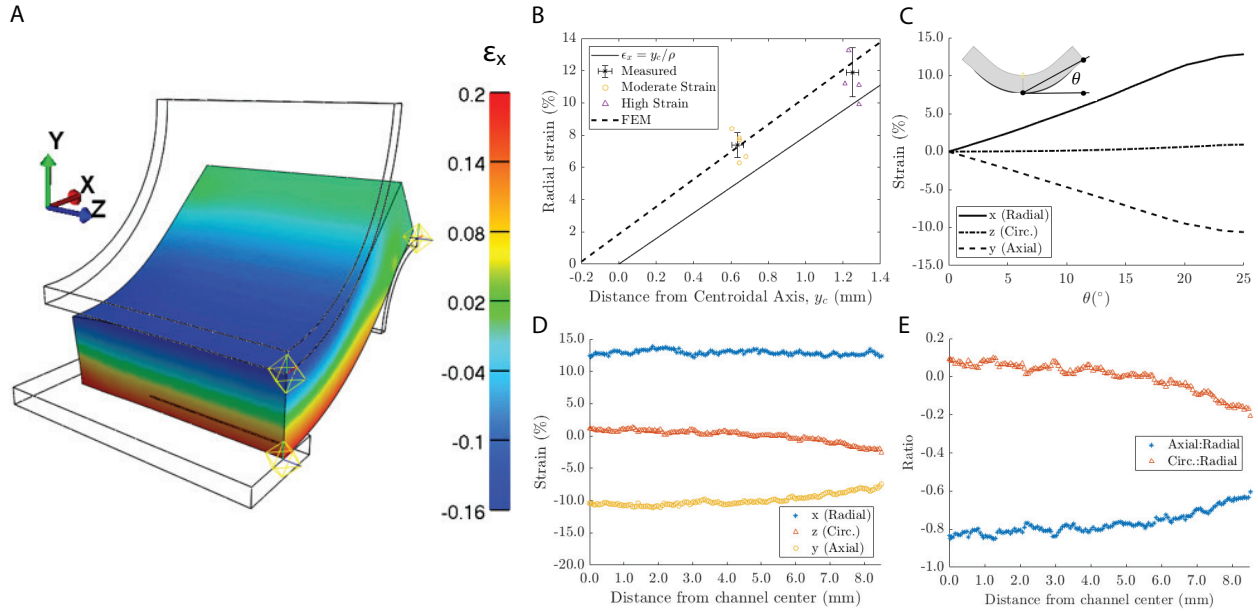


Figure 3.3: (a) Quarter symmetrical color map of strain in the x direction (radial strain) under maximum flexion. (b) Experimentally measured strains (open symbols) are plotted against the beam theory estimation (solid line) and the FE model (dashed line). Based on the model, the centroidal axis was offset from the neutral axis by 0.2 mm (difference in the intersection at the x-axis). (c) Components of 3D strains, including radial, circumferential (circ.), and axial strains, are plotted for the element at the midpoint of the channel as the device is flexed from a flat starting position to a maximum angle based on the curvature of the barrel. Tensile and compressive strains were positive and negative, respectively. Radial, axial, and circ. strains correspond to x, y, and z strains. (d) Strains plotted along the channel demonstrated uniformity in the strain fields applied throughout the channel. Data is presented only for half of the channel due to symmetry. (e) Axial:radial and circumferential:radial strain ratios for the AoC were plotted along the length of the channel.

added dynamic loading to the device.[117] Arranged in an array, these hydrogel structures are cylindrical and can receive various magnitudes of compressive strains. The same year, another form of dynamic complex strain was developed on a cartilage-on-a-chip device by Ochetta et al.[159] This example uses rectangular posts along a 300 micron wide culture chamber to apply confined hyperphysiological compression. The culture chamber enables uniformity of applied strain by minimizing gradients as compared to the unconfined structures.

Upon analysis of these existing microfluidic complex strain devices, overarching design requirements for the AoC were established. The AoC needs a confined chamber like the cartilage-on-a-chip but one subject to bending to accomplish uniform physiological relevant



strain. Like previous devices, the AoC also needs to be observable at all times during loading under a Brightfield microscope. Unlike previous devices, the AoC needs to be operational with or without a hydrogel to enable various types of modeling. Additionally, the AoC needs to be simple in both design and in operation to allow for the easy adoption of existing protocols performed on other microfluidic organ-chip platforms, such as running enzyme-linked immunosorbent assays (ELISA), Western blots, or immunofluorescence imaging necessary for future biological work.

To satisfy these design requirements, the AoC became a deformable, optically clear, mechanically actuated organ-chip device that applies strains to cells through bending (Fig. 3.1A-C). The device was made of elastomeric polydimethylsiloxane (PDMS) with a  $300\ \mu\text{m} \times 50\ \mu\text{m}$  channel created using standard soft lithography methods (further described in Device Fabrication in Methods).

The AF consists of alternating layers of fiber-reinforced tissue called lamellae. The  $300\ \mu\text{m}$  channel width was chosen to approximate the width of one lamella (average lamella thickness =  $420\ \mu\text{m} \pm 60\ \mu\text{m}$  in adults 53–76 years old).[137] The channel height (50 microns) was selected to be several times greater than the diameter of an AF cell ( $\sim 20$  microns). As a result, cells have access to media and can be distributed along the channel length as they flow unobstructed. Meanwhile, the ratio of channel width to height was kept small (6:1) to limit the possibility of channel collapse during manufacturing and testing. FE simulations later showed a 6% decrease in mean channel height at the chip’s maximum flexion state, indicative of no channel collapse.

Lastly, the channel length was chosen to be the longest possible to accommodate the greatest number of cells, minimize differences in strain along its length and fall within known lengths for nutrient diffusion in the AF. The AF relies on diffusion of nutrients and waste primarily through the disc’s cartilaginous endplates given limited peripheral vasculature reaching only the outermost AF lamellae. Diffusion across the endplate alone results in a distance of at least 7 to 8 mm [52] with greater diffusion lengths by the time AF cells at the mid-height of the AF are reached.[156] A half channel length of 8.5 mm, or 8.5 mm from the nearest port, falls within this physiological length for diffusion.

In total, the channel recapitulates a subunit of the AF at a much smaller scale than the whole disc. To account for this smaller scale, *in situ* whole disc loading, which includes a combination of axial and rotational loads, was converted to the multiaxial strains of different ratios (circumferential:radial and axial:radial) to be applied on the channel.

The device applied scalable and uniform strains on the channel when it was flexed over a rigid cylinder, or barrel structure. The design of the cylinder and device thickness were made such that the axial, radial, and circumferential (or hoop) strains (Fig. 3.1D) were scaled to match physiological levels for the outer AF by repositioning the location of the channel through the thickness of the PDMS device. In this design, radial and axial strains correspond to strains in the x and y direction, respectively (Fig. 3.1E). For proof-of-concept testing, we kept the radius of curvature for the barrel constant and adjusted the location of the channel in the device to match strains observed in the posterior AF of degenerated discs. In the future, manufacturing could be simplified such that the channel location remains fixed

while the extent of device bending dictates the applied strain.

Device flexing was achieved by powering servo motors that lift the device’s edges while keeping the channel in the focal plane of the microscope (Fig. 3.2A-B). During device development, the applied strain due to flexion was approximated using beam theory. Tensile radial strain ( $\epsilon_x$ ) was approximated using the device thickness ( $t$ ), barrel radius of curvature ( $r$ ), and the distance between the channel and the neutral axis ( $y_c$ ), which was assumed to be equivalent to the centroidal axis (Fig. 3.2C). Thus, the applied radial strain increased linearly by moving the channel further from the neutral axis (along the negative y-direction) or by decreasing the radius of curvature,  $\rho$ .

$$\epsilon_x = \frac{y_c}{\rho} = \frac{y_c}{r + \frac{t}{2}}$$

Lastly, long-term device durability against cyclic loading was assessed. We applied 10% strain at 0.5 Hz for 66K cycles to represent a week-long cell based study. Cycle count was selected based on daily activity. Rohlmann et al. measured a daily median of 4,400 spine movements (most often in flexion) or  $\sim 30$ K movements each week.[181] To ensure the AoC could withstand this week’s worth of loading cycles, an accelerated life test was performed for more than 2X the expected weekly loading cycles (66K). Visual inspection of the AoC following accelerated life testing showed that the device was durable enough to withstand long-term cell-stretching studies and showed no signs of wear or fracture. The packing tape connecting the device to plastic cylinders connected to the servo motors exhibited subtle wear, but no signs of fracture. Servo motors and the apparatus to anchor each component remained intact.

## Comparing Measured Device Strains to *in situ* Physiological Strains in the AF

To confirm that the AoC could recapitulate the complex strains within the posterior AF, we compared measured device strain ratios to those found in Amin et al.[7] To this end, two sets of five devices were fabricated using the first-order beam theory approximation (see Strain Measurement of Device Channel in Methods). While the device could be designed for higher peak strains (15-20%) as seen in other cell studies, [124, 152, 145, 29] initial device characterization and stretching process development was limited to 5-10% strain based on moderate to high physiological loading within the AF. [145] Measured applied strains in the x direction were  $7.4 \pm 0.8\%$  and  $11.9 \pm 1.5\%$ , respectively. The relatively low standard deviation in the strains indicated that the device fabrication and loading was repeatable and robust.

As expected, measured strains were consistently higher than the first-order approximation. This suggested that a more comprehensive 3D computational model was needed to describe strain fields within the device. Additionally, this model could be used to determine axial and circumferential strains (see Finite Element Modeling and Simulation of Device in Methods), which are difficult to measure experimentally.

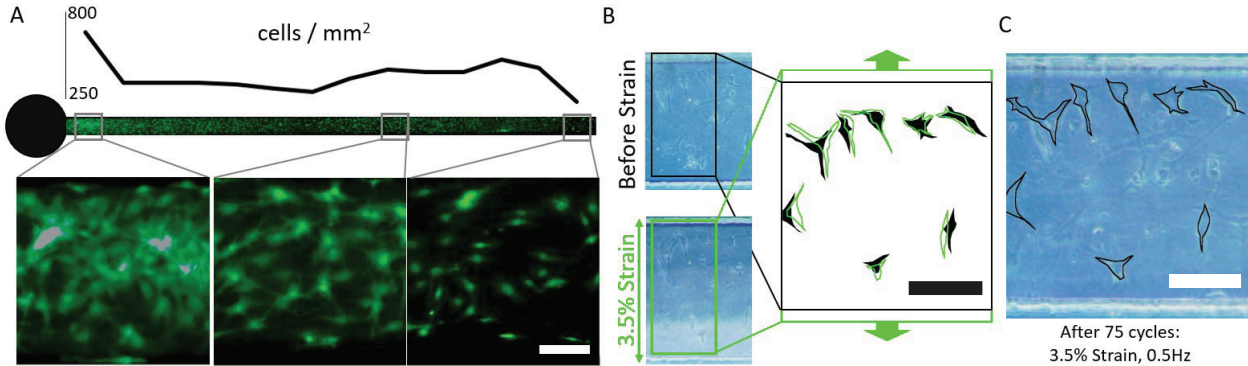


Figure 3.4: (a) Live/dead staining of an AF cell population (nearly 2000 cells/channel) after three weeks of culture. Cell density varied throughout the channel, with the greatest number near the media port (black circle). Scale bar = 100  $\mu\text{m}$ . (b) Cells with sufficient contrast were segmented with polygon selections to compare before and during strain. Scale bar = 100  $\mu\text{m}$ . (c) A Brightfield image was taken after strain was applied to confirm that cells remained attached to the channel for at least an hour after loading. Polygon selections are included to distinguish each cell. Scale bar = 100  $\mu\text{m}$ .

Table 3.1: Comparison of strain ratios in the posterior AF within bone-disc-bone segments under flexion, the AoC, and commercial uniaxial cell stretchers.

	Circumferential:Radial	Axial:Radial
Posterior AF	$0.05 \pm 0.35$ [7]	$-0.95 \pm 1.17$ [7]
Annulus-on-a-Chip	$-0.0025 \pm 0.07$	$-0.77 \pm 0.06$
Uniaxial Cell Stretcher*	n/a	$-0.55$ to $-0.4$ [56]

\*Strex Cell (Strex Inc.)

After modeling the 3D strain magnitude and orientation in the AoC, we calculated strain ratios within the channel to compare to the ratios in posterior AF tissue from degenerated human lumbar bone-disc-bone motion segments under flexion *in situ* (Table 3.1). The standard deviations within the AoC's ratios are due to the variation along the length of the device channel. We considered the AoC as physiologically relevant since the Circumferential:Radial and the Axial:Radial ratios fit within the window of posterior AF ratios. Strain ratios for a conventional PDMS uniaxial cell stretcher were included to illustrate how physiological relevant loads cannot be achieved with a traditional cell stretching method that relies on the Poisson's effect of PDMS.

## Modeling Device Strains with Finite Element Simulation

While strains in the channel were measured optically in one direction (radial), a finite element (FE) analysis was used to verify strain uniformity along the channel and assess strains in the other two directions. FE models were also used to assess strain heterogeneity, which can be used to alter the channel design for maximizing channel size and cell count. We developed models of three device configurations, with target strains of 0%, 5%, and 10% to validate our uniaxial strain measurements and establish the relationship between target strains throughout the bending cycle. We visualized the models' strain in the x-direction (Fig. 3.3A), which was considered to be the 'radial strain' with respect to orientation in the AF (Fig. 3.1E). Strains in the y- and z-directions correspond to axial and circumferential strains, respectively, and are labelled accordingly.

The FE results aligned well with our one-dimensional strain measurements taken under Brightfield microscopy (Fig. 3.3B). We then selected the 'high strain' model (10% target) and varied the bending angle to achieve specific strain magnitudes within the channel. We defined the bending angle as being the angle from beneath the device to its outer edge with respect to the horizontal plane (Fig. 3.3C, inset). For 5% and 10% target strain, the model informed us to apply a bending angle of  $9.8^\circ$  and  $19.2^\circ$ , respectively (Fig. 3.3C). Moreover, due to the linear relationship between strain and bending angle below  $20^\circ$ , we can apply controlled loading sequences of varying strains without varying the channel position. For example, we can alternate between 5% and 10% strain for each consecutive cycle or provide a 5% strain for 100 cycles before transitioning to applying a 10% strain for 100 cycles, and so on. The applied strain began to taper at  $20^\circ$ , which was due to the radius of curvature for the 3D printed barrel. For subsequent loading sequences, we utilized results from the model to modify the servo motor control sequence to ensure that the device applied 10% strain.

The model provided insights into strain uniformity along the channel length. We observed a change in strain and strain ratios towards the ends of the channel (Fig. 3.3D-E). These changes are likely due to the tendency of the device to bend into a hyperbolic paraboloid shape, imposing a unique strain distribution that cannot be estimated with the pure beam bending assumption. The curvature becomes more pronounced towards the edges of the device, resulting in strain deviations at  $\sim 2$  mm away from the center of the device. A more uniform strain distribution may be obtained by redesigning the device with a shorter channel to standardize applied strain along the full length of the channel. Alternatively, the device may be widened, and the channel length maintained to create a uniform strain distribution while avoiding a reduction in cell population within the channel. Using the model, we can iterate on the AoC design and achieve target cell populations and applied strain distributions without the need for extensive lab time or fabrication.

## AF Cell Selection and Culturing

Bovine AF cells were chosen for the AoC proof-of-concept testing due to accessibility and similarities with the human AF cells.[123, 28, 156, 54, 157, 51] Static cell culture media

was chosen instead of continuous flow to mimic AF tissue, which relies more on diffusion of nutrients than convection given its lack of vasculature.[52] To increase the reserve of nutrients without relying on convection, two pipette tips filled with 150  $\mu\text{L}$  of media were placed in each porthole and replaced every third day inside a cell culture hood like other microphysiological system designs. [36]

Prior to strain experiments, we confirmed using live/dead imaging that AF cells could sustain long-duration static culture (3-weeks; Fig. 3.4A) three times longer than required for a typical study. The highest resolution live/dead fluorescent image was captured only on the last day of culture to limit the stress on the cells while the sample was transferred to a microscope in a separate facility. Cells within the channel were found to be clustered near the ports, as expected, but also covered the remainder of the channel floor in a monolayer. The number of living cells neared 2000 without any dead cells. However, it is possible that dead cells were washed from the channel when the live/dead solution was added. Only a few cells were positioned just above the monolayer by adhering to corner surfaces between the channel floor and sidewalls. Seventy percent of manufactured devices were used in the study; the other 30% of manufactured devices were removed from testing primarily because of manufacturing defects, which included delamination of PDMS layers. Bubbles in the channel, a low cell population ( $\sim 300$  cells), and channel occlusion due to cell clumping were other, less frequent reasons to remove devices from testing. Future work will focus on reducing these losses.

The effects of a protein coating on cell adhesion in the channel was considered during chip development. In the channel, fibronectin coated PDMS at various concentrations (0, 0.03, 0.06, 0.125, 0.25, 0.5 mg/mL) were compared to the plasma treated PDMS. Cell adhesion for each treatment was determined by observing the number of cells that adhered in the channel before spreading one hour, one day, three days, and seven days after. As far as cell adhesion and spreading, fibronectin performed similarly to plasma treated PDMS in the channel. While fibronectin may play an important role in cell adhesion in the presence of excessive loading, it was eliminated from the protocol for simplicity at this stage.

We did not design the surface of the PDMS channel to include select areas for cell attachment; thus, cells were able to multiply during the culture period. The cell population was observed multiplying over multiple days using Brightfield images until a high confluency was reached and maintained.

While the cell population of the current design is too low for sufficient RNA yield for gene expression analysis, the device dimensions can be scaled to increase cell population while maintaining similar strain profiles. The devices can also be pooled to accumulate the required number of cells for the analysis.

## Applying Cyclic Load to AF Cells in the Device

To establish the feasibility of the AoC as a platform for studying cell mechanobiology within load-bearing tissues, we seeded the device's microchannel with a sparse population of bovine AF cells (100s of cells) to limit any effects of population size on cellular strain.

While a greater cell density could be used, such that more cell-cell interactions occur, a consistent cell density should be used between treatment groups. We allowed the cells to proliferate for 3 days before applying cyclic loading. A strain of 3.5% at 0.5 Hz for 75 cycles was chosen to represent low physiological loading. [204] We took Brightfield images of the channel before loading, with applied strain, and after the cyclic loading. By processing the Brightfield images with ImageJ, we observed cell deformity and strains in parallel (radial) and perpendicular (circumferential) relative to the channel. Despite the lower resolution (10X objective lens), consistent differences can be seen in annotated Brightfield images of the cells between the strained and unstrained channel (Fig. 3.4B). However, with our initial study looking at cells during chip deformation, we did not observe significant cell migration and the image resolution was not sufficient to track cell deformations. However, we do think that such a system can be used with better imaging facilities to study cell behaviors with loading. An additional Brightfield image was taken after strain was applied to confirm that cells remained adhered to the channel for at least an hour after loading (Fig. 3.4C). Meanwhile, static devices were used as controls to identify changes to cell viability, migration, and morphology due to the cell microenvironment within the chip. Cell migration was observed without mechanical loading, which will need to be considered when measuring cell changes under mechanical load.

## Limitations

The AoC has been proven to be durable and effective at applying physiological strains within 0-10%. However, *in situ* strains in the AF can be hyperphysiological (15-20% and greater).[124, 152, 145, 29, 7] Strains in the 15-20% range are achievable on the AoC by either decreasing the radius of curvature,  $\rho$  or the distance,  $y_c$  (Fig. 3.2C). However, additional long-term cyclic testing is needed to evaluate device durability given these higher strains.

Furthermore, to measure strains accurately, a reference and a deformed image can be acquired using living cell fluorescent staining (e.g., live/dead or f-actin). Digital image correlation can then convert these images to strain maps. While we detected morphological differences in strained versus unstrained bovine AF cells, measuring these differences and converting them to strains maps using digital image correlation remains challenging due to low-contrast images. Ongoing work is focused on establishing high-contrast images which would enable digital image correlation as well as automatic, live-cell segmentation.

It should also be noted, that cell access to nutrients depends on position along the length of the channel, which may play a role in viability as well as response to loads. For this reason, cell position will be taken into account as a possible variable in the future.

Additionally, the throughput in terms of cells and test replicates are limited. For a higher throughput of cells per device, all dimensions can be scaled to increase the volume and surface area of the channel while still creating a similar strain environment. For a higher throughput of tests, multiple devices with the existing dimensions could be placed in an array and actuated simultaneously.

Also, while culturing cells in the current design, pipette tips acting as media reservoirs are open to the air, which increases the possibility of contamination. To mitigate the risk of contamination, barrier pipette tips can be used instead of traditional pipette tips to close off the external environment while still allowing for any changes in pressure.

Lastly, while bovine AF cells were cultured in the AoC channel in a monolayer for proof of concept, 3D cultures and therefore 3D loading conditions have yet to be explored with bovine cells or human cells. Upcoming challenges include introducing and adhering cell-gel constructs within the channel to the PDMS surface, and visualizing 3D strains under microscopy. A gel adds complexity as it limits the diffusion of nutrients, waste, and gas; but this effect can be mitigated by perfusion channels. Tools and techniques exist for addressing each of these concerns as the AoC matures in complexity and capability. Functionalization of the PDMS surface [41, 42] can facilitate the cell-substrate adhesion and ensure proper force transfer from the surface to the construct. Visualizing fluorescent-tagged actin within the cells using confocal microscopy can allow for 3D strain measurements on the cells. Computational modeling can predict the effects of perfusion channel dimensions and spacing on diffusion and loading before upgrades are made to the existing proof-of-concept. This ongoing work is founded upon the present proof-of-concept study to validate the physiological relevancy of the AoC.

## 3.4 Methods

### Device Fabrication

Each AoC device consisted of a 17 mm-long, straight rectangular channel (300  $\mu\text{m}$  by 50  $\mu\text{m}$ ) with circular ports on either end (0.5 mm diameter; Fig. 1B). A mylar photomask printed at 10K dpi was created after designing the channel in AutoCAD (AUTODESK, San Rafael). Standard single-step photolithography was used to create the master mold with a channel comprised of SU-8 (3050) spin coated onto a four-inch silicon wafer at a thickness of 50 microns (first 500 rpm for 10s with 300 rpm/s, then 3300rpm for 30s with 300 rpm/s, Kayaku Advanced Materials, Westborough, MA). The SU-8 was baked for 14 minutes at 95°C before being exposed to 160mJ/cm<sup>2</sup> of UV (Karl Suss MA6) and baking for 4.5 minutes at 95°C. A SU-8 developer was used for 5.5 minutes to develop the partially cured SU-8 on a lab shaker. The SU-8 was then hard baked at 200°C for 30 minutes. By replica molding polydimethylsiloxane (PDMS; Sylgard 184 kit, Dow Chemical, Midland, MI) at a 10:1 ratio of base-to-crosslinker, a slab of PDMS was created with a channel featured on one side.

To achieve a desired thickness, PDMS was poured by weight onto the silicon wafers surrounded by aluminum foil and placed atop a large, leveled hotplate. The thicknesses of both slabs were controlled ( $\pm 0.05$  mm) to dictate the position of the channel. The PDMS layer thicknesses ranged from 0.5 to 3.5 mm, with a constant stacked thickness of 4 mm depending on the desired strain magnitude. PDMS was cured at 60°C overnight on the hotplate before being removed with a razor blade and covered with plastic wrap until further

processing. After punching 0.5 mm diameter ports at either end of the channel, the molded PDMS slab was bonded to a second flat PDMS slab using oxygen plasma. Within seconds of the oxygen plasma treatment (using 70 SCCM oxygen with 21W at 0.6 torr pressure for 30s), the PDMS slabs were pressed lightly together by hand and kept at room temperature. Cells suspended in media, as described below, were added to the channel within 20 minutes of bonding.

## Loading Mechanism and Device Actuation

Readily available components such as Power HD 3001HB servo motors, an Arduino UNO microcontroller, and an external 3A, 5V power supply were chosen for the loading mechanism. These components were secured with fasteners to a base cut from aluminum with a waterjet cutter.

The AoC device was designed to conform to a 3D printed barrel structure fastened to the base, which was anchored to the microscope table. Polypropylene 'packing' tape cradles the device and connects it to servo motor horns with pin joints to flex the AoC against the barrel structure (Fig. 3.2A-B). These pin joints can be made with simple bolts inside plastic cylinders. As the servo horns rotate upward, the tape forces the device to conform to the barrel structure with a radius of 10 mm (designed in SOLIDWORKS and printed with Polylactic acid on a Creality Ender 3 Pro). When the servo horns rotate downward, the device relaxes into a flat configuration. Throughout actuation, the device is fixed between the 3D printed barrel and a standard 1 mm glass slide. Thus, the channel is kept at a constant focal length from the objective lens. Frequency can be controlled between 0.5 Hz to 2 Hz.

A FlexiForce load sensor (Tekscan, Boston, MA) was placed between the glass slide and the device without blocking the viewing port to ensure that the applied pressure was consistent and repeatable during installation and operation. Additionally, reference marks on the 3D printed barrel structure were used to reliably align the device during installation within several microns of the channel center. All loading was applied at room temperature (22°C).

## Strain Measurement of Device Channel

Experimentally, radial strain was measured by imaging the channel before and after bending with a 10X objective lens on an Olympus CKX31 microscope. Images were acquired before and after applied strain and the channel width was measured in the reference and deformed image using an automated script (MATLAB, MathWorks Inc.). Based on beam bending theory, we fabricated five "moderate" and five "high" strain configurations to represent the physiological range of radial strains reported. Therefore, the moderate and high strain groups were set to 5% and 10%, respectively. We optically tracked the motion of the channel walls under Brightfield microscopy and used image processing to measure the applied strain across the channel width (i.e., radial strains). Radial strains were calculated



as engineering strain by dividing the change in channel width during loading by the initial channel width measured in the reference configuration. To assess experimental repeatability, thirty sequential measurements were acquired to assess changes in loading over an extended period of time. This loading sequence was considered to be a single set, which was repeated three times (total of 90 data points) per device to assess repeatability of measurements acquired after uninstalling and reinstalling the AoC.

To confirm that devices could physically withstand extended loading, an accelerated life test was conducted by cyclically loading devices (n=3) for 66K cycles. The devices and the loading mechanism were visually inspected by eye before and after accelerated life testing for signs of wear or crack propagation.

## Finite Element Modeling and Simulation of Device

We used a Neo-Hookean constitutive model to describe the PDMS device because of its non-linear hyperelastic stress-strain behavior. The strain-energy function was defined as:

$$W = \frac{\mu}{2}(I_1 - 3) - \mu \ln J + \frac{\lambda}{2}(\ln J)^2,$$

where  $I_1$  is the first invariant of the right Cauchy-Green deformation tensor,  $\mu$  is the bulk modulus for small deformations,  $\lambda$  is the shear modulus for small deformations, and  $J$  is the determinant of the deformation gradient tensor. [217] Material property calibration was conducted in FEBio Studio 1.3 [133] by modeling a specimen under tension using ASTM D412 standards and data in the literature. [106] The PDMS was calibrated to have an elastic modulus of 1.7 MPa and a Poisson's ratio of 0.49. The constitutive model deviated from the experimental results by 0.2% and 3.4% relative error at the target channel strains of 5% and 10%, respectively.

Models for the AoC were created in SOLIDWORKS (Dassault Systemes) with the channel positioned for three target strain configurations, including 0%, 5%, and 10% radial strain based on beam theory estimations. For these configurations, the channel was placed at 0.00 mm, 0.63 mm, and 1.26 mm below the neutral axis (assumed to be identical to the centroidal axis; Fig. 3.2C), respectively. Each of the three models were imported into FEBio Studio and meshed with 266K first order tetrahedral elements.

For the boundary conditions, we enforced zero-displacement in the direction normal to each symmetry plane of the chip, fixed the rigid barrel and microscope slide in place, and defined sliding contacts between the rigid surfaces and the chip. A y-displacement of 7 mm was applied to the end of the device using a rigid deflector, replicating the function of the tape in a computationally stable manner. This condition forced the device's curvature during the test cycle, starting from when the device begins to bend until it reaches its maximum curvature. Model-predicted device curvature was verified with the experimental setup by overlaying images of the device in the deformed condition with the model output. Strains ( $\epsilon$ ) in the x, y, and z directions corresponding to radial, axial, and circumferential strains, respectively, were evaluated along the length of the channel. Lab-based strain measurements

were limited to a 1.5 mm distance from the channel center, therefore model results were compared at the same location only. A mesh convergence analysis was then conducted for the 10% strain configuration to confirm stability of the model results within the 1.5 mm window. The percent error between the model's prediction and empirical measurements was calculated. 3D strain levels were compared to native AF tissue strains to confirm physiological relevance.

## AF Cell Sourcing

Primary bovine AF cells were obtained by harvesting four discs from a single fresh oxtail (18–24 months old) obtained from the local abattoir. The outer AF was separated from the inner AF and removed from the disc with a scalpel.[4] Outer AF cells, which are made up of only a single cell type, were isolated through an 11-hour digestion with collagenase Type IV (Worthington Biochem) in serum media supplemented with buffers to maintain pH. Isolated cells were expanded in T75 flasks with DMEM supplemented with 10% FBS and 1% penicillin/streptomycin (PS/AM; GIBCO, Texas). At 90% confluency, cells were passaged using 0.05% Trypsin (CORNING, New York). Cells were transferred to the AoC devices between passages 3 to 8.

## AF Cell Culturing in the Device Channel

After bonding the PDMS slabs to create the enclosed channel, the channel was rinsed with 70% ethanol then flushed and kept filled with deionized water. Then, 2.5  $\mu\text{L}$  of suspended cell solution was pipetted into the channel at an approximate concentration of either 2 or 10 million cells/mL. DMEM media supplemented with 20% FBS was used for AoC cultures to enhance cell proliferation. [112] The higher concentration of cells was used to evaluate the highest cell population achievable, while the lower cell concentration (2 million cells/mL) was used for cell segmentation with Brightfield imaging. Being careful not to introduce air bubbles, a droplet of media was added on top of each porthole to limit evaporation in the channel. The device with cells was then incubated in static conditions until AF cells adhered and showed signs of spread morphology (75 minutes).

An additional 300  $\mu\text{L}$  of cell culture media was split between two pipette tips and inserted on either end of the channel to act as reservoirs (VWR 20uL LTS compatible 76323-944). Right before the pipette tips were inserted into the portholes, several microliters of media were pushed to the end of the tip to form a droplet that could form a fluidic connection with the channel without introducing bubbles. Given equal volumes of media in each reservoir, fluid in the channel remained static, which left only diffusion for nutrient and waste transport. All devices were housed in optically clear containers within the incubator, which was kept at 37°C and 5% CO<sub>2</sub>. Fresh media was added every third day by replacing the pipette tips with new ones and refilling them with new media. Convection of cell media occurs if the device is tilted for an extended period of time due to a differential in media height between pipette tips. For this reason, the devices were held and stored flat.

Prior to applying cyclic loading, devices which presented the following were removed from the study: bubbles within the channel, channels with fewer than  $\sim 300$  cells, clumps of cell occluding the channel, delamination of PDMS layers, or contamination. Just prior to loading, the chip itself and loading device surfaces in contact with the chip were wiped with 70% ethanol.

## AF Cell Cyclic Loading

For initial testing with the AoC, mechanical loading was performed outside an incubator at room temperature (22°C). Devices were loaded for a total of 75 cycles with 3.5% engineering strain at 0.5 Hz as a physiologically relevant proof-of-concept. For initial studies, we chose a low level of physiological strain to ensure cell damage or detachment did not occur. We also chose a low cycle count to limit any adverse effects on cell health due to loading at room temperature (loading time  $\leq 5$  minutes, based on the average time for changing media). Further tests are needed to better understand the impact of longer duration testing at room temperature (i.e.,  $> 5$  minutes). However, the loading platform is small (15cm x 15cm x 4.4cm) enough that the entire device could be placed in the incubator for longer duration testing. Pipette tips with reservoirs of media were left plugged in during loading. Brightfield images of the cells in the channel were acquired before, during, and immediately following loading. These images were then processed using ImageJ.

## Image Processing and Preliminary Analysis

Using the lower concentration of 2 million cells/mL, cells were cultured within the channel for cell segmentation. Brightfield images of nine cells before strain and after strain within the channel were imported into ImageJ. Using custom polygons, we traced cells in images acquired before, after and during stretching to demonstrate our ability to segment cells without fluorescent markers.

## Long-term *in vitro* Cell Viability

Cell viability was evaluated at three weeks for the long-term cell culture study using the Live/Dead Viability/Cytotoxicity kit for mammalian cells using the manufacturer's instructions (Live/Dead Life Technologies Corporation, Eugene, Oregon). Rather than flush the channel, the live/dead solution was fed into the channel with gravity to minimize shear forces using a 10 $\mu$ L pipette tip with 5 $\mu$ L of live/dead solution. After a 30-minute incubation, the first pipette tip was removed and a second larger (20 $\mu$ L) pipette tip filled with phosphate buffered saline (PBS) was inserted. PBS remained in the channel throughout imaging.

## Chapter 4

# Impactful Design for Pandemic Response

In early February 2020 cases of COVID-19 were increasing rapidly for the first time on the East Coast of the United States. Personal Protective Equipment (PPE) supplies were limited throughout the country but were especially limited for hospitals beyond the cities in areas designated as rural by the US Census Bureau. Healthcare settings in these rural communities couldn't expect resupply of PPE and other disposables when bidding against large organizations and governments in the midst of an inflated global demand without the capacity for increased supply. It was reasonably assumed that most supplies purchased at a state or federal level would go to the cities first, given the greater population densities.

In a desperate effort to cope with undersupply, the best available alternatives were sought out; healthcare officials in rural settings were seen purchasing protective gear intended for other professions, such as painters or firefighters. Upon realizing that alternative forms of protection were not a reliable option, new strategies for extending the PPE lifespan of conventionally disposable products were needed. In a brainstorming meeting with a healthcare official, the need for decontamination was raised for all PPE but especially the most valuable and hardest to come by in the face of the respiratory illness, N95 respirators. At this time, the Centers for Disease Control and Prevention (CDC) recommended that N95 respirators should only be used once per patient, per visit. However, healthcare workers were given only a few per week.

These discussions began mid-March, design work commenced March 27th, 2020. What began as a solo design effort grew to eighteen volunteers brought together by their desire to shape the outcome of the pandemic in any way possible. The following chapter details the design of equipment for safely extending stockpiles of N95 respirators. Design decisions were based on the knowledge base of SARS-CoV-2 at the time. Because relevant information was updated weekly or even daily, many of the sources in this chapter are online articles or published government pamphlets instead of peer-reviewed journal articles.

Standards for properly using respirators and techniques for decontaminating respirators were rapidly changing and continued to change well after the work in this chapter was com-

pleted. Had this work been completed a mere six months later, design decisions would be greatly altered. For example, had the CDC recommended in March 2020 the use of respirators for the entire day instead of only for one patient or had they recommended that respirators be placed in a cool dry place in a paper bag and left for five days, the need for rapid design and engineering for decontamination likely would have been much less. Additionally, a different method of decontamination would have been chosen from the beginning of the design effort had the CDC determined earlier that respirator 'decontamination' needed to be 4-log reduction (viruses and bacteria) or better instead of 3-log reduction or better which is the effectiveness of the chosen Ultraviolet-C (UVC) technology.[63] Note that based on the timing of this work the chapter uses the term decontamination as a descriptor instead of the correct terminology bioburden reduction. With information and government recommendations shifting with each new week and with supply chain shortages, rapid and agile design strategies were necessary for impactful design.

Parts of this work were submitted to the MIT Solve competition designed for tackling pandemic related health problems, and submitted to the Emergency Medicine Foundation's call for COVID-19 research. In the following chapter, the terms mask or respirator have been used to refer to N95 respirators also known as filtering facepiece respirators (FFRs) instead of surgical masks or face masks.

## 4.1 Introduction

The US Department of Health and Human services estimates that 3.5 Billion N95 respirators or masks were needed in the US alone to fight an extended pandemic. However, only 1% of those needed were expected to be available due to global supply chain limitations.[134] The shortage of essential PPE created a market for underperforming counterfeit respirators and sparked price gouging for approved N95 respirators (prices increased 4X in some cases).[160] Disparities arose as N95 masks became prohibitively expensive for financially limited hospitals in rural settings which serve 20% of the US population.[25] While large scale government funded solutions for N95 respirator decontamination were erected near major cities, these solutions were limited in range and did not address the needs of small hospitals in rural areas.[178] The American Nursing Association found that 79% of 14,000 nurses surveyed did not have access to proper N95 masks for preventing airborne transmission.[75] These PPE shortages put nurses at an increased risk of contracting COVID-19 and other illnesses.

I led a team of engineers that partnered with medical providers across several states on the East Coast to develop Ultraviolet Germicidal Irradiation (UVGI) decontamination systems designed to address challenges specific to small hospitals and healthcare clinics due to PPE disparities.[161] Direct clinical feedback after each design iteration led to a novel open source UVC decontamination system that could handle the needs of a small healthcare facility at low-cost (UVC Blaster Mini in Fig. 4.1 and UVC Blaster XL in Fig. 4.2). The design was robust to supply chain issues, could ship easily, was safe, effective, and easy to use. The details of the final design outcome rather than the many design iterations are presented

in this chapter under Results and Discussion. Note that the design principles were similar between the Mini and the XL, so the Mini is highlighted while the XL is only included as a reference at several points in this chapter.

The overall UVC Blaster Mini design was based on protocols from the University of Chicago and the University of Nebraska Medical Center. The latest design iteration presented was considered successful, having met the following key metrics determined through research oriented collaboration with healthcare providers on the East Coast: 1) respirator treatment time [3-12 min] 2) respirator throughput [30-170 respirators/hour] 3) respirator dose [1 J/cm<sup>2</sup>] 4) effectiveness [99.9% reduction or 3-log reduction of pathogens].[148]

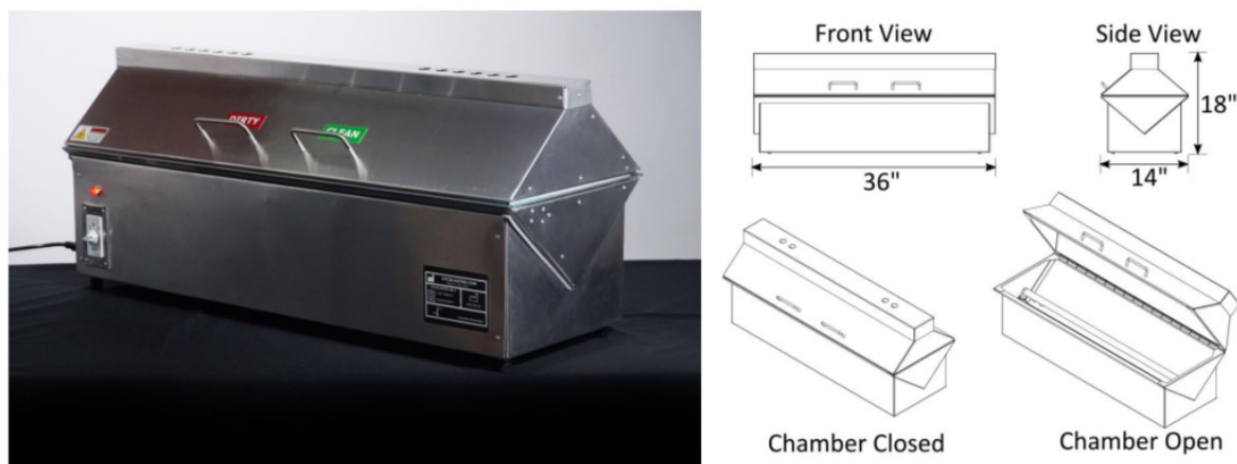


Figure 4.1: Made from readily available parts, the UVC Blaster Mini required  $< 4ft^2$  in bench space and could process five N95 respirators in ten minutes or less. (30 N95 Respirators / hour) This system processes the front and back of the respirator simultaneously. A UVC Blaster with higher capacity but greater cost was also designed.

## 4.2 Results and Discussion

The target setting was small to medium-sized hospitals that could not buy respirators at the premium they were being sold for on the superheated global market. These healthcare facilities needed low initial cost and low operating cost devices. Aided by a leading emergency physician at a time when firsthand access was restricted, the nonprofit organization Collaborative Education of Maine provided insight into the needs of frontline health workers and healthcare providers in these underserved healthcare settings across New England. Collaborative Education of Maine conducted tests in simulated clinical settings to optimize the design, calibration, and protocols and to determine key performance metrics for the UVC Blasters. Findings from these initial tests were incorporated into early versions of UVC



Figure 4.2: Iterative design resulted in two UVC Blasters models, depending on cost and throughput. The UVC Blaster Mini was designed to sit on a cart or benchtop while the UVC Blaster XL could either sit on a benchtop or be built into a temporary wall in order to separate clean and dirty zones in a hospital.

Blaster Mini with the intention of scaling for immediate use globally. The UVC Blaster Mini was designed to process the estimated total respirators needed per day to operate a small hospital, based on figures from the National Center for Immunization and Respiratory Disease. The UVC Blaster XL meanwhile was intended for medium-sized hospitals. It was determined, that given one new or treated respirator per patient, 700 respirators per day were needed for intensive care unit patients, general patients, outpatient health workers, and emergency service personnel. However, its low cost and small size allowed the UVC Blaster to be placed at the point-of-care in emergency departments, fire stations, police stations, nursing homes, hospices, prisons, dental offices, outpatient clinics, and other high risk locations. In addition, these low-cost point-of-care devices could be placed in several locations within a single hospital to keep a safe supply of N95 respirators close at hand in order to avoid contamination between clinics or contamination when shipping to a central location.

## User Needs

University of Chicago and the University of Nebraska Medical Center proved the usefulness of the UVC to treat respirators by developing decontamination protocols. Meanwhile, groups like Thor Labs, Mass General Hospital, and UVConcepts developed UVC decontamination prototypes that built these protocols into useful devices aimed at helping specific markets. Unlike competitors, the UVC Blaster was designed with a product-market fit for rural and low-income communities from the beginning. Therefore, all costs were considered, including cost of shipping, maintenance, required PPE, required space, and required personnel. As a result, the UVC Blaster Mini was the first hospital grade UVC decontamination device that completely addressed all needs of small hospitals such as proper UVC dosing, throughput, simplified training, decontamination time, and price point. The device cost less than \$5K, was capable of extending stockpiles at least 3X, and kept users safe and effective even if they hadn't been trained fully. Lastly, viral and bacterial inactivation was at least 99.9% (3-log reduction) effective (see Fig. 4.3).

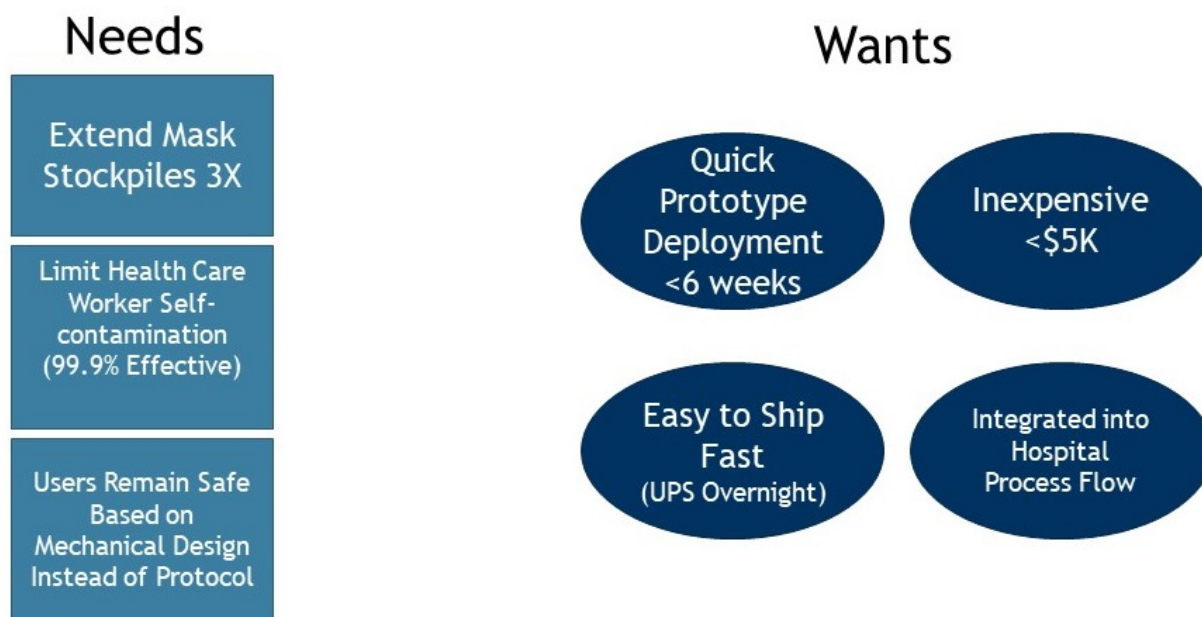


Figure 4.3: User needs and wants were defined in collaboration with rural community health-care workers.



## Decontamination Method Selection

After the Journal of American Medical Associations called for ideas to decontaminate PPE, including the many models of N95 respirators, numerous research institutes got involved. Duke University trialed vapor phase hydrogen peroxide respirator decontamination. Stanford considered various methods, including the use of steam. The University of Nebraska Medical Center trialed the use of UVC for the same purpose on-site. Except for Battelle's large-scale (10,000s of respirators) off-site method of decontaminating respirators in a shipping container with vapor phase hydrogen peroxide, all other devices remained in the prototyping phase and were yet to get FDA approved for an Emergency Use Authorization. While Battelle's system was promising for city-based hospitals, the method of decontamination was not accessible in rural locations nor was a feasible to replicate given the high cost of manufacturing and operation due to complex operating logistics. Due to the intended rural and low income/underserved community hospital use case, the decontamination method needed to be inexpensive, easy to ship, easy to operate, and non-hazardous.

The decontamination method was selected after determining the user needs. The basic requirement at the beginning of the pandemic was to be more effective than simply setting aside used N95 respirators in breathable bags until the virus was less active, an uncontrollable process extremely sensitive to initial viral load, storage temperature, and humidity (5-7 days, (22°C, 40–65% humidity).[148] Other proposed methods of decontamination included dry heat (70°C for 60 minutes), steam (70°C at 50-85% humidity for 60 minutes), hydrogen peroxide vapor (inactivates mold and bacteria present from respirator use in addition to SARS-CoV-2), and UVC (1.0J/cm<sup>2</sup>). Each protocol maintains respirator integrity and functionality after decontamination, except heat treatments above 100 degrees Celsius, which alter waterproofing in some respirators and drive filtration performance down in many. Of these methods, the level of effectiveness, the cost, and the fact it did not degrade the masks made UVC the most promising. UVC was also selected given beneficial attributes for rural hospital settings: point-of-care, minimal cost to the operate, minimal startup cost, high treatment speed, high user safety, ease of use, and portability for quick shipping/deploying. s factors in addition to treatment effectiveness and wear on the respirator.

Even though UVC was known to degrade polypropylene fibers overtime, in N95 filters and degrade the elastic band on the respirator straps, limited reuse would limit degradation. UVC also had tradeoffs to consider depending on respirator model and respirator orientation. Even though UVC decontaminates only by line-of-sight, internal layers of fabrics like the non-woven polypropylene used as the filter on respirators could still be treated. These fabrics attenuate rather than block UVC light, which means even internal layers could still be treated for pathogens with a long enough exposure. However, twisted straps that block the light would not be treated. In general, however, as long as a critical dose of UVC (1.0J/cm<sup>2</sup>) was achieved, studies indicated a high effectiveness against pathogens. Testing later in the pandemic determined that SARS-CoV-2 could be inactivated with as little as 16.9 mJ/cm<sup>2</sup> of UVC depending on the surface.[17]) In the end, UVC with 70% isopropanol / 30% deionized water for shadowed surfaces such as N95 plastic release valves and respirator straps would

be the most preferred decontamination strategy.

Protocols for UVC decontamination of N95 respirators were developed by the University of Nebraska and others using equipment such as the Surfacide Helios System and the ClorDiSys UVGI Light System, however, these systems were prohibitively expensive and were not designed specifically to treat N95 respirators.[80] UVC at 254 nm wavelength is a leading source of decontamination for smaller applications given its preservation of respirator function, lack of chemical residue, safety to the device user, low cost, potential high throughput as well as its antimicrobial efficacy on N95 respirators of at least 99.9% for Influenza A (H1N1), Avian influenza A virus (H5N1), MERS-CoV, SARS-CoV, and others. For these reasons, the CDC recommended that individual hospitals should investigate this technology.[174, 189] The UVC decontamination chamber addresses the technological challenges of providing safe and consistent treatment of N95 respirators. It is worth noting that UVC, like all forms of treatment, reduces the number of pathogens on the device, but does not eliminate them completely. For this reason, the decontamination device would be used to supplement existing PPE reprocessing practices and would not be intended as a replacement or modification of PPE use practices.

## Device Design and Development

Our system was a new application of the previously existing low pressure UVC lamps typically used in hospital settings for decontaminating entire rooms. The UVC lamps were designed to convert energy into 254 nm light, as this is a wavelength found to disrupt RNA and DNA in pathogens (see Fig. 4.9). With proper controls, exposure to UVC preserves respirator function, lacks chemical residue, is safe for the device user, is low-cost, can be point-of-care and can be high throughput. Having determined the method of decontamination, the design efforts were then challenged by unprecedented supply chain issues. As a result, the designs were constrained to off-the-shelf parts available at standard home improvement stores, except for the UVC bulbs and electronics. Just as there were shortages of PPE, there were shortages of UVC lamps. However, the UVC Blaster was designed to limit the required number of lamps by increasing their efficiency, described under the subsection UVC Dose Optimization.

The UVC Blaster Mini utilized two low pressure UVC bulbs (Tropical Marine HF Pro 55 Watts HO G55T8, 894mm long, 28 mm in diameter, 253.7 nm peak UV output, 86 Volts, 9,000 hour rating) mounted with standard bulb tombstones (Leviton 660 Watt, Medium G13 Base, Bi-Pin-Low-Profile) which could be readily sourced during a pandemic, even with disrupted supply chains. The most difficult component to source was the electronic ballasts (HEP SI254-58, 110 Watts) that were capable of controlling two bulbs at once. As a point-of-care device, the UVC Blaster Mini was built for high space efficiency (8 ft by 2 ft benchtop space) and required minimal training, minimal additional PPE, and minimal maintenance. As the heaviest components of the device, the ballasts were concealed in a secondary chamber at the bottom to prevent tipping. In addition, rubber bumpers (Rubber, 5/8 inch Outer Diameter, 1/2 inch Tall) were used as feet to prevent the device from sliding.

Instead of expensive machined parts, the UVC Blaster was made from sheet aluminum (0.032 inch Flat Sheet, 5052-H32 48 inch X 96 inch) that could be cut by hand, laser cut or water jetted before being bent and riveted (Aluminum Blind with Steel Mandrel, Domed Head, 1/8" Diameter) together. While rivets were used to permanently fasten sheets of aluminum, rivet nuts (Hilitchi 8-32, UNC Rivnut) were used to provide threads in the sheet metal to enable service access to different compartments of the device at a later date.

The tray within the device was designed to handle more than just respirators in the event that healthcare workers needed to treat personal items like electronics.

## Design for User Safety

Designs were created to guarantee user safety and respirator treatment even in the worst case of equipment malfunction or breach of protocol. Additionally, the design is based on the assumption that operators have limited training. Safety warnings explaining that UVC is a carcinogen were included on the device itself and in the user manual (see Fig. 4.4 and Fig. 4.5).

While proper PPE such as eyewear, gloves, and total coverage of the skin was required, the design of the device assumed PPE was not in use. This meant all gaps in the device panels that could let UVC light out were covered in aluminum tape. Also, the bulbs were tied to a switch (Hinge Roller Lever Microswitch, 15A, 250V) on the lid, such that only when the lid was closed would the bulbs turn on.

The device was designed to operate using a standard wall outlet (110–240V, 6A, 50/60 Hz). A ceramic-tube fuse (10A, 250V AC), a master on/off switch (Two Position Two Terminal Toggle Switch, SPST-NO, 6A), and a large red indicator light (Oil-Resistant Domed, Panel Light with Screw Terminals, 120V AC/120V DC, Red) were included to safely shut off the device. A box fan (DC axial ball bearing, 12V, 200 cubic feet / minute, 60 decibels, 120 × 120 × 38 mm), fan motor controller (Onyehn 12v 2A 30 Watt, DC Adjustable Motor Speed Controller, PWM 1803BK 1803B) and a power supply (Chanzon 12V 5A 60W AC to DC Power Supply Adapter) were built into the device to keep the chamber at a steady temperature to extend the lifespan of the bulbs and to maintain bulb UVC output which was dictated by temperature. A HEPA filter (MERV 13, 12 inch x 12 inch) was designed in line with the fan to limit the transmission of any contaminants from the exhausted air to the room housing the device. One-inch holes were created in strategic locations in the main chamber to direct air past the bulb bases and not past the respirators.

The UVC Blaster XL was designed to be inserted into the cutout of a wall or built into a temporary wall that divides a clean room from a contaminated zone in a clinical setting (see Fig. 4.2 and Fig. 4.6). Using double drawer slides (14 inch Full Extension Side Mount, Ball Bearing, Soft Close), the tray could be pushed entirely through the wall after treatment. For greater simplicity, the UVC Blaster Mini had two distinct handles labeled 'clean' and 'dirty' to indicate which handle was (Fig. 4.6) for reloading (dirty) the device and which one was for unloading (clean), without requiring a change of gloves. However, no mechanical system



#### Potential Risks of UV Exposure

Potential Risks of UV Exposure: **UVC is a carcinogen to human skin and eyes.** Safety recommendations with UVC include protecting skin and the eyes. Operators and bystanders must wear safety glasses, and cover all skin.



Potential Risks of exposure to ozone and other volatile organic compound exposure: **Ozone can lead to loss of lung function and irritation of some tissues.** This device produces ozone as a byproduct of UVC generation. This device uses bulbs that have a special quartz glass designed to block UV frequencies that produce ozone. However it is still best practice to use this device in a well ventilated area.

#### LIMITATION OF LIABILITY

The disposal and / or emission of substances used in connection with this device may be governed by various local regulations. Familiarization and compliance with any such regulation are the sole responsibility of the users of the cabinet.



Figure 4.4: In addition to preventing risks through engineering design, potential risks were displayed in the user manual as well as on the device itself.

kept the user from touching the clean handle with a dirty glove, which limits the fail-safety value.

## UVC Dose Optimization

UVC shadows can be minimized if surfaces have even partial UVC reflectance. Polished aluminum was chosen for its high UVC reflectance among common materials that were also easy to work with (bending, forming, and cleaning).[60] To further increase reflectivity, expanded polytetrafluoroethylene (ePTFE) with near perfect UVC reflectivity (95% or better) was placed on many inside surfaces of the chamber so that UVC light not absorbed by the respirator would reflect off the chamber walls and hit the respirator at different angles with minimal loss in intensity (see Fig. 4.7). In this way, most surfaces on the respirator could be

## SAFETY WARNINGS


- Read all instructions before proceeding and observe the installation procedure and environmental/electrical requirements.
- Anyone working with, on or around this equipment should read this manual. Failure to read, understand and follow the instructions given in this documentation may result in damage to the unit, injury to operating personnel, and / or poor equipment performance.
- Any internal adjustment, modification or maintenance to this equipment must be undertaken by qualified service personnel.
- Before you proceed, you should thoroughly understand the installation procedures and take note of the environmental/electrical requirements of the cabinet.
- In this manual, important safety related points will be marked with this symbol. 
- If the equipment is used in a manner not specified by this manual, the protection provided by this equipment may be impaired.
- Respirators should be decontaminated only twice.
- The bulbs in this device are most efficient when operating at the correct temperature range. Operate this device in an environment that has been temperature controlled to 65-72F (18-22C)
- **This is not an FDA cleared device and is to be used during the COVID-19 Public Health Emergency**

Figure 4.5: The device was created to be safe by mechanical design instead of safe by protocol. However, safety warnings were displayed in the user manual to add a layer of safety for the user.

treated even if respirator straps were twisted, thus treating pathogens that could harbor in folds and behind fibers. Additionally, the irradiance of UVC increases, meaning the overall treatment time decreases for the desired dose.

An indicator strip was placed in each batch as a low-cost mechanism to ensure consistent operation of the device. Failure of the indicator strip to turn from yellow to green would indicate failure of a bulb or another mechanism in the device, like the timer, which is linked to the bulb power supply.

## Comparison to State-of-the-Art

The University of Nebraska stood out as the most promising UVC method (see Fig. 4.8, Left). But significant obstacles remained. In addition to the steep initial investment, the protocol required a dedicated room, depended on slow batch processing, and relied on scarce equipment that is hard to source during a pandemic. In addition, the device was only

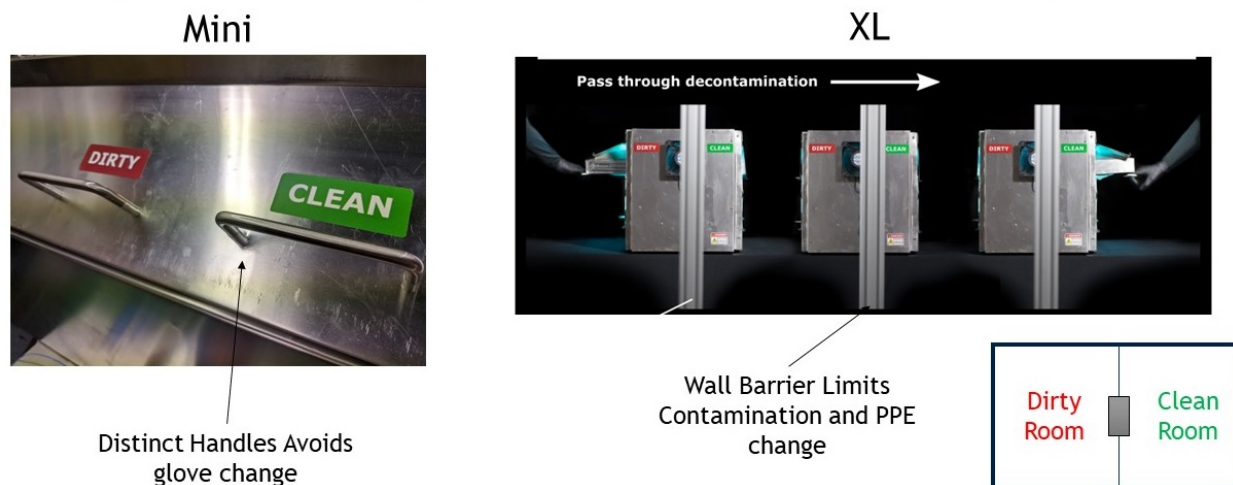


Figure 4.6: Design elements were included to ensure user safety and treatment effectiveness. A clean and dirty handle on the Mini eliminated the need for additional personnel or additional PPE to operate the device. A barrier separating a clean room from a dirty room afford better process control.

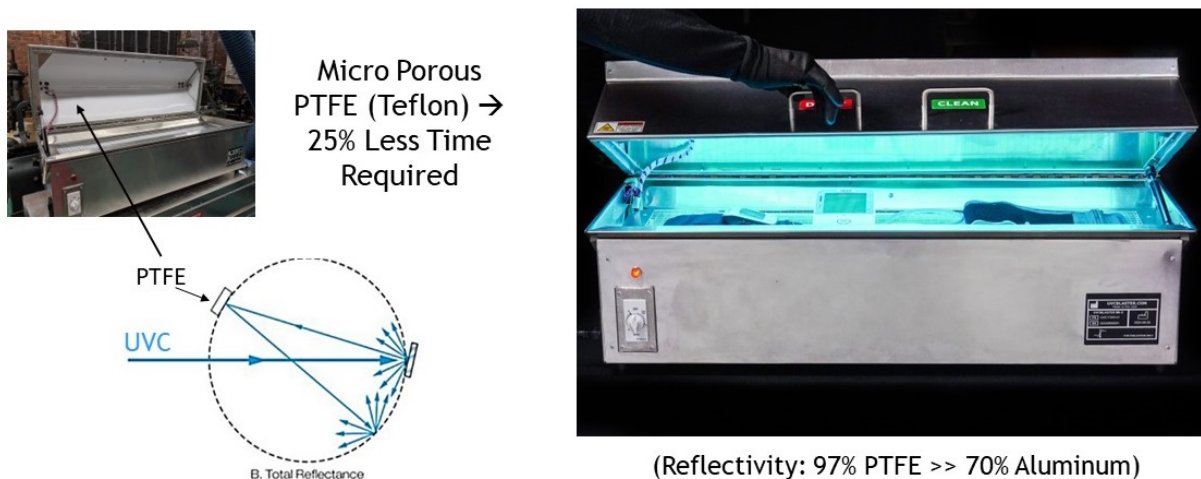


Figure 4.7: Compared to aluminum, ePTFE was chosen as a more UVC reflective surface, which improved chamber performance by increasing UVC intensity and UVC scattering (Image from Porex Corporation). Treatment time was reduced, and treatment coverage improved qualitatively.

safe by protocol rather than safe by mechanical design. The Battelle was also only safe by protocol in that users needed to be diligent when collecting, shipping, and repositioning the

contaminated respirators from dozens of distant facilities to avoid transmission (see Fig. 4.8, Middle). For this reason, hazmat suits were required when handling the respirators, which were treated as biohazardous material.

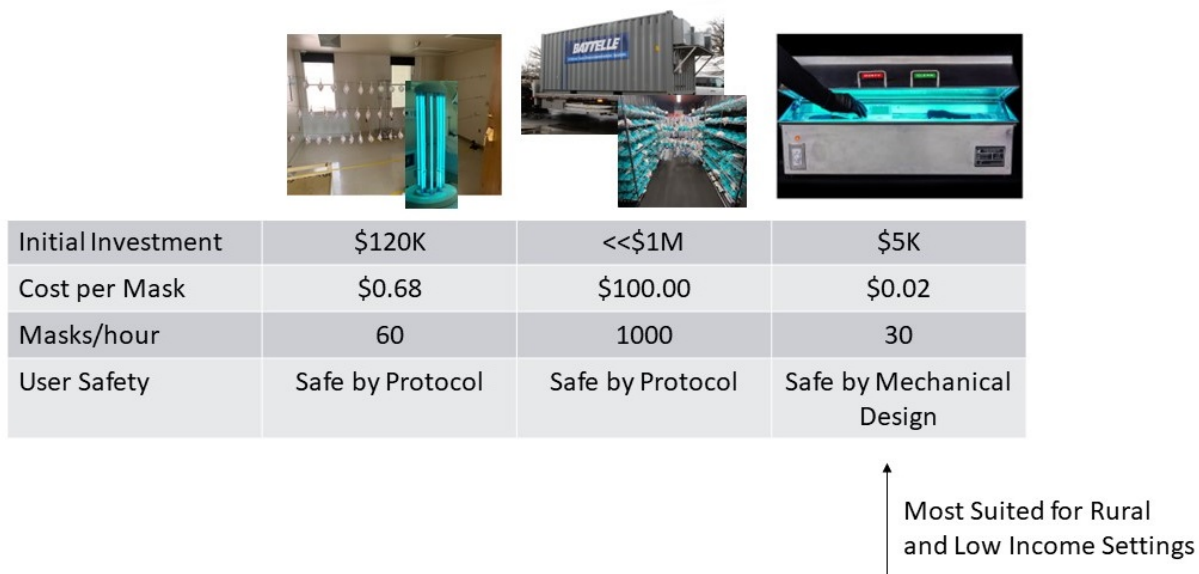


Figure 4.8: The UVC Blaster Mini compared favorably to the state-of-the-art systems of the time with respect to metrics important for rural and low income healthcare settings. (Left) The University of Nebraska Medicine Center paved the way for UVC use for decontaminating respirators in hospitals, but the initial investment was too expensive. (Middle) Costs for the Battelle hydrogen peroxide vapor system were almost entirely covered by the federal government and could treat respirators at scale but could not treat respirators outside its range in rural settings. (Right) In addition to the low cost, the UVC Blaster Mini was designed to be easy to operate with built-in safety elements that could keep nearly any healthcare worker safe even without training.

## 4.3 Methods

### Measuring UVC Spatially and Temporally

Irradiance values ( $mW/cm^2$ ) were measured in a grid pattern throughout the UVC Blaster Mini Chamber (see UVC Blaster Mini in Fig. 4.10 and UVC Blaster XL in 4.11). In addition to up and down, the light meter was also placed at different angles (45 degrees to the bulb) to capture UVC light at various orientations that are relevant for the highly



contoured shapes of the respirators. For all orientations, UVC intensity diminished around the edges of the chamber, which indicated where PPE could not be placed. Tests were also run with the presence of PPE to see how respirators would shade the rest of the chamber.

Distribution of dose across the respirator was observed using UVC Intensity Labels from UVC Process Supply, Inc (Chicago) as seen in Figure 4.9. These labels were pasted in a grid pattern across all faces of the respirator, including the respirator straps and behind the respirator strap fixation points. After exposure, the respirators were checked qualitatively for changes in color. While a taped section of the label remained yellow as a control, the rest of the labels turned a dark green, indicating a dose of anywhere from 300-750  $mJ/cm^2$  of UVC light was applied. In this test, the UVC dose compared from one location on the respirator to another was more important than the actual dose in any one location. Comparison of colors indicated that shadows cast by the mesh screen (19-Gauge Galvanized Steel Hardware Cloth) holding the respirators were negligible and did not require further research into shadowless materials like quartz rod (similar in material to the quartz housing on the UVC bulb), which is nearly transparent to UVC but proved too brittle for practical use. Of concern were straps that were misplaced, which created UVC shadowing and could warrant the use of alcohol wipes.

## UVC Measurement

Prior to shipping the device to a simulated hospital setting, continuous irradiance was measured (Sper Scientific UVC Light Meter, 850010) in the chamber. Measurements indicated UVC chamber performance, but should not be used to calculate necessary time to accumulate desired dose onsite. The Sper Scientific UVC Light Meter measures from 220 nm to 275 nm and is calibrated at 254 nm (see Fig. 4.12). N95 respirators at the very center of the chamber received peak irradiance across the germicidal wavelength 220-270 nm (+/- 4% accuracy). However, irradiance varies along the length of the bulb, perpendicular to the bulb length, and varies depending on if there are other respirators present. Given that these variations can't be easily controlled and given the understanding that respirator performance isn't affected by extended exposure to UVC, the worst case irradiance values at the corners of the chamber were used to calculate the dose or expected time to fully treat the respirators. This worst case dose was further increased to account for changes in output during the lifespan of the lamp, variations between lamps, and variations in output during the warm-up phase of the lamp. As a result, the worst case time to exceed the recommended dose of 1  $J/cm^2$  was calculated to be 10 minutes for the UVC Blaster Mini. This dose falls orders of magnitude short of a dose known to degrade respirator performance, in other words the respirator filter material and the respirator straps would have to be exposed to UVC for many hours before substantial changes of material properties and performance were noticed.[126]



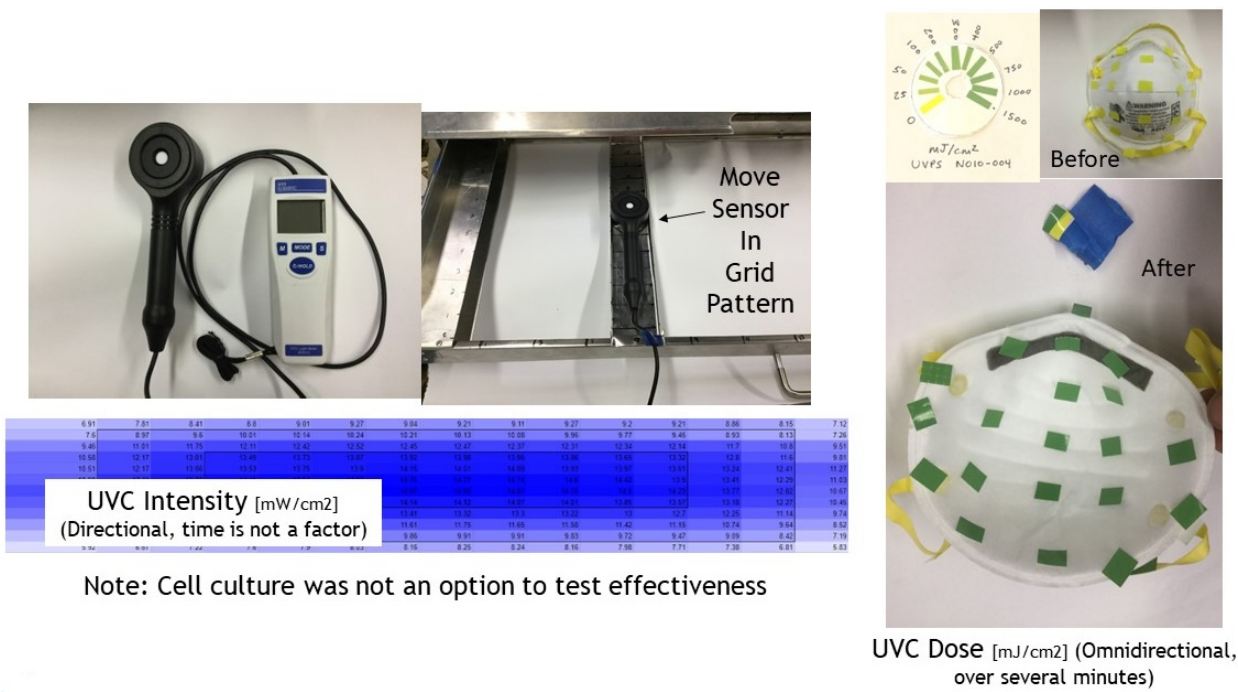


Figure 4.9: A Sper light meter was used to measure UVC intensity, while test strips were used to measure UVC dose (intensity per time). A jig was created to move the light meter sensor reliably to various coordinates within the chamber. Intensity was recorded in spreadsheets as depicted in this figure. The test strips which turned green in the presence of sufficient UVC light were pasted at various locations on the respirator including the inside, any edges, and the straps. Dose was recorded by photographing the test strips and comparing color to a reference shown in the top right.

## Limitations

### Respirator Functionality

N95 respirators come in many shapes and sizes and have variations in materials, particularly in the strap and nose piece designs. The ability to treat a variety of respirators comes down to the operator placing them correctly in the device. The functionality of respirators is highly dependent on the integrity of the straps. Therefore, the effectiveness of respirator treatment is dependent on tracking how many times a respirator has been processed.[162]

### Variation in UVC Measurement

Measured UVC irradiance may vary in the chamber depending on the light meter used (see Fig. 4.12). For example, the smaller the numerical aperture the less off-angle light mea-

<b>A</b>	Sensor upwards [mW/cm <sup>2</sup> ]		
6	4.93	8.63	4.1
3.5	5.94	9.89	5.26
1	4.58	8.15	4.28
Position (in)	1	16	31
<b>B</b>	Sensor downwards [mW/cm <sup>2</sup> ]		
6	3.72	6.37	3.47
3.5	6.61	11.26	5.82
1	3.24	6.27	4.02
Position (in)	1	16	31
<b>C</b>	Sensor sideways toward right wall [mW/cm <sup>2</sup> ]		
6	n/a	5.34	1.65
3.5	n/a	6.38	1.97
1	n/a	5	1.51
Position (in)	1	16	31

Figure 4.10: A grid of irradiance values ( $mW/cm^2$ ) measured throughout the chamber was faster and more reliable than simulating values.

sured, the greater the underestimation of irradiance and therefore the greater the calculated

12	4.65	5.56	5.84	6.06	6.51	6.50	6.48	6.51	6.57	6.58	6.50	6.44	6.20	5.64	4.80
11	5.74	7.20	7.76	8.12	8.31	8.38	8.56	8.57	8.70	8.67	8.69	8.52	8.27	7.60	6.56
10	8.29	9.20	9.63	10.14	10.28	10.40	10.52	10.55	10.46	10.59	10.4	10.22	10.18	8.88	7.74
9	7.75	9.88	10.65	11.18	11.42	11.68	11.64	11.72	11.76	11.74	11.66	11.46	11.04	10.41	8.54
8	9.51	11.13	11.54	11.94	12.10	12.25	12.31	12.35	12.40	12.45	12.36	12.15	11.71	10.72	9.56
7	8.88	10.76	11.77	12.26	12.46	12.60	12.68	12.70	12.70	12.71	12.61	12.44	12.00	11.01	9.75
6	8.76	10.80	11.89	12.32	12.47	12.65	12.76	12.85	12.91	12.81	12.69	12.54	12.15	11.07	9.30
5	8.79	11.07	11.53	11.97	12.19	12.36	12.46	12.52	12.52	12.51	12.35	12.19	11.84	10.89	9.45
4	8.32	10.14	11.01	11.4	11.68	11.83	11.91	11.86	11.88	11.81	11.68	11.46	11.07	10.20	8.70
3	7.41	8.99	9.60	9.85	10.05	10.20	10.32	10.37	10.40	10.20	10.04	9.88	9.55	9.04	7.30
2	5.82	6.61	7.30	7.82	7.81	7.96	8.14	8.08	7.98	7.99	7.87	7.94	7.50	6.72	5.67
1	4.48	5.64	6.11	6.52	6.85	6.95	7.05	7.01	7.04	6.94	6.87	6.73	6.45	5.75	4.09
Position in Inches	1	3	5	7	9	11	13	15	17	19	21	23	25	27	29

Figure 4.11: A grid of irradiance values ( $mW/cm^2$ ) for the XL model was also measured. Besides a higher intensity, the pattern of values similar with respect to edge effects.

dosage. Sensors may also vary depending on the germicidal spectrum that is sampled, which can have slight variations depending on the manufacturer. Expected variations between sensors can be accounted for by increasing the treatment time to ensure that the proper dose is reached.

### Undesirable Smell

Healthcare workers testing the device commonly complained of a burned or toasted odor in the device and on the respirators following treatment. A carbon layer added to the HEPA filter had little effect on the odor. The odor was determined to be from the breakdown of skin cells, which indicates the need to keep respirators clean and to put establish criteria for when respirators can not be retreated.[23]

### Controlling Dose

For simplicity of design, the device had a built-in timer (Intermatic SW15MWK 15-Minute Spring Wound Timer) that would shut off the bulbs when complete. While this system was easy to understand, it allowed for the user to set the wrong treatment duration or allowed to alter the treatment by opening the lid, which turned off bulbs but kept the

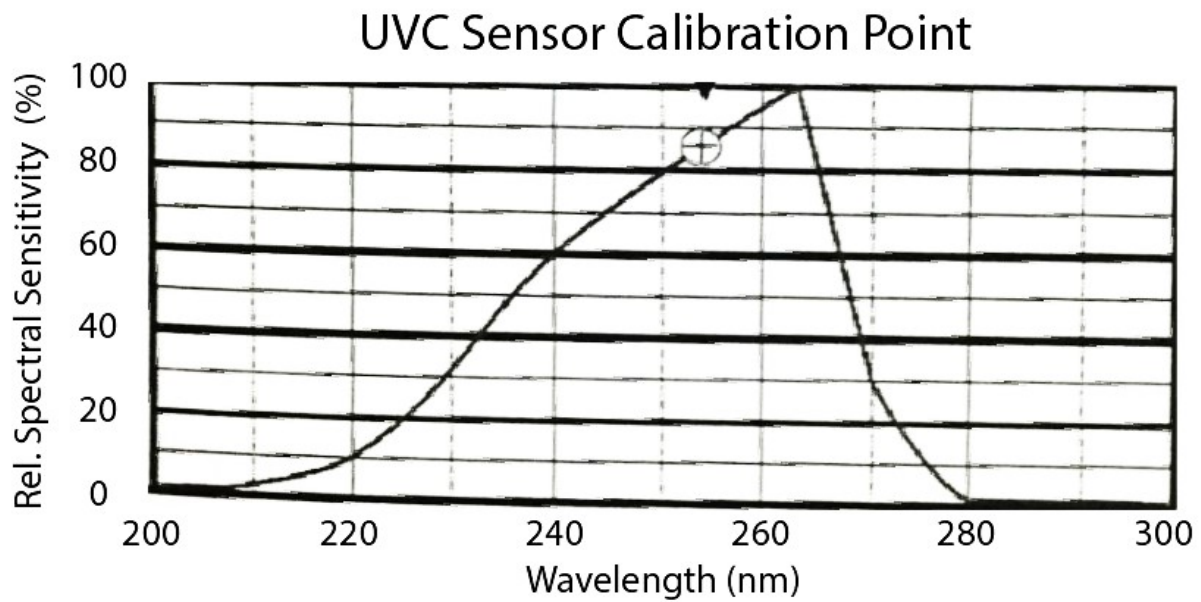


Figure 4.12: Relative spectral intensity by wavelength from the Sper Scientific UVC Light Meter user manual. The crosshairs indicate the calibration point.

timer running. Ultimately, a digital timer with set treatment times are needed. In general, fail-safe or Poka-Yoke methodology is needed to prevent, correct or draw attention to human error during operation with design elements. As an example, these design elements might include color coded guides for respirator placement. Further observations in a simulated hospital setting are first needed.

# Chapter 5

## Conclusions and Outlook

### 5.1 Design and Development of the Annulus-on-a-Chip

We designed, modelled, and fabricated a flexing organ-chip, referred to as the flexing Annulus-on-a-Chip (AoC). Our chip was designed to replicate complex loading observed in the intervertebral disc to study annulus fibrosis (AF) mechanobiology. We also conducted preliminary cell-based experiments to show that a population of cells could be maintained within a confined Polydimethylsiloxane (PDMS) channel with limited nutrient flow.

Biological treatments to delay or prevent early onset of degeneration have been limited.[206, 40] A platform or microphysiological system which can replicate conditions of early to moderate disc degeneration could enable rapid testing of cellular therapies. The AoC's design provides a mechanism to study cell responses to loading such as orientation, gene expression, and response to drugs added to the culture media. Furthermore, the AoC could be used to model most load bearing annular structures, such as cardiovascular vessels, lymphatic vessels, and the cervix. The device design and loading mechanism provides a platform for tailoring applied dynamic strains.

From the computational modeling perspective, we seek to quantify the strains at localized regions within the cell monolayer encased in the channel using image processing. This high-resolution strain data would enable us to correlate the strain distribution across the microchannel with cell behavior such re-orientation, spreading, proliferation, or apoptosis. Moreover, it would allow us to create descriptive computational models to investigate cell biomechanics, including the potential to estimate cell elasticity and identify loading modalities that lead to cell softening and stiffening. [38] Taken together, these experimental and computational approaches would inform our understanding of AF cell mechanobiology and potentially identify the initiation and development of disc degeneration. Future work will investigate the response of human AF cells within the device, as well as 3D cell-laden constructs.

It is my hope that the Annulus-on-a-Chip will inspire a series of next generation cellular

disc models that can alter the course of the growing back pain epidemic by improving the translatability of drug development. However, the translatability of such drugs will not be improved by a single model, instead a combination of animal models, micro-bioreactors, macro-bioreactors, and clinical studies are needed.

## 5.2 Rapid Design for Pandemic Response

Engineering design played an enabling role when targeting disparities in healthcare working conditions during the pandemic. Whether in the healthcare industry or outside the industry, many felt the need to help improve working conditions at a time when many were barred from accessing work, including graduate students who conducted wet lab experiments. However, due to the unprecedented nature of the pandemic there was neither a playbook nor research that could be leveraged to solve the problems at hand, there was only trial and error. When focused on addressing the needs of healthcare workers, engineering design provided an actionable framework to systematically generate insights by way of prototype iteration or controlled trial and error. This design process enabled one to go from limited knowledge to generating new knowledge in the space in just a short period of time, given the quick pace of rapid prototyping. Without this incremental progress being possible with engineering design, the task of bettering healthcare working conditions could have been an intractable problem. The UVC Blaster Mini and XL prototypes presented in the last chapter represented nearly a dozen design iterations, each with incorporated feedback from the end users in the hospitals. A device ready for scale-up and global deployment may have taken a dozen more iterations to hone the system, either way, the path to global impact from a design point of view was clear. However, the CDC stated that 4-log reduction in pathogens was required over 3-log which was the capability of UVC technology, the UVC Blasters were obsolete overnight as a result. With these shifting government guidelines and the rapid evolution of the pandemic in general, it became clear that engineering design alone could only impact the world so much. Additional capability was needed by engineering PhDs to strategize and adapt the vision that drives design.

## 5.3 Business Minor Specifically Designed for Engineering PhDs

Capabilities to better understand the shifting healthcare landscape, to foster collaborations, and to map a go-to-market strategy were needed not only to maximize the reach of the engineering design work but to influence the design itself. Not until taking Lean Tech Transfer, a course in the Haas School of Business, did I grow my understanding that these capabilities couldn't be gleaned from textbooks or peer-reviewed journals. Instead, it came in the form of business acumen around collecting higher quality information to establish design assumptions, talking with experts systematically to substantiate these design

assumptions, and predicting possible changes in the decontamination landscape that could affect design assumptions (such as the shift away from 3-log effectiveness making the UVC Blasters obsolete) in a rapidly shifting world.

At a later time, I went on to take two additional courses in the business school titled *Entrepreneurship* and *Opportunity Recognition: Technology and Entrepreneurship* that could have served me as a design engineer for both the Annulus-on-a-Chip and the pandemic response work. In many instances, I tailored my business coursework directly to my research, which put me in the habit of calling world experts on my research topic daily to satisfy course requirements but also to deepen my own expertise. It became apparent that my previous complete focus on engineering coursework was both a strength and a weakness. I felt that exposure to business coursework could translate the engineering accomplishments into real world impact. I also felt that the business courses brought greater clarity in the end goal of the research, which could strengthen one's research vision and publications. Overall, the business exposure helped me to keep the end user in mind, which is a key concept when engineering research and medical tools.

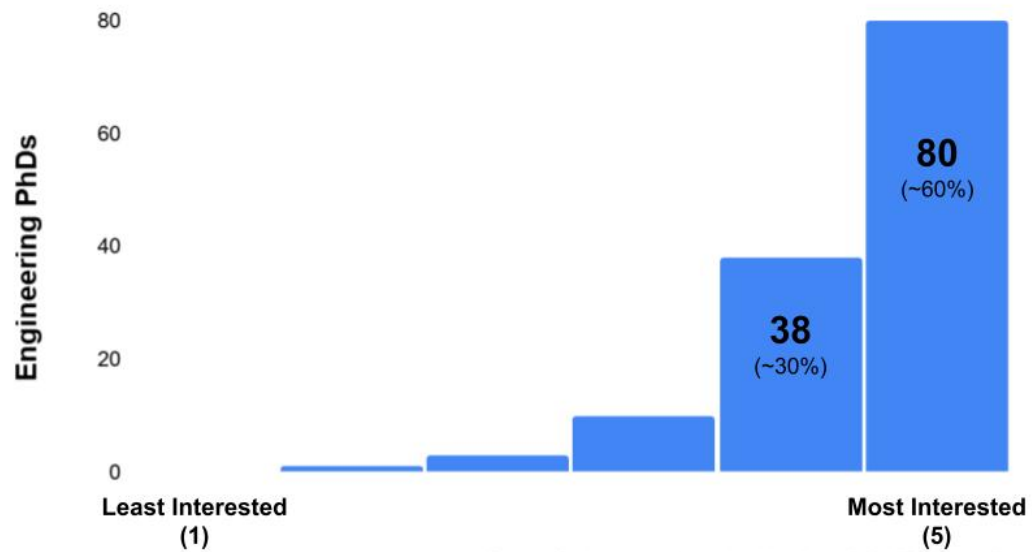
My self-made business course experience came with many uncertainties; not knowing which classes would be most helpful for my research, not knowing if I could even enroll after sitting in class for weeks, and not knowing what courses would count toward my degree. I was convinced that if knowledge of the courses was compiled, the process was formalized by creating a business minor degree, and if professors in both colleges were on hand to support the process, hundreds of engineering PhDs could benefit from a similar experience as mine.

I set out to prove or disprove the hypothesis that engineering PhDs wanted a business minor by conducting surveys and interviews with the students. The following data were collected independently by sending surveys to each UC Berkeley Engineering College PhD student in October 2020. PhD students responded to the survey when asked: Are you interested in a new minor in business designed specifically for PhD engineering students? The 132 responses were almost entirely in favor of a business minor. Graphs illustrated the extent of the support for the idea, while open-ended responses in the surveys provided ideas for designing the business minor (see Fig. 5.1 and Fig. 5.2).

While I worked with students, Professor Lee Fleming went to great lengths to substantiate and champion the business minor proposal at a faculty level. After two years, the proposal received resounding approval with the engineering faculty. Information for the business minor for engineering PhDs can now be found hosted on the UC Berkeley Fung Institute for Engineering Leadership website (<https://funginstitute.berkeley.edu/phd-minor/>).

In closing, during my time at UC Berkeley, I have discovered that the best designs and the best experiences come from strong communities, or teams, built on the desire for personal and communal growth. Build an empowering community, and you will have a lasting, enabling, and rewarding experience.

**On a scale from 1 (least) to 5 (most) how interested are you in a business minor designed for engineering PhDs?**

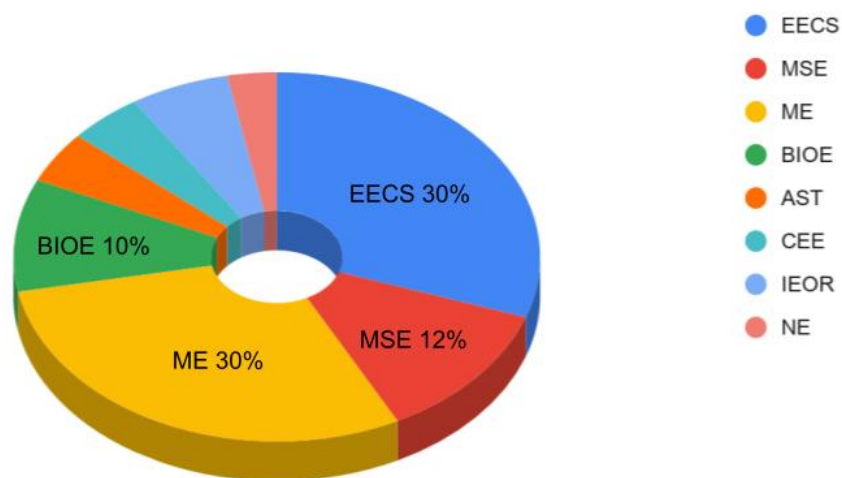


*Survey Conducted by Jonathan McKinley, PhD ME from 10/9 -10/20 2020*

Figure 5.1: The entire Engineering PhD student body was surveyed regarding their interest in a business minor. Favorable responses from 132 PhDs indicated that there was a need.



## Business Minor Interest by Engineering Department



*Survey Conducted by Jonathan McKinley, PhD ME from 10/9 -10/20 2020*

Figure 5.2: Engineering PhD students interested in a business minor were spread across numerous departments in the college including Electrical Engineering and Computer Science (EECS), Mechanical Engineering (ME), Material Science Engineering (MSE), BioEngineering (BioE), Applied Science and Technology (AST), Civil and Environmental Engineering (CEE), Industrial Engineering Operations Research (IEOR), and Nuclear Engineering (NE).

# Bibliography

- [1] Rosalyn D. Abbott et al. “Live free or die: Stretch-induced apoptosis occurs when adaptive reorientation of annulus fibrosus cells is restricted”. In: *Biochemical and Biophysical Research Communications* 421 (2 May 2012), pp. 361–366. ISSN: 0006291X. DOI: 10.1016/j.bbrc.2012.04.018.
- [2] MA Adams and WC Hutton. “The effect of posture on diffusion into lumbar intervertebral discs.” In: *Journal of anatomy* 147 (1986), p. 121.
- [3] Shehnaz Ahmed et al. “New generation of bioreactors that advance extracellular matrix modelling and tissue engineering”. In: *Biotechnology letters* 41 (2019), pp. 1–25.
- [4] Guus GH van den Akker et al. “Transcriptional profiling distinguishes inner and outer annulus fibrosus from nucleus pulposus in the bovine intervertebral disc”. In: *European Spine Journal* 26.8 (2017), pp. 2053–2062.
- [5] B Alkhatib et al. “Acute mechanical injury of the human intervertebral disc: link to degeneration and pain”. In: *Eur Cell Mater* 28.514 (2014), 98e110.
- [6] Kalliopi Alpantaki et al. “Diabetes mellitus as a risk factor for intervertebral disc degeneration: a critical review”. In: *European Spine Journal* 28.9 (2019), pp. 2129–2144.
- [7] DB Amin, CM Moawad, and JJ Costi. “New findings confirm regional internal disc strain changes during simulation of repetitive lifting motions”. In: *Annals of biomedical engineering* 47.6 (2019), pp. 1378–1390.
- [8] Lauren Banh et al. “Advances in organ-on-a-chip systems for modelling joint tissue and osteoarthritic diseases”. In: *Osteoarthritis and Cartilage* (2022).
- [9] Michele C Battié and Tapio Videman. “Lumbar disc degeneration: epidemiology and genetics”. In: *JBJS* 88.suppl\_2 (2006), pp. 3–9.
- [10] Laura Baumgartner et al. “Multiscale regulation of the intervertebral disc: achievements in experimental, in silico, and regenerative research”. In: *International Journal of Molecular Sciences* 22.2 (2021), p. 703.
- [11] Amanda M Beatty, Anton E Bowden, and Laura C Bridgewater. “Functional validation of a complex loading whole spinal segment bioreactor design”. In: *Journal of Biomechanical Engineering* 138.6 (2016).

- [12] Michel Benoist. “Natural history of the aging spine”. In: *The aging spine* (2005), pp. 4–7.
- [13] Nikolaus Berger-Roscher et al. “Influence of complex loading conditions on intervertebral disc failure”. In: *Spine* 42.2 (2017), E78–E85.
- [14] Allison L Berrier and Kenneth M Yamada. “Cell–matrix adhesion”. In: *Journal of cellular physiology* 213.3 (2007), pp. 565–573.
- [15] Semih E Bezci and Grace D O’Connell. “Osmotic pressure alters time-dependent recovery behavior of the intervertebral disc”. In: *Spine* 43.6 (2018), E334–E340.
- [16] Semih E Bezci et al. “Radial variation in biochemical composition of the bovine caudal intervertebral disc”. In: *JOR spine* 2.3 (2019), e1065.
- [17] Mara Biasin et al. “UV-C irradiation is highly effective in inactivating SARS-CoV-2 replication”. In: *Scientific Reports* 11.1 (2021), p. 6260.
- [18] Abbie LA Binch et al. “Cell-based strategies for IVD repair: clinical progress and translational obstacles”. In: *Nature Reviews Rheumatology* 17.3 (2021), pp. 158–175.
- [19] Edward D Bonnevie et al. “Aberrant mechanosensing in injured intervertebral discs as a result of boundary-constraint disruption and residual-strain loss”. In: *Nature biomedical engineering* 3.12 (2019), pp. 998–1008.
- [20] DJ Botsford, SI Esses, and DJ Ogilvie-Harris. “In vivo diurnal variation in intervertebral disc volume and morphology.” In: *Spine* 19.8 (1994), pp. 935–940.
- [21] Katrin Bott et al. “The effect of matrix characteristics on fibroblast proliferation in 3D gels”. In: *Biomaterials* 31.32 (2010), pp. 8454–8464.
- [22] Robby D Bowles et al. “Self-assembly of aligned tissue-engineered annulus fibrosus and intervertebral disc composite via collagen gel contraction”. In: *Tissue Engineering Part A* 16.4 (2010), pp. 1339–1348.
- [23] Normand Brais, P Eng, Benoit Despatis, et al. “Root Cause of the Odor Generated by Germicidal UV Disinfection with Mobile Units”. In: *Carbon* 9 (), pp. 10–2.
- [24] Robijn Bruinsma. “Theory of force regulation by nascent adhesion sites”. In: *Biophysical journal* 89.1 (2005), pp. 87–94.
- [25] US Census Bureau. *New Census Data Show Differences Between Urban and Rural Populations*. 2016. URL: <https://www.census.gov/newsroom/press-releases/2016/cb16-210.html> (visited on 12/08/2016).
- [26] Peter G Bush et al. “Viability and volume of in situ bovine articular chondrocytes—changes following a single impact and effects of medium osmolarity”. In: *Osteoarthritis and cartilage* 13.1 (2005), pp. 54–65.
- [27] Joo Hyeon Byeon et al. “Degenerative changes of spine in helicopter pilots”. In: *Annals of rehabilitation medicine* 37.5 (2013), pp. 706–712.

- [28] Martina Calió et al. “The Cellular Composition of Bovine Coccygeal Intervertebral Discs: A Comprehensive Single-Cell RNAseq Analysis”. In: *International journal of molecular sciences* 22.9 (2021), p. 4917.
- [29] Elena Cambria et al. “TRPV4 Inhibition and CRISPR-Cas9 Knockout Reduce Inflammation Induced by Hyperphysiological Stretching in Human Annulus Fibrosus Cells”. In: *Cells* 9.7 (2020), p. 1736.
- [30] James L Carey, Ann E Remmers, and David C Flanigan. “Use of MACI (autologous cultured chondrocytes on porcine collagen membrane) in the United States: preliminary experience”. In: *Orthopaedic Journal of Sports Medicine* 8.8 (2020).
- [31] APG Castro and D Lacroix. “Micromechanical study of the load transfer in a polycaprolactone collagen hybrid scaffold when subjected to unconfined and confined compression”. In: *Biomechanics and Modeling in Mechanobiology* 17 (2018), pp. 531–541.
- [32] Chaenyung Cha et al. “Tailoring hydrogel adhesion to polydimethylsiloxane substrates using polysaccharide glue”. In: *Angewandte Chemie International Edition* 52.27 (2013), pp. 6949–6952.
- [33] Samantha CW Chan, Stephen J Ferguson, and Benjamin Gantenbein-Ritter. “The effects of dynamic loading on the intervertebral disc”. In: *European spine journal* 20.11 (2011), pp. 1796–1812.
- [34] Samantha CW Chan and Benjamin Gantenbein-Ritter. “Preparation of intact bovine tail intervertebral discs for organ culture”. In: *JoVE (Journal of Visualized Experiments)* 60 (2012), e3490.
- [35] Samantha CW Chan et al. “Region specific response of intervertebral disc cells to complex dynamic loading: an organ culture study using a dynamic torsion-compression bioreactor”. In: *PloS one* 8.8 (2013), e72489.
- [36] Bérénice Charrez et al. “Heart muscle microphysiological system for cardiac liability prediction of repurposed COVID-19 therapeutics”. In: *Frontiers in Pharmacology* 12 (2021).
- [37] Umber Cheema et al. “Oxygen diffusion through collagen scaffolds at defined densities: implications for cell survival in tissue models”. In: *Journal of tissue engineering and regenerative medicine* 6.1 (2012), pp. 77–84.
- [38] Chun-Teh Chen and Grace X Gu. “Learning hidden elasticity with deep neural networks”. In: *Proceedings of the National Academy of Sciences* 118.31 (2021), n.p.
- [39] Kellen Chen et al. “Role of boundary conditions in determining cell alignment in response to stretch”. In: *Proceedings of the National Academy of Sciences* 115.5 (2018), pp. 986–991.
- [40] Genglei Chu et al. “Strategies for annulus fibrosus regeneration: from biological therapies to tissue engineering”. In: *Frontiers in bioengineering and biotechnology* 6 (2018), p. 90.

- [41] Yon Jin Chuah et al. “Simple surface engineering of polydimethylsiloxane with polydopamine for stabilized mesenchymal stem cell adhesion and multipotency”. In: *Scientific reports* 5.1 (2015), pp. 1–12.
- [42] Yon Jin Chuah et al. “The effects of poly (dimethylsiloxane) surface silanization on the mesenchymal stem cell fate”. In: *Biomaterials science* 3.2 (2015), pp. 383–390.
- [43] Yon Jin Chuah et al. “Three-dimensional development of tensile pre-strained annulus fibrosus cells for tissue regeneration: An in-vitro study”. In: *Experimental cell research* 331.1 (2015), pp. 176–182.
- [44] William W Clark et al. “Development of a piezoelectrically actuated cell stretching device”. In: *Smart Structures and Materials 2000: Industrial and Commercial Applications of Smart Structures Technologies*. Vol. 3991. SPIE. 2000, pp. 294–301.
- [45] A Cochis et al. “Bioreactor mechanically guided 3D mesenchymal stem cell chondrogenesis using a biocompatible novel thermo-reversible methylcellulose-based hydrogel”. In: *Scientific reports* 7.1 (2017), pp. 1–12.
- [46] Joana Costa et al. “Bioreactor with electrically deformable curved membranes for mechanical stimulation of cell cultures”. In: *Frontiers in Bioengineering and Biotechnology* 8 (2020), p. 22.
- [47] John J Costi, Brian JC Freeman, and Dawn M Elliott. “Intervertebral disc properties: challenges for biodevices”. In: *Expert review of medical devices* 8.3 (2011), pp. 357–376.
- [48] John Jack Costi et al. “Direct measurement of intervertebral disc maximum shear strain in six degrees of freedom: motions that place disc tissue at risk of injury”. In: *Journal of biomechanics* 40.11 (2007), pp. 2457–2466.
- [49] Marita Cross et al. “The global burden of rheumatoid arthritis: estimates from the global burden of disease 2010 study”. In: *Annals of the rheumatic diseases* 73.7 (2014), pp. 1316–1322.
- [50] Jun Dai et al. “Microfluidic disc-on-a-chip device for mouse intervertebral disc: pitching a next-generation research platform to study disc degeneration”. In: *ACS biomaterials science & engineering* 5.4 (2019), pp. 2041–2051.
- [51] Chris Daly et al. “A review of animal models of intervertebral disc degeneration: pathophysiology, regeneration, and translation to the clinic”. In: *BioMed research international* 2016 (2016).
- [52] Christopher M De Geer. “Intervertebral disk nutrients and transport mechanisms in relation to disk degeneration: a narrative literature review”. In: *Journal of chiropractic medicine* 17.2 (2018), pp. 97–105.
- [53] Carlos Gomes De Oliveira and Jurandir Nadal. “Transmissibility of helicopter vibration in the spines of pilots in flight”. In: *Aviation, space, and environmental medicine* 76.6 (2005), pp. 576–580.

- [54] Jane Desrochers and Neil A Duncan. “Strain transfer in the annulus fibrosus under applied flexion”. In: *Journal of biomechanics* 43.11 (2010), pp. 2141–2148.
- [55] Joseph A DiMasi, Henry G Grabowski, and Ronald W Hansen. “Innovation in the pharmaceutical industry: new estimates of R&D costs”. In: *Journal of health economics* 47 (2016), pp. 20–33.
- [56] Sedat Dogru et al. “Poisson’s ratio of PDMS thin films”. In: *Polymer Testing* 69 (2018), pp. 375–384.
- [57] Yixiao Dong, Allison N Ramey-Ward, and Khalid Salaita. “Programmable Mechanically Active Hydrogel-Based Materials”. In: *Advanced Materials* 33.46 (2021).
- [58] Yiming Dou et al. “Intervertebral disk degeneration: The microenvironment and tissue engineering strategies”. In: *Frontiers in bioengineering and biotechnology* 9 (2021), p. 592118.
- [59] Jonas F Eichinger et al. “Mechanical homeostasis in tissue equivalents: a review”. In: *Biomechanics and modeling in mechanobiology* 20.3 (2021), pp. 833–850.
- [60] Tomonori Endo et al. “Discussion on effect of material on UV reflection and its disinfection with focus on Japanese Stucco for interior wall”. In: *Scientific Reports* 11.1 (2021), p. 21840.
- [61] George C Engelmayr Jr et al. “Cyclic flexure and laminar flow synergistically accelerate mesenchymal stem cell-mediated engineered tissue formation: Implications for engineered heart valve tissues”. In: *Biomaterials* 27.36 (2006), pp. 6083–6095.
- [62] Eric W Esch, Anthony Bahinski, and Dongeun Huh. “Organs-on-chips at the frontiers of drug discovery”. In: *Nature reviews Drug discovery* 14.4 (2015), pp. 248–260.
- [63] FDA. *FAQs for Filtering Facepiece Respirator (FFR) Decontamination and Bioburden Reduction Systems*. 2021. URL: <https://www.fda.gov/medical-devices/coronavirus-covid-19-and-medical-devices/faqs-filtering-facepiece-respirator-ffr-decontamination-and-bioburden-reduction-systems> (visited on 04/25/2021).
- [64] Bailey V Fearing et al. “Mechanotransduction and cell biomechanics of the intervertebral disc”. In: *JOR spine* 1.3 (2018), e1026.
- [65] Elisa Figallo et al. “Micro-bioreactor array for controlling cellular microenvironments”. In: *Lab on a Chip* 7.6 (2007), pp. 710–719.
- [66] Miriam Filippi et al. “Microfluidic Tissue Engineering and Bio-Actuation”. In: *Advanced Materials* 34.23 (2022), p. 2108427.
- [67] Dale E Fournier et al. “Vascularization of the human intervertebral disc: A scoping review”. In: *JOR spine* 3.4 (2020), e1123.
- [68] Eliot H Frank et al. “A versatile shear and compression apparatus for mechanical stimulation of tissue culture explants”. In: *Journal of biomechanics* 33.11 (2000), pp. 1523–1527.

- [69] Leslie Frapin et al. “Lessons learned from intervertebral disc pathophysiology to guide rational design of sequential delivery systems for therapeutic biological factors”. In: *Advanced Drug Delivery Reviews* 149 (2019), pp. 49–71.
- [70] JW Frymoyer et al. “Risk factors in low-back pain. An epidemiological survey.” In: *JBJS* 65.2 (1983), pp. 213–218.
- [71] Hamish TJ Gilbert, Judith A Hoyland, and Sarah J Millward-Sadler. “The response of human annulus fibrosus cells to cyclic tensile strain is frequency-dependent and altered with disc degeneration”. In: *Arthritis & Rheumatism* 62.11 (2010), pp. 3385–3394.
- [72] Hamish TJ Gilbert et al. “Acidic pH promotes intervertebral disc degeneration: Acid-sensing ion channel-3 as a potential therapeutic target”. In: *Scientific reports* 6.1 (2016), pp. 1–12.
- [73] Christopher L Gilchrist et al. “Measurement of intracellular strain on deformable substrates with texture correlation”. In: *Journal of biomechanics* 40.4 (2007), pp. 786–794.
- [74] Alessio Gizzi et al. “Computationally informed design of a multi-axial actuated microfluidic chip device”. In: *Scientific reports* 7.1 (2017), pp. 1–11.
- [75] Jessica Glenza. *Survey finds 87% of America’s nurses forced to reuse protective equipment*. 2020. URL: <https://www.theguardian.com/world/2020/may/20/survey-finds-87-of-americas-nurses-are-forced-to-reuse-protective-equipment> (visited on 09/01/2020).
- [76] Shakti A Goel, Vicky Varghese, and Tyfik Demir. “Animal models of spinal injury for studying back pain and SCI”. In: *Journal of Clinical Orthopaedics and Trauma* 11.5 (2020), pp. 816–821.
- [77] MP Grant et al. “Tungsten accumulates in the intervertebral disc and vertebrae stimulating disc degeneration and upregulating markers of inflammation and pain”. In: *Eur. Cells Mater* 41 (2021), pp. 517–530.
- [78] Christian M Griffith et al. “Microfluidics for the study of mechanotransduction”. In: *Journal of physics D: Applied physics* 53.22 (2020), p. 224004.
- [79] Linda G Griffith and Melody A Swartz. “Capturing complex 3D tissue physiology in vitro”. In: *Nature reviews Molecular cell biology* 7.3 (2006), pp. 211–224.
- [80] Christi A Grimm. *Hospital Experiences Responding to the COVID-19 Pandemic: Results of a National Pulse Survey March 23–27, 2020*. 2020. URL: <https://oig.hhs.gov/oei/reports/oei-06-20-00300.pdf> (visited on 04/01/2020).
- [81] Helen E Gruber and Edward N Hanley. “Human disc cells in monolayer vs 3D culture: cell shape, division and matrix formation”. In: *BMC musculoskeletal disorders* 1.1 (2000), pp. 1–6.

- [82] Heather Anne L Guerin and Dawn M Elliott. “Degeneration affects the fiber reorientation of human annulus fibrosus under tensile load”. In: *Journal of biomechanics* 39.8 (2006), pp. 1410–1418.
- [83] Eline E van Haaften et al. “Decoupling the effect of shear stress and stretch on tissue growth and remodeling in a vascular graft”. In: *Tissue Engineering Part C: Methods* 24.7 (2018), pp. 418–429.
- [84] Lisbet Haglund et al. “Development of a bioreactor for axially loaded intervertebral disc organ culture”. In: *Tissue Engineering Part C: Methods* 17.10 (2011), pp. 1011–1019.
- [85] Woojin M Han et al. “Macro-to microscale strain transfer in fibrous tissues is heterogeneous and tissue-specific”. In: *Biophysical journal* 105.3 (2013), pp. 807–817.
- [86] Jan Hartvigsen et al. “What low back pain is and why we need to pay attention”. In: *The Lancet* 391.10137 (2018), pp. 2356–2367.
- [87] Frank Heuer, Hendrik Schmidt, and Hans-Joachim Wilke. “The relation between intervertebral disc bulging and annular fiber associated strains for simple and complex loading”. In: *Journal of biomechanics* 41.5 (2008), pp. 1086–1094.
- [88] Simon P Hoerstrup et al. “Tissue engineering of small caliber vascular grafts”. In: *European journal of cardio-thoracic surgery* 20.1 (2001), pp. 164–169.
- [89] Timothy M Hosea and Jo A Hannafin. “Rowing injuries”. In: *Sports health* 4.3 (2012), pp. 236–245.
- [90] Timothy M. Hosea and Jo A. Hannafin. “Rowing Injuries”. In: *Sports Health* 4 (3 May 2012), pp. 236–245. ISSN: 19417381. DOI: 10.1177/1941738112442484.
- [91] Hsin-Yi Hsieh et al. “Gradient static-strain stimulation in a microfluidic chip for 3D cellular alignment”. In: *Lab on a Chip* 14.3 (2014), pp. 482–493.
- [92] Dongeun Huh. “A human breathing lung-on-a-chip”. In: *Annals of the American Thoracic Society* 12.Supplement 1 (2015), S42–S44.
- [93] Dongeun Huh et al. “Microengineered physiological biomimicry: organs-on-chips”. In: *Lab on a Chip* 12.12 (2012), pp. 2156–2164.
- [94] Min Ho Hwang et al. “Spine-on-a-chip: Human annulus fibrosus degeneration model for simulating the severity of intervertebral disc degeneration”. In: *Biomicrofluidics* 11.6 (2017), p. 064107.
- [95] Donald E Ingber. “Human organs-on-chips for disease modelling, drug development and personalized medicine”. In: *Nature Reviews Genetics* 23.8 (2022), pp. 467–491.
- [96] Brett C Isenberg, Chrysanthi Williams, and Robert T Tranquillo. “Small-diameter artificial arteries engineered in vitro”. In: *Circulation research* 98.1 (2006), pp. 25–35.
- [97] Hirokazu Ishihara et al. “Proteoglycan synthesis in the intervertebral disk nucleus: the role of extracellular osmolality”. In: *American Journal of physiology-Cell physiology* 272.5 (1997), pp. C1499–C1506.



- [98] Hiroaki Ito and Makoto Kaneko. “On-chip cell manipulation and applications to deformability measurements”. In: *Robomech Journal* 7.1 (2020), pp. 1–11.
- [99] Alicia R Jackson, Chun-Yuh Huang, and Wei Yong Gu. “Effect of endplate calcification and mechanical deformation on the distribution of glucose in intervertebral disc: a 3D finite element study”. In: *Computer methods in biomechanics and biomedical engineering* 14.02 (2011), pp. 195–204.
- [100] Nathan T Jacobs et al. “Effect of orientation and targeted extracellular matrix degradation on the shear mechanical properties of the annulus fibrosus”. In: *Journal of the mechanical behavior of biomedical materials* 4.8 (2011), pp. 1611–1619.
- [101] David Jamison and Michele S Marcolongo. “The effect of creep on human lumbar intervertebral disk impact mechanics”. In: *Journal of Biomechanical Engineering* 136.3 (2014), p. 031006.
- [102] Paul A Janmey, Daniel A Fletcher, and Cynthia A Reinhart-King. “Stiffness sensing by cells”. In: *Physiological reviews* 100.2 (2020), pp. 695–724.
- [103] Li Jin, Gary Balian, and Xudong Joshua Li. “Animal models for disc degeneration-an update”. In: *Histology and histopathology* 33.6 (2018), p. 543.
- [104] Moonsoo Jin et al. “Tissue shear deformation stimulates proteoglycan and protein biosynthesis in bovine cartilage explants”. In: *Archives of biochemistry and biophysics* 395.1 (2001), pp. 41–48.
- [105] Zariel I Johnson, Irving M Shapiro, and Makarand V Risbud. “Extracellular osmolarity regulates matrix homeostasis in the intervertebral disc and articular cartilage: evolving role of TonEBP”. In: *Matrix Biology* 40 (2014), pp. 10–16.
- [106] ID Johnston et al. “Mechanical characterization of bulk Sylgard 184 for microfluidics and microengineering”. In: *Journal of Micromechanics and Microengineering* 24.3 (2014), p. 035017.
- [107] Derek G Ju, Linda E Kanim, and Hyun W Bae. “Intervertebral disc repair: current concepts”. In: *Global Spine Journal* 10.2\_suppl (2020), 130S–136S.
- [108] Svenja Jünger et al. “Effect of limited nutrition on in situ intervertebral disc cells under simulated-physiological loading”. In: *Spine* 34.12 (2009), pp. 1264–1271.
- [109] Kattika Kaarj and Jeong Yeol Yoon. “Methods of delivering mechanical stimuli to Organ-on-a-Chip”. In: *Micromachines* 10 (10 Oct. 2019). ISSN: 2072666X. DOI: 10.3390/mi10100700.
- [110] Leonid Kalichman et al. “Computed tomography-evaluated features of spinal degeneration: prevalence, intercorrelation, and association with self-reported low back pain”. In: *The spine journal* 10.3 (2010), pp. 200–208.
- [111] Jeffrey N Katz. “Lumbar disc disorders and low-back pain: socioeconomic factors and consequences”. In: *JBJS* 88.suppl.2 (2006), pp. 21–24.

- [112] Ramada R. Khasawneh et al. “Addressing the impact of different fetal bovine serum percentages on mesenchymal stem cells biological performance”. In: *Molecular Biology Reports* 46 (4 Aug. 2019), pp. 4437–4441. ISSN: 15734978. DOI: 10.1007/s11033-019-04898-1.
- [113] Suzanne E Koch et al. “A multi-cue bioreactor to evaluate the inflammatory and regenerative capacity of biomaterials under flow and stretch”. In: *JoVE (Journal of Visualized Experiments)* 166 (2020), e61824.
- [114] Yuha Koike, Yoshiyuki Yokoyama, and Takeshi Hayakawa. “Light-driven hydrogel microactuators for on-chip cell manipulations”. In: *Frontiers in Mechanical Engineering* 6 (2020), p. 2.
- [115] Fan-Yun Lan et al. “An investigation of a cluster of cervical herniated discs among container truck drivers with occupational exposure to whole-body vibration”. In: *Journal of occupational health* 58.1 (2016), pp. 118–127.
- [116] Donghee Lee et al. “A Microfluidic Platform for Stimulating Chondrocytes with Dynamic Compression”. In: *JoVE (Journal of Visualized Experiments)* 151 (2019), e59676.
- [117] Donghee Lee et al. “Pneumatic microfluidic cell compression device for high throughput study of chondrocyte mechanobiology”. In: *Lab on a Chip* 18.14 (2018), pp. 2077–2086.
- [118] P Lee et al. “Mechanical forces in musculoskeletal tissue engineering”. In: *Regenerative Engineering of Musculoskeletal Tissues and Interfaces*. Elsevier, 2015, pp. 77–93.
- [119] Chak Ming Leung et al. “A guide to the organ-on-a-chip”. In: *Nature Reviews Methods Primers* 2.1 (2022), pp. 1–29.
- [120] George E Lewinnek and Carol A Warfield. “Facet joint degeneration as a cause of low back pain.” In: *Clinical orthopaedics and related research* 213 (1986), pp. 216–222.
- [121] Siyuan Li et al. “The effects of cyclic tensile strain on the organisation and expression of cytoskeletal elements in bovine intervertebral disc cells: an in vitro study”. In: *Eur Cell Mater* 21 (2011), pp. 508–522.
- [122] Zening Li et al. “Microfluidic Organ-on-a-Chip System for Disease Modeling and Drug Development”. In: *Biosensors* 12.6 (2022), p. 370.
- [123] Zhen Li et al. “Preclinical ex-vivo testing of anti-inflammatory drugs in a bovine intervertebral degenerative disc model”. In: *Frontiers in Bioengineering and Biotechnology* 8 (2020), p. 583.
- [124] Morakot Likhitpanichkul et al. “Do mechanical strain and TNF- $\alpha$  interact to amplify pro-inflammatory cytokine production in human annulus fibrosus cells?” In: *Journal of biomechanics* 49.7 (2016), pp. 1214–1220.

- [125] Zixuan Lin et al. “Osteochondral tissue chip derived from iPSCs: modeling OA pathologies and testing drugs”. In: *Frontiers in bioengineering and biotechnology* 7 (2019), p. 411.
- [126] William G Lindsley et al. “Effects of ultraviolet germicidal irradiation (UVGI) on N95 respirator filtration performance and structural integrity”. In: *Journal of occupational and environmental hygiene* 12.8 (2015), pp. 509–517.
- [127] Markus Loibl et al. “Controversies in regenerative medicine: Should intervertebral disc degeneration be treated with mesenchymal stem cells?” In: *JOR spine* 2.1 (2019), e1043.
- [128] Jeffrey C Lotz. “Animal models of intervertebral disc degeneration: lessons learned”. In: *Spine* 29.23 (2004), pp. 2742–2750.
- [129] Jeffrey C Lotz and Jennie R Chin. “Intervertebral disc cell death is dependent on the magnitude and duration of spinal loading”. In: *Spine* 25.12 (2000), pp. 1477–1483.
- [130] Lucie A Low et al. “Organs-on-chips: into the next decade”. In: *Nature Reviews Drug Discovery* 20.5 (2021), pp. 345–361.
- [131] Katariina Luoma et al. “Low back pain in relation to lumbar disc degeneration”. In: *Spine* 25.4 (2000), pp. 487–492.
- [132] Feng-Juan Lyu et al. “IVD progenitor cells: a new horizon for understanding disc homeostasis and repair”. In: *Nature Reviews Rheumatology* 15.2 (2019), pp. 102–112.
- [133] Steve A Maas et al. “FEBio: finite elements for biomechanics”. In: *Journal of biomechanical engineering* 134.1 (2012), p. 011005.
- [134] Rhea Mahbubani. *US medical workers will need 3.5 billion face masks if the coronavirus reaches pandemic status. Right now, the country only has 1% of that number.* 2020. URL: <https://www.businessinsider.com/usa-1-percent-3-billion-face-masks-needed-coronavirus-pandemic-2020-3> (visited on 03/04/2020).
- [135] Andrea Mainardi et al. “Intervertebral Disc-on-a-Chip as Advanced In Vitro Model for Mechanobiology Research and Drug Testing: A Review and Perspective”. In: *Frontiers in Bioengineering and Biotechnology* 9 (2021).
- [136] Daniel J Maltman and Stefan A Przyborski. “Developments in three-dimensional cell culture technology aimed at improving the accuracy of in vitro analyses”. In: *Biochemical Society Transactions* 38.4 (2010), pp. 1072–1075.
- [137] Francoise Marchand and Abdul M Ahmed. “Investigation of the laminate structure of lumbar disc anulus fibrosus.” In: *Spine* 15.5 (1990), pp. 402–410.
- [138] A Maroudas et al. “Factors involved in the nutrition of the human lumbar intervertebral disc: cellularity and diffusion of glucose in vitro.” In: *Journal of anatomy* 120.Pt 1 (1975), p. 113.

- [139] Anna Marsano et al. “Beating heart on a chip: a novel microfluidic platform to generate functional 3D cardiac microtissues”. In: *Lab on a Chip* 16.3 (2016), pp. 599–610.
- [140] John T Martin et al. “In vivo fluid transport in human intervertebral discs varies by spinal level and disc region”. In: *JOR Spine* (2022), e1199.
- [141] Shamik Mascharak et al. “YAP-dependent mechanotransduction is required for proliferation and migration on native-like substrate topography”. In: *Biomaterials* 115 (2017), pp. 155–166.
- [142] Jonathan P. McKinley et al. “Design of a flexing organ-chip to model in situ loading of the intervertebral disc”. In: *Biomicrofluidics* 16.5 (2022), p. 054111.
- [143] James A Miller, Christine Schmatz, and AB Schultz. “Lumbar disc degeneration: correlation with age, sex, and spine level in 600 autopsy specimens.” In: *Spine* 13.2 (1988), pp. 173–178.
- [144] Maria Molinos et al. “Inflammation in intervertebral disc degeneration and regeneration”. In: *Journal of the Royal Society Interface* 12.104 (2015), p. 20141191.
- [145] Sara Molladavoodi, John McMorran, and Diane Gregory. “Mechanobiology of annulus fibrosus and nucleus pulposus cells in intervertebral discs”. In: *Cell and Tissue Research* 379 (2020), pp. 429–444.
- [146] Jamie Moy et al. “Modeling Joint Pain on a Chip: integrating sensory neurons in the microJoint to model osteoarthritis”. In: *The Journal of Pain* 22.5 (2021), p. 583.
- [147] Kunihiko Murai et al. “Primary immune system responders to nucleus pulposus cells: evidence for immune response in disc herniation”. In: *Eur Cell Mater* 19.6 (2010), pp. 13–21.
- [148] N95Decon. *Publications*. 2023. URL: <https://www.n95decon.org/publications#time>.
- [149] Cornelia Neidlinger-Wilke et al. “Interactions of environmental conditions and mechanical loads have influence on matrix turnover by nucleus pulposus cells”. In: *Journal of Orthopaedic Research* 30.1 (2012), pp. 112–121.
- [150] Cornelia Neidlinger-Wilke et al. “Mechanical loading of the intervertebral disc: from the macroscopic to the cellular level”. In: *European Spine Journal* 23.3 (2014), pp. 333–343.
- [151] Nandan L Nerurkar, Dawn M Elliott, and Robert L Mauck. “Mechanical design criteria for intervertebral disc tissue engineering”. In: *Journal of biomechanics* 43.6 (2010), pp. 1017–1030.
- [152] Li Ning et al. “Mechanical Stretch Induces Annulus Fibrosus Cell Senescence through Activation of the RhoA/ROCK Pathway”. In: *BioMed Research International* 2021 (2021), n.p.

- [153] Grace D O’Connell, J Kent Leach, and Eric O Klineberg. “Tissue engineering a biological repair strategy for lumbar disc herniation”. In: *BioResearch open access* 4.1 (2015), pp. 431–445.
- [154] Grace D O’Connell, Isabella B Newman, and Michael A Carapezza. “Effect of long-term osmotic loading culture on matrix synthesis from intervertebral disc cells”. In: *BioResearch open access* 3.5 (2014), pp. 242–249.
- [155] Grace D O’Connell, Edward J Vresilovic, and Dawn M Elliott. “Human intervertebral disc internal strain in compression: the effect of disc region, loading position, and degeneration”. In: *Journal of orthopaedic research* 29.4 (2011), pp. 547–555.
- [156] Grace D O’Connell et al. “Human internal disc strains in axial compression measured noninvasively using magnetic resonance imaging”. In: *Spine* 32.25 (2007), pp. 2860–2868.
- [157] Grace D O’Connell, Edward J Vresilovic, and Dawn M Elliott. “Comparison of animals used in disc research to human lumbar disc geometry”. In: *Spine* 32.3 (2007), pp. 328–333.
- [158] Grace D. O’Connell, Heather L. Guerin, and Dawn M. Elliott. “Theoretical and Uniaxial Experimental Evaluation of Human Annulus Fibrosus Degeneration”. In: *Journal of Biomechanical Engineering* 131.11 (Oct. 2009). 111007, n.p. ISSN: 0148-0731. DOI: 10.1115/1.3212104. eprint: <https://asmedigitalcollection.asme.org/biomechanical/article-pdf/131/11/111007/5489057/111007\1.pdf>. URL: <https://doi.org/10.1115/1.3212104>.
- [159] Paola Occhetta et al. “Hyperphysiological compression of articular cartilage induces an osteoarthritic phenotype in a cartilage-on-a-chip model”. In: *Nature biomedical engineering* 3.7 (2019), pp. 545–557.
- [160] US Attorney’s Office. *Brooklyn Company Admits Price Gouging KN95 Masks During COVID-19 Pandemic*. 2022. URL: <https://www.justice.gov/usao-nj/pr/brooklyn-company-admits-price-gouging-95-masks-during-covid-19-pandemic> (visited on 03/29/2022).
- [161] Natalia V Oster et al. *COVID-19 and the Rural Health Workforce: The Impact of Federal Pandemic Funding to Address Workforce Needs*. 2022. URL: <https://familymedicine.uw.edu/chws/wp-content/uploads/sites/5/2022/03/Covid-19-and-the-Rural-Health-Workforce-PB-2022.pdf> (visited on 03/01/2022).
- [162] David Ozog et al. “The importance of fit testing in decontamination of N95 respirators: A cautionary note”. In: *Journal of the american academy of dermatology* 83.2 (2020), pp. 672–674.
- [163] Hannu Paaajanen et al. “Diurnal fluid changes of lumbar discs measured indirectly by magnetic resonance imaging”. In: *Journal of Orthopaedic Research* 12.4 (1994), pp. 509–514.

- [164] Carlo Alberto Paggi et al. “Monolithic microfluidic platform for exerting gradients of compression on cell-laden hydrogels, and application to a model of the articular cartilage”. In: *Sensors and Actuators B: Chemical* 315 (2020), p. 127917.
- [165] Jonathon Parrish et al. “New frontiers for biofabrication and bioreactor design in microphysiological system development”. In: *Trends in biotechnology* 37.12 (2019), pp. 1327–1343.
- [166] Avinash G Patwardhan et al. “A follower load increases the load-carrying capacity of the lumbar spine in compression”. In: *Spine* 24.10 (1999), pp. 1003–1009.
- [167] WCG Peh. “Provocative discography: current status”. In: *Biomedical Imaging and Intervention Journal* 1.1 (2005).
- [168] Baogan Peng and Yongchao Li. “Concerns about cell therapy for intervertebral disc degeneration”. In: *NPJ Regenerative medicine* 7.1 (2022), pp. 1–5.
- [169] Judith-Johanna Pfannkuche et al. “Intervertebral disc organ culture for the investigation of disc pathology and regeneration—benefits, limitations, and future directions of bioreactors”. In: *Connective tissue research* 61.3-4 (2020), pp. 304–321.
- [170] Belinda Pinguan-Murphy and Illida Nawi. “Upregulation of matrix synthesis in chondrocyte-seeded agarose following sustained bi-axial cyclic loading”. In: *Clinics* 67.8 (2012), pp. 939–944.
- [171] Alexandre Poulin et al. “An ultra-fast mechanically active cell culture substrate”. In: *Scientific reports* 8.1 (2018), pp. 1–10.
- [172] MC Powell et al. “Prevalence of lumbar disc degeneration observed by magnetic resonance in symptomless women”. In: *The Lancet* 328.8520 (1986), pp. 1366–1367.
- [173] Harris Pratsinis et al. “Cyclic tensile stress of human annulus fibrosus cells induces MAPK activation: involvement in proinflammatory gene expression”. In: *Osteoarthritis and cartilage* 24.4 (2016), pp. 679–687.
- [174] Milad Raeiszadeh and Babak Adeli. “A critical review on ultraviolet disinfection systems against COVID-19 outbreak: applicability, validation, and safety considerations”. In: *Acs Photonics* 7.11 (2020), pp. 2941–2951.
- [175] Ahmad Jabir Rahyussalim, Muhammad Luqman Labib Zufar, and Tri Kurniawati. “Significance of the association between disc degeneration changes on imaging and low back pain: a review article”. In: *Asian spine journal* 14.2 (2020), p. 245.
- [176] François Rannou et al. “Monolayer anulus fibrosus cell cultures in a mechanically active environment: local culture condition adaptations and cell phenotype study”. In: *Journal of Laboratory and Clinical Medicine* 136.5 (2000), pp. 412–421.
- [177] Duncan A Reid and Peter J McNair. “Factors contributing to low back pain in rowers”. In: *British journal of sports medicine* 34.5 (2000), pp. 321–322.

- [178] Battelle Media Relations. *Battelle Develops System to Decontaminate Personal Protective Equipment to Meet Growing Demand during COVID-19 Crisis*. 2020. URL: <https://www.battelle.org/insights/newsroom/press-release-details> (visited on 03/29/2020).
- [179] Chloé Roffay et al. “Passive coupling of membrane tension and cell volume during active response of cells to osmosis”. In: *Proceedings of the National Academy of Sciences* 118.47 (2021), e2103228118.
- [180] Antonius Rohlmann et al. “Activities of everyday life with high spinal loads”. In: *PloS one* 9.5 (2014), e98510.
- [181] Antonius Rohlmann et al. “Measurement of the number of lumbar spinal movements in the sagittal plane in a 24-hour period”. In: *European Spine Journal* 23.11 (2014), pp. 2375–2384.
- [182] J Rosser et al. “Microfluidic nutrient gradient-based three-dimensional chondrocyte culture-on-a-chip as an in vitro equine arthritis model”. In: *Materials Today Bio* 4 (2019), p. 100023.
- [183] Devon I Rubin. “Epidemiology and risk factors for spine pain”. In: *Neurologic clinics* 25.2 (2007), pp. 353–371.
- [184] Maximilian Rudert and Bernhard Tillmann. “Lymph and blood supply of the human intervertebral disc: Cadaver study of correlations to discitis”. In: *Acta Orthopaedica* 64 (1 1993), pp. 37–40. ISSN: 17453674. DOI: 10.3109/17453679308994524.
- [185] Aleksandra Sadowska et al. “Osmosensing, osmosignalling and inflammation: how intervertebral disc cells respond to altered osmolarity”. In: *European cells & materials* 36 (2018), pp. 231–250.
- [186] Prasanthi Sampara et al. “Understanding the molecular biology of intervertebral disc degeneration and potential gene therapy strategies for regeneration: a review”. In: *Gene therapy* 25.2 (2018), pp. 67–82.
- [187] Jaya Sanapati et al. “Do regenerative medicine therapies provide long-term relief in chronic low back pain: a systematic review and metaanalysis”. In: *Pain Physician* 21.6 (2018), p. 515.
- [188] Tara C Schmitz et al. “Characterization of biomaterials intended for use in the nucleus pulposus of degenerated intervertebral discs”. In: *Acta Biomaterialia* 114 (2020), pp. 1–15.
- [189] Max A Schumm et al. “Filtering facepiece respirator (N95 respirator) reprocessing: a systematic review”. In: *Jama* 325.13 (2021), pp. 1296–1317.
- [190] Anthony C Schwarzer et al. “The prevalence and clinical features of internal disc disruption in patients with chronic low back pain.” In: *Spine* 20.17 (1995), pp. 1878–1883.

- [191] Amra Secerovic et al. “Toward the Next Generation of Spine Bioreactors: Validation of an Ex Vivo Intervertebral Disc Organ Model and Customized Specimen Holder for Multiaxial Loading”. In: *ACS biomaterials science & engineering* 8.9 (2022), pp. 3969–3976.
- [192] Clare Selden and Barry Fuller. “Role of bioreactor technology in tissue engineering for clinical use and therapeutic target design”. In: *Bioengineering* 5.2 (2018), p. 32.
- [193] Lori A Setton and Jun Chen. “Cell mechanics and mechanobiology in the intervertebral disc”. In: *Spine* 29.23 (2004), pp. 2710–2723.
- [194] Kifah Shahin and Pauline M Doran. “Shear and compression bioreactor for cartilage synthesis”. In: *Cartilage Tissue Engineering*. Springer, 2015, pp. 221–233.
- [195] Narjes Momeni Shahraki et al. “Prediction of clinically relevant initiation and progression of tears within annulus fibrosus”. In: *Journal of Orthopaedic Research* 35 (1 Jan. 2017), pp. 113–122. ISSN: 1554527X. DOI: 10.1002/jor.23346.
- [196] Alyah H Shamsah et al. “Tissue engineering the annulus fibrosus using 3D rings of electrospun PCL: PLLA angle-ply nanofiber sheets”. In: *Frontiers in bioengineering and biotechnology* 7 (2020), p. 437.
- [197] Changgui Shi et al. “Animal models for studying the etiology and treatment of low back pain”. In: *Journal of Orthopaedic Research* 36.5 (2018), pp. 1305–1312.
- [198] Changgui Shi et al. “Development of an in vivo mouse model of discogenic low back pain”. In: *Journal of cellular physiology* 233.10 (2018), pp. 6589–6602.
- [199] Brent L. Showalter et al. “Novel human intervertebral disc strain template to quantify regional three-dimensional strains in a population and compare to internal strains predicted by a finite element model”. In: *Journal of Orthopaedic Research* 34 (7 July 2016), pp. 1264–1273. ISSN: 1554527X. DOI: 10.1002/jor.23137.
- [200] Ravi Sinha et al. “Endothelial cell alignment as a result of anisotropic strain and flow induced shear stress combinations”. In: *Scientific reports* 6.1 (2016), pp. 1–12.
- [201] Joanna Skommer and Donald Wlodkowic. “Successes and future outlook for microfluidics based cardiovascular drug discovery”. In: *Expert opinion on drug discovery* 10.3 (2015), pp. 231–244.
- [202] R Lane Smith et al. “Effects of fluid-induced shear on articular chondrocyte morphology and metabolism in vitro”. In: *Journal of Orthopaedic Research* 13.6 (1995), pp. 824–831.
- [203] Gwendolyn Sowa and Sudha Agarwal. “Cyclic tensile stress exerts a protective effect on intervertebral disc cells”. In: *American journal of physical medicine & rehabilitation/Association of Academic Physiatrists* 87.7 (2008), p. 537.
- [204] Gwendolyn Sowa et al. “Determination of annulus fibrosus cell response to tensile strain as a function of duration, magnitude, and frequency”. In: *Journal of Orthopaedic Research* 29.8 (2011), pp. 1275–1283.



- [205] Manos Stefanakis et al. “Mechanical influences in progressive intervertebral disc degeneration.” In: *Spine Journal Meeting Abstracts*. LWW. 2014, pp. 38–39.
- [206] Janja Stergar et al. “Intervertebral disc tissue engineering: A brief review”. In: *Bosnian Journal of Basic Medical Sciences* 19 (2 2019), pp. 130–137. ISSN: 18404812. DOI: 10.17305/bjbms.2019.3778.
- [207] Ian AF Stokes and James C Iatridis. “Mechanical conditions that accelerate intervertebral disc degeneration: overload versus immobilization”. In: *Spine* 29.23 (2004), p. 2724.
- [208] Zhen Sun, Bing Liu, and Zhuo-Jing Luo. “The immune privilege of the intervertebral disc: implications for intervertebral disc degeneration treatment”. In: *International journal of medical sciences* 17.5 (2020), p. 685.
- [209] Alireza Tajeddin and Nur Mustafaoglu. “Design and fabrication of organ-on-chips: Promises and challenges”. In: *Micromachines* 12.12 (2021), p. 1443.
- [210] Shirley N Tang et al. “Controversies in spine research: Organ culture versus in vivo models for studies of the intervertebral disc”. In: *JOR spine* (2022), e1235.
- [211] Andrew J Teichtahl et al. “Fat infiltration of paraspinal muscles is associated with low back pain, disability, and structural abnormalities in community-based adults”. In: *The Spine Journal* 15.7 (2015), pp. 1593–1601.
- [212] M Teraguchi et al. “Prevalence and distribution of intervertebral disc degeneration over the entire spine in a population-based cohort: the Wakayama Spine Study”. In: *Osteoarthritis and cartilage* 22.1 (2014), pp. 104–110.
- [213] Vanessa Terraciano et al. “Differential response of adult and embryonic mesenchymal progenitor cells to mechanical compression in hydrogels”. In: *Stem cells* 25.11 (2007), pp. 2730–2738.
- [214] Clare L Thompson et al. “Mechanical stimulation: a crucial element of organ-on-chip models”. In: *Frontiers in Bioengineering and Biotechnology* 8 (2020), p. 602646.
- [215] Krzysztof A Tomaszewski et al. “Age-and degeneration-related variations in cell density and glycosaminoglycan content in the human cervical intervertebral disc and its endplates”. In: *Polish Journal of Pathology* 66.3 (2015), pp. 296–300.
- [216] Olivia M Torre et al. “Annulus fibrosus cell phenotypes in homeostasis and injury: implications for regenerative strategies”. In: *Annals of the New York Academy of Sciences* 1442.1 (2019), pp. 61–78.
- [217] LRG Treloar. “The elasticity and related properties of rubbers”. In: *Reports on progress in physics* 36.7 (1973), p. 755.
- [218] Dominique Tremblay et al. “A microscale anisotropic biaxial cell stretching device for applications in mechanobiology”. In: *Biotechnology letters* 36.3 (2014), pp. 657–665.

- [219] Yoshihiro Ujihara et al. “Computational studies on strain transmission from a collagen gel construct to a cell and its internal cytoskeletal filaments”. In: *Computers in Biology and Medicine* 56 (2015), pp. 20–29.
- [220] Jill PG Urban, Stanton Smith, and Jeremy CT Fairbank. “Nutrition of the intervertebral disc”. In: *Spine* 29.23 (2004), pp. 2700–2709.
- [221] JPG Urban, S Roberts, and JR Ralphs. “The nucleus of the intervertebral disc from development to degeneration”. In: *American Zoologist* 40.1 (2000), pp. 53–61.
- [222] Gianluca Vadalà et al. “Interaction between mesenchymal stem cells and intervertebral disc microenvironment: from cell therapy to tissue engineering”. In: *Stem Cells International* 2019 (2019).
- [223] P-PA Vergroesen et al. “Mechanics and biology in intervertebral disc degeneration: a vicious circle”. In: *Osteoarthritis and cartilage* 23.7 (2015), pp. 1057–1070.
- [224] Barrie Vernon-Roberts, Nicola L Fazzalari, and Beverley A Manthey. “Pathogenesis of tears of the annulus investigated by multiple-level transaxial analysis of the T12-L1 disc”. In: *Spine* 22.22 (1997), pp. 2641–2646.
- [225] Barrie Vernon-Roberts, Robert J Moore, and Robert D Fraser. “The natural history of age-related disc degeneration: the pathology and sequelae of tears”. In: *Spine* 32.25 (2007), pp. 2797–2804.
- [226] Geoffrey Verrall and Andrew Darcey. “Lower back injuries in rowing national level compared to international level rowers”. In: *Asian journal of sports medicine* 5.4 (2014).
- [227] Michael Von Korff et al. “Back pain in primary care. Outcomes at 1 year.” In: *Spine* 18.7 (1993), pp. 855–862.
- [228] Theo Vos et al. “Years lived with disability (YLDs) for 1160 sequelae of 289 diseases and injuries 1990–2010: a systematic analysis for the Global Burden of Disease Study 2010”. In: *The lancet* 380.9859 (2012), pp. 2163–2196.
- [229] Michelle E Wall et al. “Comparison of cellular strain with applied substrate strain in vitro”. In: *Journal of biomechanics* 40.1 (2007), pp. 173–181.
- [230] Zhixin Wang, Alex A Volinsky, and Nathan D Gallant. “Crosslinking effect on polydimethylsiloxane elastic modulus measured by custom-built compression instrument”. In: *Journal of Applied Polymer Science* 131.22 (2014).
- [231] Benjamin Werbner et al. “Saline-polyethylene glycol blends preserve in vitro annulus fibrosus hydration and mechanics: An experimental and finite-element analysis”. In: *Journal of the Mechanical Behavior of Biomedical Materials* 125 (2022), p. 104951.
- [232] Augustus White and Manohar Panjabi. *Clinical Biomechanics of the Spine*. Lippincott, 1978.
- [233] Hans-Joachim Wilke et al. “New in vivo measurements of pressures in the intervertebral disc in daily life”. In: *Spine* 24.8 (1999), pp. 755–762.

- [234] Joshua Scott Will, David C Bury, and John A Miller. “Mechanical low back pain”. In: *American family physician* 98.7 (2018), pp. 421–428.
- [235] Benjamin L Wong et al. “Shear deformation kinematics during cartilage articulation: effect of lubrication, degeneration, and stress relaxation”. In: *Molecular & cellular biomechanics: MCB* 5.3 (2008), p. 197.
- [236] Aimin Wu et al. “Global low back pain prevalence and years lived with disability from 1990 to 2017: estimates from the Global Burden of Disease Study 2017”. In: *Annals of translational medicine* 8.6 (2020).
- [237] K Wuertz et al. “Influence of extracellular osmolarity and mechanical stimulation on gene expression of intervertebral disc cells”. In: *Journal of Orthopaedic Research* 25.11 (2007), pp. 1513–1522.
- [238] Katsuhisa Yamada, Norimasa Iwasaki, and Hideki Sudo. “Biomaterials and Cell-Based Regenerative Therapies for Intervertebral Disc Degeneration with a Focus on Biological and Biomechanical Functional Repair: Targeting Treatments for Disc Herniation”. In: *Cells* 11.4 (2022), p. 602.
- [239] Bo Yang and Grace D. O’Connell. “Intervertebral disc swelling maintains strain homeostasis throughout the annulus fibrosus: A finite element analysis of healthy and degenerated discs”. In: *Acta Biomaterialia* 100 (Dec. 2019), pp. 61–74. ISSN: 18787568. DOI: 10.1016/j.actbio.2019.09.035.
- [240] Haiou Yang et al. “Low Back Pain Prevalence and Related Workplace Psychosocial Risk Factors: A Study Using Data From the 2010 National Health Interview Survey”. In: *Journal of Manipulative and Physiological Therapeutics* 39 (7 Sept. 2016), pp. 459–472. ISSN: 15326586. DOI: 10.1016/j.jmpt.2016.07.004.
- [241] Edmond WK Young and David J Beebe. “Fundamentals of microfluidic cell culture in controlled microenvironments”. In: *Chemical Society Reviews* 39.3 (2010), pp. 1036–1048.
- [242] Lawrence Zeldin et al. “Spatial mapping of collagen content and structure in human intervertebral disk degeneration”. In: *JOR spine* 3.4 (2020), e1129.
- [243] Hua Zhang et al. “Effects of Changes in Osmolarity on the Biological Activity of Human Normal Nucleus Pulposus Mesenchymal Stem Cells”. In: *Stem Cells International* 2022 (2022).
- [244] Tianzi Zhang et al. “Investigating fibroblast-induced collagen gel contraction using a dynamic microscale platform”. In: *Frontiers in bioengineering and biotechnology* 7 (2019), p. 196.
- [245] Ting-Ting Zhang et al. “Obesity as a risk factor for low Back pain”. In: *Clinical spine surgery* 31.1 (2018), pp. 22–27.

- [246] Minhao Zhou, Benjamin Werbner, and Grace D O'Connell. "Fiber engagement accounts for geometry-dependent annulus fibrosus mechanics: a multiscale, Structure-Based Finite Element Study". In: *journal of the mechanical behavior of biomedical materials* 115 (2021), p. 104292.
- [247] Minhao Zhou et al. "Torque-and Muscle-Driven Flexion Induce Disparate Risks of In Vitro Herniation: A Multiscale and Multiphasic Structure-Based Finite Element Study". In: *Journal of biomechanical engineering* 144.6 (2022), p. 061005.
- [248] Pinghui Zhou et al. "Regulation of differentiation of annulus fibrosus-derived stem cells using heterogeneous electrospun fibrous scaffolds". In: *Journal of Orthopaedic Translation* 26 (2021), pp. 171–180.